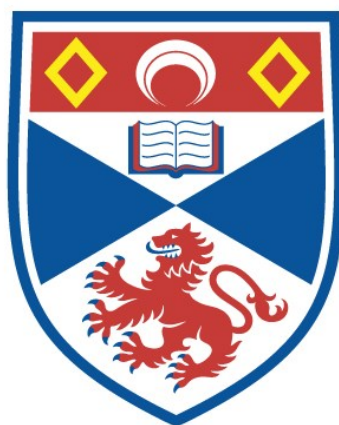


THE FORMULAE AND STRUCTURES OF SOME
AROMATIC AMINE AND HYDROCARBON
COMPLEXES OF ANTIMONY TRICHLORIDE

Donald Joseph Edgar Mullen

A Thesis Submitted for the Degree of PhD
at the
University of St Andrews



1970

Full metadata for this item is available in
St Andrews Research Repository
at:

<http://research-repository.st-andrews.ac.uk/>

Please use this identifier to cite or link to this item:

<http://hdl.handle.net/10023/15172>

This item is protected by original copyright

THE FORMULAE AND STRUCTURES OF SOME AROMATIC AMINE AND
HYDROCARBON COMPLEXES OF ANTIMONY TRICHLORIDE.

being a thesis presented by
DONALD JOSEPH EDGAR MULLEN
to the University of St. Andrews
in application for the degree of
Doctor of Philosophy.



DEDICATIONS:

To Christine;

To Albert Camus (1923 - 1960)

ProQuest Number: 10171170

All rights reserved

INFORMATION TO ALL USERS

The quality of this reproduction is dependent upon the quality of the copy submitted.

In the unlikely event that the author did not send a complete manuscript and there are missing pages, these will be noted. Also, if material had to be removed, a note will indicate the deletion.



ProQuest 10171170

Published by ProQuest LLC (2017). Copyright of the Dissertation is held by the Author.

All rights reserved.

This work is protected against unauthorized copying under Title 17, United States Code
Microform Edition © ProQuest LLC.

ProQuest LLC.
789 East Eisenhower Parkway
P.O. Box 1346
Ann Arbor, MI 48106 – 1346

Tn 5755

DECLARATION.

I declare that this thesis is a record of the results of work carried out by me, and that the thesis is my own composition and has not previously been presented for a higher degree.

The research was carried out in the Department of Chemistry, University of St. Andrews under the direction of Mr. R. Hulme.

September, 1970.

CERTIFICATE.

I certify that Donald J.E. Mullen has spent nine terms at research work under my direction, that he has fulfilled the conditions of Ordinance 16 (St. Andrews) and is qualified to submit the accompanying Thesis in application for a degree of Doctor of Philosophy.

September, 1970.

Director of Research.

UNIVERSITY CAREER.

I first matriculated in King's College, University of London in October, 1964, and subsequently graduated B.Sc. with Lower Second Class Honours in Chemistry in August, 1967.

I was admitted as a Research Student in the Department of Chemistry, University of St. Andrews in October, 1967.

I was awarded a Research Scholarship by the Department of Chemistry, University of St. Andrews for the whole period of my research.

ACKNOWLEDGEMENTS.

I would like to express my gratitude to Mr. Hulme who supervised the work for this thesis, and without whose guidance it would not have been completed.

I would also like to thank Professor P.A.H. Wyatt and Professor Lord J.M. Tedder for the provision of laboratory facilities.

For the grant which made possible my research I am indebted to the Department of Chemistry, University of St. Andrews.

Thanks are also due to those who typed this thesis.

SUMMARY.

The crystal structure of the complex $2\text{SbCl}_3 \cdot \text{p-xylene}$ (space group: $P2_1/c$; $a=9.13\text{\AA}$, $b=8.44\text{\AA}$, $c=12.79\text{\AA}$; $\beta=125^\circ 21'$) was investigated at low temperatures, and it proves to be a layer structure with packing p-xylene molecules.

The compound $\text{C}_5\text{H}_5\text{NH}^+ \text{SbCl}_4^-$ (space group: $C2/c$; $a=13.12\text{\AA}$, $b=13.07\text{\AA}$, $c=7.44\text{\AA}$, $\beta=122^\circ 19'$) was identified as a hydrolysis product of the $\text{SbCl}_3/\text{pyridine}$ system by means of a partial structure analysis.

The complex $2\text{SbCl}_3 \cdot 3\text{C}_5\text{H}_5\text{N}$ (space group: $Pca2_1$; $a=26.14\text{\AA}$, $b=11.93\text{\AA}$, $c=7.51\text{\AA}$) was prepared and its structure elucidated. Its general structural features include an infinite Sb - Cl chain, pyridine ligands attached to the antimony atom, and the presence, in addition, of a "solvating" pyridine molecule.

The complex $2\text{SbCl}_3 \cdot \text{C}_5\text{H}_5\text{N}$ (space group: $P\bar{1}$; $a=10.93\text{\AA}$, $b=9.92\text{\AA}$, $c=9.30\text{\AA}$, $\alpha=106^\circ 48'$, $\beta=102^\circ 48'$, $\gamma=116^\circ 36'$) was prepared. This has an extensively bridged Sb - Cl system and non-bonding pyridine molecules, occurring in alternate layers.

The complex $\text{SbCl}_3 \cdot \text{C}_5\text{H}_5\text{N}$ (space group: $P2_1/c$; $a=13.00\text{\AA}$, $b=17.87\text{\AA}$, $c=12.17\text{\AA}$, $\beta=121^\circ 11'$) was prepared.

CONTENTS

Chapter

Introduction	1
A). Theoretical Aspects of Molecular Complexes	
B). Molecular Complexes: A Brief Survey	
I Preparation of the Compounds	28
A). The Antimony Trichloride/p-xylene System	
B). The Antimony Trichloride/pyridine System	
II Construction of a Low Temperature X-Ray Apparatus	36
III Identification of an Air-Stable Hydrolysis Product of the Antimony Trichloride/Pyridine System by Means of a Partial Structure Determination.	42
IV The Structure of the Complex $2\text{SbCl}_3 \cdot \text{p-xylene}$ at -110°C .	49
V The Structure of the Complex $2\text{SbCl}_3 \cdot 3\text{C}_5\text{H}_5\text{N}$.	66
VI The Complex $\text{SbCl}_3 \cdot \text{C}_5\text{H}_5\text{N}$.	85
VII The Structure of the Complex $2\text{SbCl}_3 \cdot \text{C}_5\text{H}_5\text{N}$.	91
VIII Comparison and Discussion.	107
References.	120
Appendices I - VI.	

I N T R O D U C T I O N

A) Theoretical Aspects of Molecular Complexes.

The term 'molecular complexes' is used to describe compounds which are built up from components which in general have a separate existence of their own. There are no strong interactions between the components, and geometrical or 'packing' considerations in the main decide the structural features of these complexes. The intermolecular distances are generally much larger than those expected of covalent electron-pair bonds. The components pack together without allowing the specification of a covalent bond between them, and in such a manner that the structure cannot be reduced conceptually to a simple ionic lattice. The simplification of regarding the component molecules as close-packing spheres, with molecules of one species fitting into the cavities in the close-packed lattice of the other, allows a quantitative rationalisation of the structural features in terms of a relative radius ratio.¹

Under the above description of molecular compounds we include Van der Waals type complexes and charge-transfer type complexes. A third type of intermolecular association occurs in the formation of a dative bond in a donor-acceptor

interaction. This is a stronger interaction resulting in the formation of a formal bond through lone-pair donation.

These three basic models for intermolecular interactions will be considered below. This classification in terms of interaction is not unambiguous, and its weakness lies in that there are many borderline cases.

(i) Van der Waals Forces.

In 1937 London² described a model for molecular interactions involving no formal bond. He proposed to follow Van der Waals' treatment of interactions in the gaseous state, in that he attributed the intermolecular forces to small perturbations of one molecule by another in the manner that Van der Waals had attributed deviation from the ideal gas law to such perturbations.

Three principal factors were responsible for the Van der Waals force, according to London : the 'Orientation effect', the 'Induction effect' and the 'Dispersion effect'.

The first ideas about the 'Orientation effect' are due to Keesom³. Since molecules are usually uncharged, he regarded the dipole moment, μ , as the operative factor in determining intermolecular forces. The orientations of molecules relative to each other therefore become a crucial factor in deciding the

sizes and directions of these forces. Orientations of lower energy are statistically favoured, so that the average dipole is non-zero. It is also temperature dependent. Keesom gave an 'orientational' interaction energy of

$$\bar{U} = -\frac{2}{3} \frac{\mu_I^2 \mu_{II}^2}{R^6} \cdot \frac{1}{kT} \quad (\mu_I \mu_{II} / kT \ll kT),$$

where μ_I, μ_{II} are the dipoles of the two molecules, and R the distance between the dipole centres. The expression above represents an attractive force.

Debye⁴ pointed out that the Keesom 'orientation effect' led to a force between molecules: which vanished rapidly with increasing temperature, in contrast to the less steep decline of the empirical Van der Waals corrections. The charge distribution in a molecule may be altered by an electric field produced by a neighbouring molecule: The effect is mutual to the two molecules. The result is an induced dipole in each molecule with an interaction energy given by:

$$\bar{U} = -\frac{1}{R^6} (\alpha_I \mu_{II}^2 + \alpha_{II} \mu_I^2),$$

where α_I, α_{II} are the polarisabilities of the molecules, and μ_I, μ_{II} permanent dipoles. It will be noted that this interaction is temperature independent. Molecules without permanent dipoles

were assumed to have quadrupoles, and these would induce dipoles in each other.

Wave mechanical considerations showed that the rare-gas molecules were spherically symmetrical and possessed no multipoles at all. However, these molecules possess a zero point motion, and London considered that this motion gave rise to quickly varying dipoles which induced further dipoles in neighbouring molecules. These induced dipoles are in phase with and interacting with the instantaneous dipoles which produced them, giving rise to an attractive force which London termed the 'dispersion effect'. This effect he expressed as:

$$U_{\rho k} = U_{\rho \rightarrow k} + U_{k \rightarrow \rho} = -\frac{2}{3hR^6} \sum_{l\sigma} \frac{\mu_{kl}^2 \mu_{\rho\sigma}^2}{\nu_{kl} + \nu_{\rho\sigma}},$$

where μ_{kl}, ν_{kl} are the periodic dipoles and oscillation frequency of one molecule, and $\mu_{\rho\sigma}, \nu_{\rho\sigma}$ the corresponding functions of the other molecule. k, ρ and l, σ are lower and upper states of the two oscillating molecules.

The total Van der Waals force was postulated as the sum of these three effects. In order to realise these interactions, the various molecules must be allowed to approach each other closely enough for the different dipolar forces to be operative: hence the term 'packing complexes'.

(ii) Charge-Transfer Interactions.

It is possible for molecules to approach closer to each other than the 3.5\AA generally accepted as the 'Van der Waals distance' without forming a definite and localised chemical bond. However, at distances significantly less than this figure, interactions become attributable to increasingly localised and directed forces or 'bonds'. Instead of considering overall charge distributions in molecules (which give rise to the dipoles), it becomes pertinent to think in terms of the magnitudes of electron densities on individual atoms and the relative directions of molecular orbitals,

Charge-transfer complexes involve donation of electrons by one molecule and acceptance by another. The donor must be a molecule possessing non-bonding electrons, and the acceptor a molecule with sufficiently low-lying vacant orbitals with respect to their energy.

However, charge-transfer complexes can be distinguished from normal donor-acceptor complexes involving co-ordinate bonds to ligands by typical bands in their U.V. spectra. Several early attempts to explain charge-transfer interactions suggested straight-forward covalent bonding schemes. The objection to this was the large distances involved. Briegleb⁶(1936)

suggested dipole-dipole and dipole-induced dipole interactions. Pauling⁷ (1939) attempted to explain the marked colouring of charge-transfer complexes in terms of dipole-dipole interactions, but it was found that these weak interactions were insufficient to explain the colours. Weiss⁸ (1942) regarded these complexes as donor-acceptor complexes, and Brackman⁹ in 1949 developed this idea in suggesting "complex-resonance" between 'bonded' and 'non-bonded' structures.

Mulliken⁵ has given a wave mechanical treatment of charge-transfer interactions, and he regards these interactions as "partial electron transfer . . . occurring in loosely bound organic molecular complexes". Mulliken's treatment of charge-transfer emphasises the importance of orientational effects as against dispersion effects, in line with the idea that the forces involved are more directional than in Van der Waals interaction. In this treatment, the wave-function of the ground state of the complex is given by:

$$\psi_0 = \psi(D, A) + b_0 \psi(D^+, A^-),$$

where D is the donor molecule, A the acceptor molecule, D^+ , A^- the respective ions, and $b_0 \ll 1$. The ionic state makes only a small contribution to the ground state of the complex, and the energy associated with ψ_0 is lower than that of $\psi(D, A)$ or $\psi(D^+, A^-)$, therefore accounting for the stability of the complex.

The excited state is given by:

$$\psi_1 = a_0 \psi(D^+, A^-) + a_1 \psi(D, A) ; \quad (a_1 \ll 1)$$

Transitions $\psi_0 \rightarrow \psi_1$, give rise to the characteristic charge-transfer bands.

(iii) Donor-Acceptor or Metal-Ligand Bonding.

If the ionic function $\psi(D^+, A^-)$ makes as large a contribution to the ground state as the no-bond state $\psi(D, A)$ (i.e. is of similar energy), the ground state is stabilised, the excited state de-stabilised and a large intermolecular binding energy is found. The ground state/excited state separation becomes too large to allow charge-transfer bands to occur. This situation corresponds (formally) to the donation of a lone-pair of electrons to the acceptor atom. The orbitals involved in bonding generally afford a larger overlap than the delocalised molecular orbitals found in many organic (aromatic) charge-transfer complexes.

Several factors contribute to the stability of these "lone-pair" bonds. An assessment of co-ordinate bond strength in terms of donor-power computed from considerations of basicity of the donor alone is inadequate to account for the bonding in all the observed complexes. Chatt¹⁰ has found that a more elaborate bonding scheme than simple σ -bonding is required. The σ -bond formed by donation ($L \rightarrow M$) is supplemented by a π -contribution ($L \rightleftharpoons M$), and this he has called the "synergic effect". The effect of this multiple-bonding scheme is

to afford stability to the complexes. The ligand must have vacant π^* -orbitals to accept the "back-bonded" electrons, and the metal atom must have orbitals of suitable symmetry, size and energy for overlap with these (Fig.I)

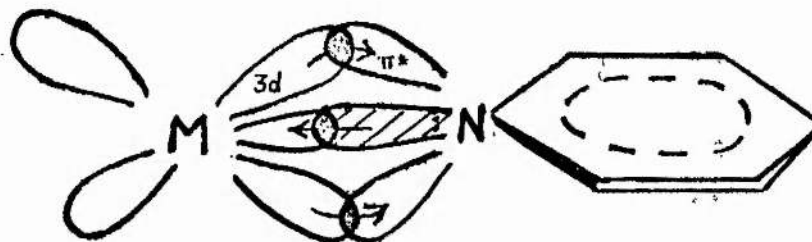


Fig.I. - Synergic Effect.

While donor and acceptor actions may be individually weak, their combined effect is unexpectedly strong¹¹. A measure of the strength of these metal-ligand bonds is found in the magnitude of the overlap integral of the orbitals involved.

Craig and Nyholm¹² have suggested that synergic π -back-bonding from metal to ligand is enhanced by "inner screening" of the metal $d\pi$ -electrons by the lone-pair donated from the ligand. The effect of this screening is to decrease the effective nuclear charge at the $d\pi$ -orbital, to increase the size of the $d\pi$ -orbital, and therefore to enhance its overlap with the ligand π^* -acceptor orbital. A further and specific examination of donor-acceptor behaviour is given in the "Discussion of Results" in regard to the aniline and pyridine ligands. Factors considered include availability of donor and acceptor orbitals, orbital overlap, ligand competition, and availability of lone-pairs.

B). Molecular Complexes : A Brief Survey.

With the above bonding considerations in mind, it is now proposed to survey the area of molecular complexes, in particular those of antimony trichloride with aromatics.

Van der Waals or "Packing" Complexes.

It is convenient to sub-divide this type of complex into groups which emphasise the nature/^{of} packing of the components, and the various types are considered in turn below.

i). Clathrates.

In typical clathrates, one compound forms a 'cage' lattice with suitable 'holes' which are occupied by molecules of the other component, the two molecular species being designated the 'host lattice' and the 'guest molecule' respectively. The framework of the cage is frequently held together by hydrogen bonding, and there is no bonding between the lattice and the guest molecule.

Von Stackelberg and Muller¹³ in 1951 reported clathrates of the noble gas hydrates for argon, krypton and xenon. In these complexes, hydrogen-bonded water molecules form the cage, and two types of such cage were reported, giving rise to different sizes of cavities. In addition to the noble gases, molecules such as CHCl_3 , H_2S and Br_2 are possible guests in the above hydrate lattices.

A second series of clathrates is that formed by β -quinol¹⁴.

Powell and his co-workers have made detailed structural examinations of clathrates of the type $Mx - 3 C_6H_4(OH)_2$, where the β -quinol acts as a host lattice for various molecules, M ,¹⁵⁻¹⁹ including SO_2 , HCl , CO_2 , CH_3OH and the noble gases argon, krypton and xenon. The quinol framework is held together by extensive hydrogen bonding, such that there is one cavity for every three quinol molecules. Van der Waals forces are operative between the lattice and guest molecules.

Not all of the cavities need be filled, and more than one type of guest molecule may be present in the same compound, giving rise to non-stoichiometric compounds.

The rare gas clathrates¹⁶ are of particular interest in establishing the idea that a molecular complex may be formed without invoking any valency bonding forces.

A further type of clathrate is that formed with a tri-*o*-thymotide framework²⁰. Here, however, the tri-*o*-thymotide units are held together by Van der Waals forces. Inclusion compounds with benzene and chloroform have been reported. In these compounds, the tri-*o*-thymotide forms a trigonal spiral with the spiral directions parallel to the *a* axis of the unit cell. Channel type complexes with tri-*O*-thymotide are also formed, and are discussed in the next section.

Powell and Rayner^{21,22} have described a clathrate with an inorganic framework, $Ni(CN)_2 \cdot NH_3 \cdot C_6H_6$. The host lattice

is a face-centred arrangement with Ni atoms at two opposite face-centres. These are interlinked by cyanide groups to form extensive layers. The ammonia is bound to the nickel atoms at the corners of the unit cell and in a direction perpendicular to the Ni-CN layers. The remaining four face centres are occupied by benzene rings. There is no interaction between the benzene molecules and the Ni layers, the usual Van der Waals distances being observed. Similar complexes can be formed by several other aromatic molecules such as pyrrole, furan, pyridine, phenol and aniline, where the molecules have about the same Van der Waals volume²³.

(i) "Channel" Type Complexes.

Tri-o - thymotide exhibits in addition to 'cavity' complexes, certain examples of adducts where the host molecules spiral around long guest molecules, forming channel-like structures²⁰. These compounds belong to the space-group P_{61} , and the tri-o - thymotide molecules form a six-fold spiral. Guest molecules include n-alcohols and n-alkyl halides, running in channels parallel to the c-axis of the cell.

A further example of a 'channel' inclusion compound is the urea-hydrocarbon complex^{24,25}. Here the hexagonal spiral of urea is held together by hydrogen bonding

iii) Other Van der Waals Complexes.

In addition to the inclusion compounds noted above, there are many examples of Van der Waals complexes in which

the inclusion is limited and the structure is layer-like.

Powell and co-workers have reported a complex between p- iodoaniline and s- trinitrobenzene²⁶. The structure consists essentially of alternate planar molecules of the two components stacked together in columns. The separations of the ^{phenyl} rings are of the order of 3.5 Å, but the nitrogen atoms of the amino-groups and the oxygen atoms of the nitro-groups approach each other as closely as 3.1 - 3.2 Å, and hydrogen bonding has been suggested to account for this.

Molecular compounds between picryl iodide and hexamethylbenzene, and picryl chloride and hexamethylbenzene, have been studied structurally²⁷. They consist of alternate layers of the two components with separations between the ^{phenyl} rings of about 3.5 Å.

A series of complexes, all of which display this layer-like structure, is formed by 4,4' dinitrodiphenyl with several aromatic molecules^{28,29}. These include 4 - hydroxydiphenyl, diphenyl³⁰, 4,4' - dihydroxydiphenyl, benzidine, 4-iododiphenyl and 4-bromodiphenyl. All these complexes show a Van der Waals separation between the component molecules, and are similar in that they are governed by geometrical considerations. Wallwork called these aromatic layer complexes 'polarisation-bonded complexes', and his ideas on this are developed in the section on 'charge-transfer compounds', p. 21 ff.

(iv) Complexes of Antimony Trihalides with Aromatic Molecules.

Menshutkin in 1912 prepared and characterised a number of complexes between antimony trihalides and various substituted aromatic molecules^{31,-34}. His examination of these systems was chiefly concerned with phase diagram studies, and since then other workers have used various physico-chemical methods to extend the examination. The interest in these systems has arisen in the main from a need to account for the non-bonded interactions which apparently exist between the component molecules.

Ewell³⁷ (1937) found that the SbCl_3 /benzene system showed deviations from ideal solution laws in its solid-solution behaviour. Shriver (1938) measured cryoscopically the equilibrium constants for complex formation in the SbCl_3 /benzene system.

The relative stabilities of a number of SbCl_3 /aromatic complexes (considered as donor-acceptor complexes) were measured by Shinomiya³⁸ in 1938. He considered this stability as a function of the degree of dissociation of the complex in a fused state, computed on the basis of melting point measurements.

Ashkanazi³⁹ (1936) examined the Raman spectra of a SbCl_3 /benzene complex and found new lines at 477cm^{-1} and 1236cm^{-1} which he assigned to bending and stretching frequencies of a new Sb-benzene bond.

Raskin⁴⁰ (1955) looked at Raman spectra for a SbCl_3 /naphthalene complex and discovered Sb-Cl frequency shifts. He also found that C - C frequencies had shifted to lower values, and new lines and splitting had appeared. These he assigned to π -orbital interaction of naphthalene with SbCl_3 . The Sb - Cl shifts he attributed to the formation of a naphthalene - Sb bond

and its consequent effect on the Sb-Cl bonds in SbCl_3 .

Structural studies of several SbX_3 / aromatic complexes, using X-ray techniques, have been carried out by Hulme⁴¹⁻⁴⁴ and co-workers, with the aim of investigating further the nature of the bonding in these complexes. A table of these complexes, including those prepared by Menshutkin and those investigated by Hulme and co-workers, is given below. (Table I)

TABLE I.

(a) SbCl_3 Complexes with Aromatics.

AROMATIC	SbCl_3 Ar ratio	M.P. (°C)	Ref.No.
Benzene	2:1	79	31
Propylbenzene	2:1	10	32
"	1:1	1.5	32
Toluene	2:1	42.5	34
"	1:1	15	34
Ethylbenzene	2:1	57	34
"	1:1	39	34
Isoamylbenzene	1:1	1.5	34
p-xylene	2:1	70	34
"	1:1	56	34, 40
m-xylene	2:1	38	34
"	1:1	8	34
o-xylene	2:1	35.8	34
"	1:1	19	34
p-cymene	2:1	40	34
"	1:1	6	34

Mesitylene	2:1	75	34
"	1:1	43	34,41
Pseudocumene	2:1	56	34
"	1:1	0	34
Diphenyl	2:1	71	35,44
Diphenylmethane	2:1	100	35,44
Triphenylmethane	2:1	49.5	35,44
Naphthalene	2:1	86	36,41
α -chloronaphthalene	2:1	46	36
β -chloronaphthalene	1:1	29.5	36
α -bromonaphthalene	1:1	35	36
Fluorobenzene	1:1	10	36
Stilbene	4:1	-	43
Dibenzyl	2:1	76	43,44
"	4:1	77.5	43

(b) SbBr_3 Complexes with Aromatics.

AROMATIC	$\text{SbBr}_3 \cdot \text{Ar}$ Ratio	M.P. ($^{\circ}\text{C}$)	Ref. No.
Benzene	2:1	92.5	31,42
Toluene	2:1	39	34
"	1:1	9	34
Ethylbenzene	1:1	33	34
Propylbenzene	1:1	1	34
p-xylene	2:1	67.5	34
m-xylene	1:1	13.5	34
o-xylene	1:1	24	34
p-cymene	1:1	10	35

Mesitylene	2:1	69.5	34
"	1:1	39	34
Pseudocumene	2:1	36	34
"	1:1	-	34
Diphenyl	2:1	60.5	35
Diphenylmethane	2:1	90	35
Naphthalene	2:1	66	36

(c). SbI_3 Complexes with Aromatics.

AROMATIC	SbI_3 .Ar Ratio	M.P. ($^{\circ}\text{C}$)	Ref. No.
Diphenyl	2:1	161	35

The structures of these SbX_3 aromatic complexes appear to be layer-like, with layers of SbCl_3 alternating with layers of the aromatic. The separation distances between the layers are of the order of the normally accepted Van der Waals distances of about 3.5\AA . A further point of interest is that the "incipient dimer" configuration of the SbCl_3 molecules which ^{possibly} occurs in the antimony trichloride structure⁴⁵, is preserved in these aromatic complexes. SbCl bond lengths and the bond angles Cl-Sb-Cl are similar to those found in the uncomplexed molecule, 2.36\AA and 95.2° respectively. The aromatic molecules in general show no significant distortion from their uncomplexed form, in keeping with the idea of very weak dipole interaction. For X-ray structural details of some of these complexes the reader is referred to several theses of recent years⁴¹⁻⁴⁴. The structure of the complex $2\text{SbCl}_3 \cdot \text{p-xylene}$ and its comparison with the 1:1 analogue is discussed in a later chapter.

The prominent chemical feature of all these complexes, and of SbCl_3 itself, is their readiness to hydrolyse, resulting in the formation of oxychlorides. A discussion of hydrolysis in terms of structural features is deferred until a later chapter, when the nature of the bonding in SbCl_3 complexes has been examined in more detail.

Recent work with a view to examining the SbCl_3 aromatic interaction has made use of I.R., N.M.R. and E.S.R. techniques. Perkampus and Baumgarten⁴⁶ examined I.R. spectra of SbCl_3 / methylbenzene complexes and came to the conclusion

that they were not σ -type complexes.

Grechischkin and Kyuntse⁴⁷ (1963) observed shifts for Sb^{121} in N.Q.R. frequency measurements on SbBr_3 /aromatic complexes, but no significant change in Br frequencies. A similar situation was found with SbCl_3 , and the conclusion reached was that there was no significant interaction between the halogen and the aromatic, and any interaction that existed occurred between the antimony atom and the aromatic molecule. An extensive N.Q.R. study of Menshutkin complexes of SbCl_3 has been recently reported by the above workers.⁴⁸

An E.S.R. study of several aromatics in molten SbCl_3 ⁴⁹ indicated that there was significant interaction with aromatics having a low ionisation potential (e.g. tetracene, where charge transfer forces are operative), but not with simpler hydrocarbons with higher ionisation potentials like naphthalene.

From measurements of the dielectric constants of SbCl_3 in solution in benzene, p-xylene and mesitylene, Gerbier⁵⁰ concluded that the complexes formed between the trihalide and the aromatics show a polar moment due to electron transfer from the aromatic to the SbCl_3 molecule, accompanied by an induced polarisation of the acceptor molecule.

A recent N.M.R. study⁵¹ of SbCl_3 in benzene and toluene at various concentrations and at temperatures between 7°C and 70°C

suggested that rapid exchange occurs between free solvent molecules and disolvated SbCl_3 , further testimony to the

relatively weak nature of the aromatic -SbCl_3 linkages.

(v) Some Novel Packing Complexes: 'Solvated Complexes'.

Hitherto, all the packing complexes discussed have involved the packing together of a simple unliganded molecules, for example SbCl_3 and an aromatic molecule. Recently, the structures of certain compounds have been reported where the liganding species plays the dual roles of lone-pair donor and solvating molecule. This is well illustrated in the complex $[\text{C}_5\text{H}_5\text{N}]_2\text{Cu}(\text{NO}_3)_2 \cdot 2\text{C}_5\text{H}_5\text{N}$, reported by Cameron and co-workers⁵². This crystallises in the space group $\text{P2}_1/\text{c}$, with two units of $[(\text{py})_2\text{Cu}(\text{NO}_3)_2] \cdot 2\text{-(py)}$ per unit cell. The dimer $[(\text{py})_2\text{Cu}(\text{NO}_3)_2]_2$ is centrosymmetric with two bidentate nitrate-groups effecting asymmetric bridging through oxygen atoms. The second nitrate-group co-ordinates with each copper atom in chelate fashion through two oxygen atoms. Two pyridine rings are bonded trans to each copper atom, and perpendicular to the plane of the nitrate-groups. The third pyridine molecule is unbonded, and lies at a centre of symmetry, there being two such ~~pyridine molecules~~ ^{pyridine molecules} ~~pyridine molecules~~ per unit cell. This gives rise to statistical disorder of these molecules in the lattice, producing an overall "centrosymmetric average".

The trimeric nitrito-complex $[\text{Ni}(\beta\text{-picoline})_2(\text{NO}_2)_2]_3 \cdot \text{C}_6\text{H}_6$ described recently by Rogers and co-workers⁵³, is similar to the above copper complex in that the nitrito bridging groups are coplanar and the β -picoline units are bonded trans and perpendicular to the plane containing the bridging groups. Both compounds

contain solvating aromatic molecules, in the copper complex pyridine, and in the nickel complex benzene.

A further example of this type of packing is found in the complex reported by Stalick and Ibers⁵⁴, $2\text{NiBr}_3(\text{P}(\text{C}_6\text{H}_5)(\text{CH}_3)_2)_2 \cdot \text{NiBr}_2(\text{P}(\text{C}_6\text{H}_5)(\text{CH}_3)_2)_2 \cdot 2\text{C}_6\text{H}_6$. This crystallises in the space-group $\overline{P}1$, the NiBr_2L_2 ($\text{L}=\text{P}(\text{C}_6\text{H}_5)(\text{CH}_3)_2$) molecules being at a centre of symmetry with one molecule per unit cell, the NiBr_3L_2 and benzene molecules lying in general positions with two molecules of each per unit cell. The structure basically consists of alternate layers of NiBr_2L_2 and NiBr_3L_2 , with benzene molecules packing in holes between NiBr_2L_2 units and lying in the NiBr_2L_2 layers rather than the NiBr_3L_2 layers. The NiBr_2L_2 units is square planar and centrosymmetric about nickel. The NiBr_3L_2 is trigonal bipyramidal with equatorial halogens.

Powell and co-workers have recently investigated an addition compound⁵⁵, $\text{LiI}(\text{OP}(\text{C}_6\text{H}_5)_3)_4 \cdot \text{OP}(\text{C}_6\text{H}_5)_3$. This complex crystallises in space group $\text{Pna}2_1$. The lithium ion is co-ordinated tetrahedrally through oxygen to four triphenylphosphine oxide groups. Iodide ions are more than 8.5\AA away from the lithium ions. The fifth triphenylphosphine oxide unit is unbonded to any other molecule, being more than 9\AA from the nearest lithium ion and over 8\AA from the nearest iodide ion. This fifth unit is therefore playing the role of an "included" or "solvating" species.

Further examples of this type of inclusion complex are those formed by Ni(II) with methylpyrazine⁵⁶ and with certain α -arylalkylamines⁵⁷. These have seven ligand species per nickel atom and are explained by having an octahedrally-co-ordinated metal atom with the remaining ligand species occupying a packing position.

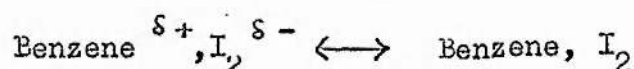
Another packing complex of the above type is that reported by Drew and co-workers⁵⁸. This is the complex $[\text{PyH}^+][\text{TlI}_4^-] \cdot \text{Py}$. ~~Py~~ (where py = pyridine). The compound crystallises in the space group $P2_1/C$ with four $[\text{PyH}][\text{TlI}_4] \cdot \text{py}$ molecules per unit cell. The anion is tetrahedral. It has not been possible for the authors to distinguish between the 'solvating' pyridine molecule and the pyridinium ion, but they have suggested that the molecule with the higher of the two average ring temperature factors (7.6 and 10.8) corresponds to the pyridine of solvation. The authors do not specify that there is no interaction between the two pyridine rings; for example a hydrogen bonded cation $(\text{py}-\text{H}---\text{Py})^+$ may occur in the structure, analogous with the $(\text{Py}-\text{I}-\text{Py})^+$ ion which is known. However, in that they call one ring a 'molecule of solvation' it is assumed that it has a purely packing role. No co-ordinates are published at the time of writing.

Charge Transfer Complexes.

The halogen/aromatic system (in particular with benzene) affords a classical and long-investigated charge-transfer system.

Benezi and Hildebrand's early studies⁵⁹ of solutions of iodine in benzene (in which they observed the formation of a brown colour), led them to postulate association between the benzene and iodine molecules. The aromatic was said to behave as a π -donor and the halogen as an acceptor.

Mulliken (1950)⁶⁰ proposed a charge-transfer type interaction with the diatomic axis lying parallel to the aromatic plane. Ferguson⁶¹ (1956) found that the complex had hexagonal symmetry, with the diatomic axis perpendicular to the ring and directed to its centre at a distance of 3.4 Å away. Benezi and Hildebrand considered this interaction between halogen and aromatic to be essentially a Lewis acid - Lewis base type of association, while Mulliken's description emphasised the charge-transfer nature of the forces involved, in terms of a resonance of the type:



Mulliken's views on the relative contributions of charge-transfer and dipole-dipole forces in the I_2 /benzene complex need to be modified somewhat in the light of recent studies by several workers, among them Hanna and Williams⁶². After I.R. investigations they have come to the conclusion that the interaction making the dominant contribution to the observed I.R. shifts is the benzene-quadrupole halogen-induced dipole interaction. Charge-transfer interactions are not as important in determining the ground state properties of these compounds as had previously been supposed, and electrostatic forces are by no means negligible.

The same comments apply to the ICl/benzene system, except that ICl has, additionally, a permanent dipole.

Pyridine also forms complexes with iodine and iodine monochloride, and Person and co-workers have conducted I.R. studies of these complexes⁶³. They have concluded from these that charge-transfer contributions were much greater in ICl complexes than in the corresponding I_2 complexes. Further, ICl complexes are more stable than I_2 complexes with pyridine because of the dipole-induced dipole forces arising from the permanent dipole of ICl.

Mulliken and Person⁶⁴ have found that the ionisation potential of the donor for the systems I_2 /aromatic and I_2 /aromatic amine is linearly related to the energy, $E (=h\nu_{c.t.})$, of the charge-transfer band.

A novel pyridine/iodine complex (pyridine. $2I_2$) has been reported by Hassel and co-workers⁶⁵. This is composed of $[Py - I - Py]^+$ units, I_3^- ions and I_2 molecules, the N - I - N configuration of the cation being linear.

Carbon tetrabromide can form a 1:1 complex with p-xylene⁶⁶, in which the intermolecular association is attributed to charge-transfer. The p-xylene π - system donates electrons to low-lying d- orbitals of the halogen. Half of the bromine atoms are directed to the centres of the aromatic rings and lie 3.34\AA from the ring centres and 3.62\AA from the nearest carbon atom. There is a bromine atom on either side of each aromatic ring.

The distance of 3.62Å between halogen and ring carbon is compatible with Van der Waals forces, and the validity of invoking charge-transfer for this particular intermolecular association is doubtful. A table of the relevant intermolecular distances in some charge-transfer complexes is given below (Table 2).

TABLE 2		
Complex	Intermolecular Distance(Å)	Ref. No.
$\text{CBr}_4 \cdot \text{p-xylene}$	Br-Aromatic = 3.54 *	66
Benzene. Cl_2	Cl-Aromatic = 3.28 *	67
Benzene. Br_2	Br-Aromatic = 3.36 *	67
1,4 - dioxan. Br_2	O - Br = 2.71	68
1,4 - dioxan. ICl	O - I = 2.60	68
Acetone. Br_2	O - Br = 2.82	69
Pyridine. ICl	N - I = 2.26	63
Pyridine. I_2	N - I = 2.16	63

* Distances to aromatic ring centres.

Wallwork has coined the term "polarisation" bonded complex⁷⁰ for a group of molecular complexes in which the interactions between molecules are weak (charge-transfer or Van der Waals) and the components are polarising and polarisable units. Polarisation complexes are typified by compounds between two aromatic components, in which the structure consists of plane-to-plane stacking of the rings, resulting in overlap of the π -orbitals of the component molecules. The table below (Table 3)

summarises the relevant details for a few such complexes.

TABLE 3.

Complex	Ratio	Perpendicular Sepn. (Å)	Ref. No.
Anthracene - s - nitrobenzene	1:1	3.29	71
Hexamethylbenzene-chloranil	1:1	3.51	72
Phenol-p-benzoquinone	2:1	3.33	73
Pyrene -1,3,5,7-tetramethyl- uric acid	1:1	3.40	74

While charge-transfer has been suggested as a significant contribution to SbCl_3 interaction with polycyclic aromatics such as tetracene and perylene, there is no fully convincing evidence to indicate that it plays a significant part in bonding in SbCl_3 complexes with simpler aromatics such as substituted benzenes.

Donor-Acceptor Complexes of Antimony trichloride.

Antimony trichloride is known to act as an acceptor. The antimony atom can expand its octet from a Sp^3 tetrahedral configuration to a Sp^3d trigonal bipyramidal hybrid, accommodating a donated lone-pair from one ligand, and even further to Sp^3d^2 (octahedral), accommodating two ligands.

Kinell, Lindquist and Zackrisson⁷⁵ have examined the system $\text{SbCl}_3 - \text{POCl}_3$ in which an oxygen lone-pair is donated to SbCl_3 . Zackrisson and Alden⁷⁶ report the donor acceptor complexes $\text{SbCl}_3 \cdot \text{Me}_3\text{PO}$ and $\text{SbCl}_3 \cdot 2\text{Me}_2\text{CO}$. Menshutkin⁵⁶ in 1912 prepared

several SbCl_3 complexes with potential donors such as aniline. These included the complexes $\text{SbCl}_3 \cdot 6\text{PhNH}_2$, $\text{SbCl}_3 \cdot 4\text{PhNH}_2$, $\text{SbCl}_3 \cdot 3\text{PhNH}_2$, $\text{SbCl}_3 \cdot 2\text{PhNH}_2$, (where PhNH_2 = aniline). The latter complex and the complex $\text{SbCl}_3 \cdot \text{PhNH}_2$ have subsequently been confirmed as donor-acceptor type compounds by the X-ray analysis of Scruton⁷⁷. The 1:1 complex crystallises in the space-group $P2_1/C$ and has a trigonal bipyramidal configuration with an equatorial lone-pair. The 1:2 complex crystallises in the space-group Cm and has a distorted octahedral configuration with cis ligands.

Holmes and Bertaut⁷⁸ have characterised amine and phosphine complexes of SbCl_3 . They report the compounds $\text{SbCl}_3 \cdot \text{Me}_3\text{N}$, $\text{SbCl}_3 \cdot \text{Et}_3\text{N}$, $\text{SbCl}_3 \cdot 2\text{Et}_3\text{N}$, $\text{SbCl}_3 \cdot 2\text{Me}_3\text{P}$ (where Me = methyl group)

Antimony trichloride displays two modes of intermolecular association, a Van der Waals type or dipole interaction as with aromatic π -systems, or a donor-acceptor interaction in which it expands its octet by accepting a lone-pair. The possibility arises of studying these two types of interaction in competition with each other by including both functions (the aromatic π -system and the donor-lone-pair) in the same molecule. To this end, the complexes of SbCl_3 with aniline were examined structurally by Scruton. In the present work, aniline is replaced by pyridine in an extension of this competitive study of the π -system and lone-pair interactions with SbCl_3 . It affords, in addition, a comparative study of aniline and pyridine as ligands with respect to SbCl_3 .

SbCl_3 /pyridine complexes which have been reported are appended in the table below (Table 4.)

TABLE 4.

COMPLEX	REFERENCE NO.
$\text{SbCl}_3 - \text{C}_5\text{H}_5\text{N}$	79
$2\text{SbCl}_3 - 3\text{C}_5\text{H}_5\text{N}$	80
$[2\text{SbI}_3 - 3\text{C}_5\text{H}_5\text{N}]$	81
$\text{SbCl}_3 - 2\text{C}_5\text{H}_5\text{N}$	82
$\text{SbCl}_3 - 3\text{C}_5\text{H}_5\text{N}$	83
$2\text{SbCl}_3 - \text{C}_5\text{H}_5\text{N}$	This Work

CHAPTER I

A). The p-xylene - SbCl_3 System.

I). Purification of Materials.

In view of the existence of o- and m-xylene/ SbCl_3 complexes, the A.R. p-xylene was fractionally frozen in ice several times to remove traces of o- and m-xylene (f.p. of o-, m-, p-xylene: -25.2°C , -47.9°C , 13.2°C respectively). The purified p-xylene was finally checked for traces of o- and m-xylene by examining its I.R. spectrum for characteristic peaks.

Carbon tetrachloride (commercial grade) was dried by standing over calcium hydride (lab. rgt. grade) for several hours. It was then distilled from the calcium hydride. No further purification was carried out.

Chloroform (commercial grade) was dried by standing for a few hours over phosphorus pentoxide (L.R. grade) and then distilling off from the P_2O_5 reagent.

Antimony trichloride (L.R. grade) was recrystallised three times from dried chloroform. Decantation of solvent from crystals and bottling of crystals were carried out in a dry box.

2.) Preparation of the complex $2\text{SbCl}_3 \cdot \text{p-xylene}$.

The hygroscopic nature of SbCl_3 and its complexes with p-xylene make it necessary to carry out all preparative work under rigorously dry conditions in a dry box. A crystallographic

dry-box, with a microscope mounted through the top, was constructed for this purpose. The drying agent used was phosphorus pentoxide.

The preparation was carried out in a small conical flask (10 ml.). About 0.3 ml. p-xylene was added to about 0.25 g. antimony trichloride and the two components melted together. No solvent system was used. It was found, however, that a diluent was needed to prevent rapid solidification of the mass, and to allow crystallisation to take place⁴¹. Accordingly, a small volume (less than 0.5 ml.) of carbon tetrachloride was added while the components were being melted. It appears that the ratio of components present is not critical for production of reasonable crystals of 2:1 complex, so long as an excess of SbCl_3 is present. Slow cooling yields crystals of suitable size and quality. The 2:1 complex crystallises as rather flat needles, and optical examination through crossed polars showed extinction along the needle (a) axis. The b axis is perpendicular to the larger face of the "plate-like" needle and c lies in the plane of the plate.

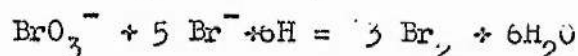
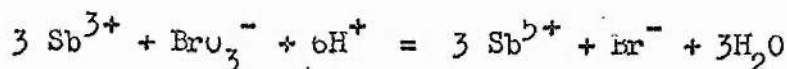
Because of the hygroscopic nature of these crystals, it was necessary to mount them in Lindemann glass tubes (0.5 m.m. in diameter) prior to x-ray photography.

3.) Analysis and Density.

Analysis for antimony was carried out by dissolving 0.05g.

of the sample in concentrated hydrochloric acid and titrating against N/10 potassium bromate, using methyl red indicator.

The reaction is as follows:-



The end-point corresponds to the production of a colourless solution when the indicator is bleached by the bromine produced by an excess of bromate.

The analysis for antimony gave a result corresponding to the ratio 2SbCl_3 .p-xylene (1.94:1)

Flotation of the crystals in a mixture of chloroform ($\rho=1.49$) and ethyl iodide ($\rho=1.93$) gave a value of 1.55 for the density of the complex. (Calculated $\rho = 1.582$ for 2SbCl_3 .p-xylene).

B) The Pyridine - SbCl_3 System

1) Purification of Materials.

Pyridine (L.R. grade) was dried with potassium hydroxide pellets from which it was separated by distillation. No further purification was carried out.

The chloroform solvent and antimony trichloride were treated in the same way as for the p-xylene system.

2a) Preparation of the Complex $2\text{SbCl}_3 - 3\text{C}_5\text{H}_5\text{N}$.

Addition of about 0.3 ml. pyridine dropwise into a cold saturated solution (about 2 ml.) of antimony trichloride

in chloroform yields a mass of minute, colourless crystals.

If this material is redissolved in an excess of dry chloroform and the resultant solution allowed to cool, fibrous, colourless needles of the complex $2\text{SbCl}_3 \cdot 3\text{C}_5\text{H}_5\text{N}$ are deposited. Alternatively, slow addition of the same quantity of pyridine to about 2 ml. of a warm saturated SbCl_3 solution, followed by slow cooling, deposits the 2:3 complex. The compound is very hygroscopic and was prepared in a dry-box. A suitable crystal was sealed in a 0.5 m.m. Lindemann glass tube prior to photography.

Optical examination between crossed polars showed extinction along the direction of the needle (c) axis. The a and b axes lie perpendicular to the needle axis and are themselves mutually perpendicular.

2b) Analysis and Density.

The potassium bromate method for the estimation of antimony gave results which varied from sample to sample. The range was from 30% to 50% approximately. 31.3% corresponds to a composition of $\text{SbCl}_3 \cdot 2$ pyridine, and 45.4% corresponds to $2\text{SbCl}_3 \cdot \text{pyridine}$.

The measured density, 2.30, (obtained by flotation of single crystals in a chloroform ($\rho=1.499$)/bromoform ($\rho=2.89$) mixture) did not allow a rationalisation of the cell volume in terms of an acceptable number of SbCl_3 and pyridine molecules in the unit cell.

The results of the analysis and the density measurements are most obviously explained by contamination of the complex

with free SbCl_3 . The correct ratio was only inferred on interpretation of the 3-D Patterson map. (see P. 69)

3a) Preparation of the Complex $\text{SbCl}_3 \cdot \text{C}_5\text{H}_5\text{N}$.

If a large excess of pyridine (about 3 ml.) is added rapidly to about 1 ml. of a warm saturated solution of SbCl_3 in chloroform, and the solution allowed to cool slowly, colourless, tabular crystals of the 1:1 complex are deposited after a few hours. Alternatively, if a warm saturated solution of SbCl_3 in pyridine is allowed to cool slowly, crystals of the 1:1 complex are deposited.

These crystals are very hygroscopic and must be prepared in a dry-box and mounted in Lindemann glass tubes for photography. In shape, they are square plates. On optical examination through crossed polars, they showed straight extinction. The b axis is parallel with one extinction direction, the c axis with the other. The a axis lies inclined at an angle of about 60° with the plane of the plate.

3b) Analysis and Density.

Again, analysis and density measurements are inconsistent, and the ratio was inferred from the interpretation of Patterson projections (see P. 89).

Analysis for antimony using the potassium bromate method gave values ranging from 24% to 30% (26.0% corresponds to a 1:3 SbCl_3 /pyridine ratio, and 39.4% to a 1:1 ratio).

Analysis for pyridine using a quantitative U.V. method and making measurements on a characteristic peak at $255\text{ m}\mu$ gave a value of 48.9% pyridine. This corresponds most closely to the ratio $\text{SbCl}_3 \cdot 3$ pyridine (calculated : 51.0% pyridine). 1:1, 25.8% py.

Flotation of single crystals in a mixture of chloroform ($\rho = 1.499$) and ethyl iodide ($\rho = 1.93$) gave a value of 1.49 for the density of the complex. (Calculated for $\text{SbCl}_3 \cdot 3$ pyridine = 1.470). 1:1, 1.70.

4a) Preparation of the Complex $2\text{SbCl}_3 \cdot \text{C}_5\text{H}_5\text{N}$.

Rapid addition of about 0.3 ml. pyridine dropwise into a warm saturated solution (about 1.5 ml.) of SbCl_3 in chloroform yields a mass of minute crystals which are very hygroscopic. They are colourless and needle-shaped.

Optical examination showed that extinction occurred in the direction of the needle axis, b.

4b) Analysis and Density.

Analysis of the complex for pyridine by a quantitative U.V. method gave 15.8% pyridine (calculated : 14.8% pyridine for $2\text{SbCl}_3 \cdot \text{pyridine}$). About 0.04g. of the complex was dissolved in about 2 ml. of concentrated hydrochloric acid and made up to be about 0.01N in HCl. Measurements were made on a peak at $255\text{ m}\mu$.

Flotation in a mixture of carbon tetrachloride ($\rho = 1.63$) and bromoform ($\rho = 2.89$) gave a value of 2.34 for the density of the material (calculated for $2\text{SbCl}_3 \cdot \text{pyridine} = 2.34$).

5a) Preparation of an Air-Stable Hydrolysis Product, Q, from Pyridine and Antimony Trichloride.

About 0.5 ml. pyridine was added dropwise to a warm saturated solution (about 3 ml.) of SbCl_3 in chloroform, and the addition was carried out in the atmosphere. The clear liquid was decanted from the white precipitate of oxychloride. Crystallisation from this decanted solution apparantly produced a mixture of compounds, mostly microcrystalline.

A single crystal was picked out and its composition was determined only as a result of its structure being elucidated from X-ray diffraction data. This is discussed in Chapter III .

5b) Analysis and Density.

Analysis for antimony using the potassium bromate method gave a value of 44.6% Sb.

Analysis for chlorine by titrating conductimetrically against N/10 AgNO_3 (using silver and glass electrodes) gave a value of 37.9% Cl. 0.04g of complex was boiled in 5N-NaOH for $\frac{1}{2}$ hour. The cooled solution was titrated as above.

Pyridine was estimated using the quantitative U.V. method described in previous sections. This gave a value of 13.6% pyridine. Tabulated below are these measured values and the percentage compositions of some possible complexes:

	%Sb	%Cl	% $\text{C}_5\text{H}_5\text{N}$
Found	44.6	37.9	13.6
Calc. ($2\text{SbCl}_3 \cdot \text{Pyridine}$)	45.5	39.8	14.7
Calc. ($\text{SbCl}_4^- \text{Pyridinium}^+$)	35.6	41.5	23.2

Flotation of crystals in a mixture of carbon tetrachloride ($\rho=1.63$) and bromoform ($\rho=2.89$) gave a value of 2.31 for the density of the material. (calculated : 2.34 for $2\text{SbCl}_3\text{pyridine}$).

2.11 " $\text{pyH}^+\text{SbCl}_4^-$.

CHAPTER II

CONSTRUCTION OF A LOW-TEMPERATURE X-RAY APPARATUS

Low Temperature Crystallography

The thermal parameter, B, is a function of temperature such that a lowering of the temperature of the crystal results in a decrease in the magnitude of B. The electron density function in terms of the positional atomic parameters is modified by a function $\exp(-B \sin^2 \theta / \lambda^2)$ to make allowance for temperature effects. The lower the value of B, the higher the magnitudes of the electron density maxima. A sharper resolution of the electron density maxima is obtained. In physical terms, a lower temperature results in a decrease in the molecular vibrations. The effect of a temperature decrease is felt relatively to a greater degree by the lighter atoms which at room temperature have, in general, higher temperature factors.

Another important aspect of low temperature work lies in the increased stability at low temperatures of an unstable crystal to decomposition through hydrolysis or oxidation.

Description of the Apparatus

The basic model for the apparatus is similar to that described by Altona⁸⁹, in that it consists of a system of two dewars, a large storage dewar and a small 'transfer' dewar. The complete apparatus is shown in Fig. 2.

The Storage Dewar.

The main dewar (25 l. capacity) is adapted to blow liquid air through an insulated pipe into the small 'transfer' dewar. The 25 l. dewar is fitted with a brass collar which holds in place a brass plate. A flat cork ring between the brass plate and the rim of the dewar effects a satisfactory seal when the collar is screwed down. Soldered through this plate are two pipes, one for the transfer of liquid air and the other terminating in a valve. This valve is activated by the level controlling thermistor in the transfer dewar. When the level in the transfer dewar drops below the thermistor, the valve is shut and a heater (10W.) in the storage dewar is switched on. The liquid air boils and the resultant build up of pressure forces the liquid into the transfer dewar. After the transfer dewar is filled (i.e. the level in the transfer dewar reaches the level of the thermistor), the valve is opened again and the heater in the main dewar switched off. This releases the pressure in the main dewar, stopping the filling process.

The main dewar is also fitted with a safety valve (ball-and-spring type) which is adjusted to open at a pressure slightly above that at which the filling process operates.

The Transfer Dewar

This is, in essence, a small dewar vessel (of about 150-200 ml. capacity) with a double-walled, evacuated side-arm. This side-arm is designed to fit into a former which runs concentrically inside a layer-line screen of the Weissenberg camera. The former consists of two asbestos rings with an external diameter equal to the internal diameter of the layer-line screen, and its purpose is to centre the side-arm so that the flow of cold air is directed at the mounted crystal.

Liquid air is delivered through an insulated funnel into the dewar. This funnel, and the wires for the heater (10 W.) and thermistor pass through a "Teflon" lid. Sunk into this lid is a cork ring, and the lid is screwed down onto the box containing and protecting the dewar. The dewar rim makes contact with the cork ring, the seal being made air-tight by the pressure effected by screwing down the lid.

Measurement of Temperature

The temperature in the vicinity of the crystal is measured by means of a copper/constantan thermocouple with one junction at room temperature and the other placed at the mouth of the delivery tube inside the Weissenberg camera (about 2 cm. from the end of the Lindemann tube or glass fibre mounting). The temperature is read directly from a specially calibrated milliammeter (graded in $^{\circ}\text{C}$) in conjunction with an amplifier.

Heating Screens

In order to prevent condensation of moisture on the layer-line screens, with subsequent freezing, cylindrical heating elements are inserted inside the screens, one for each of the two screens⁴¹. These elements consist of two thin layers of fibre-glass with the heating ribbon "sandwiched" between them and the whole shaped into a uniform cylinder of external diameter equal to the internal diameter of the layer-line screens. An additional heating coil is situated around the end of the tube delivering cold air inside the camera. The power through all three heating elements is adjustable by means of variacs, the two heating screens operating at about 15-20 W. and the coil at about 5-6 W. when the working temperature at the crystal is of the order of -120°C .

Operation and Results

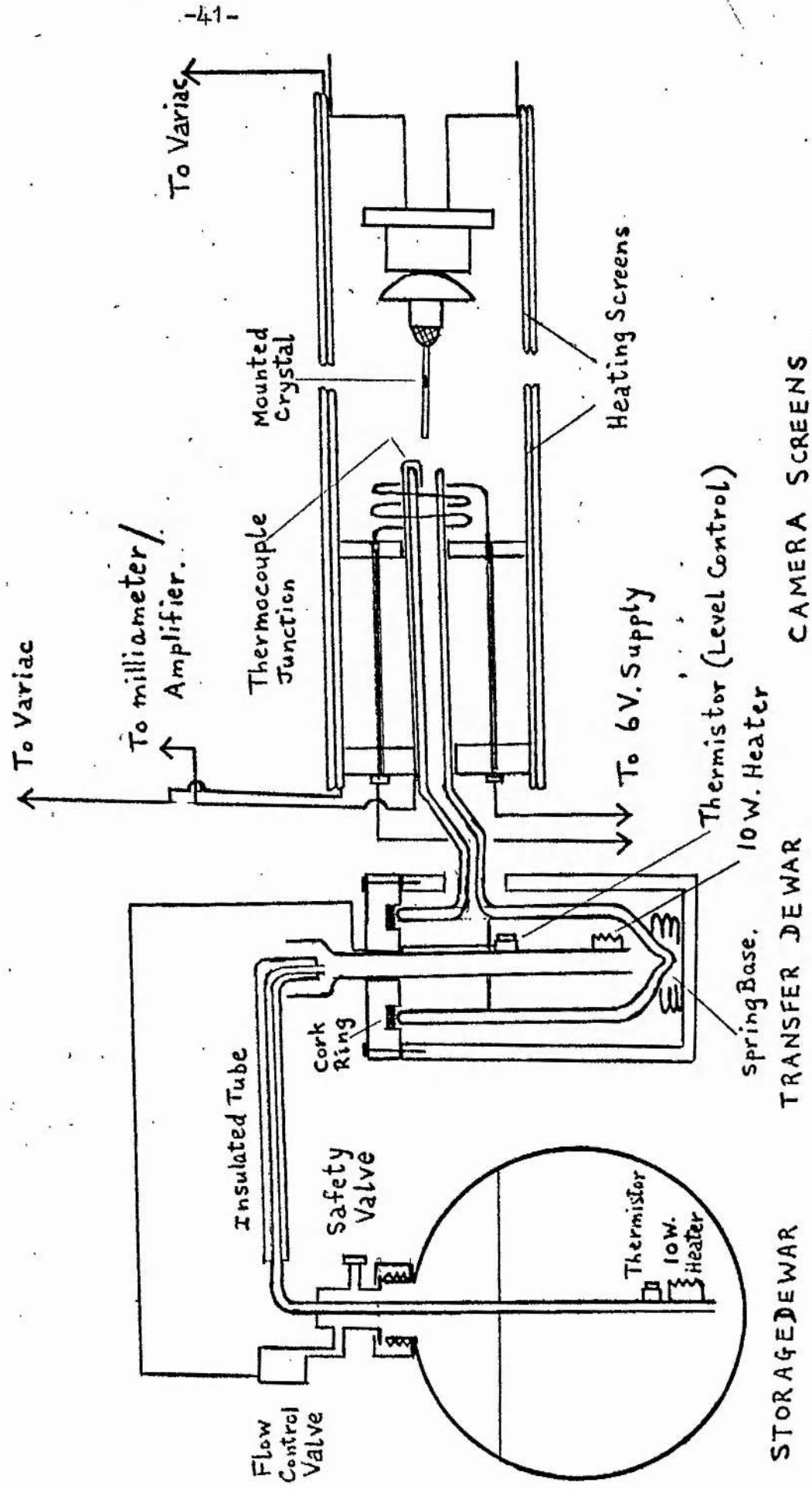
The present apparatus has a high liquid air consumption, about 2.5 l. per hour. With a simple single-dewar apparatus it was possible to achieve consumption rates as low as 1 l. per hour.

The temperature at the end of the delivery pipe is varied

by varying the rate of boiling of the liquid air in the transfer dewar (i.e. by varying the power through the heater by means of a variac). A minimum temperature of the order of $-120 \pm 5^{\circ}\text{C}$ at the end of the delivery tube is possible with the existing apparatus. The temperature at the crystal is about 10°C higher than that at the end of the delivery tube.

With the above apparatus limited low temperature data (-110°C) has been obtained from single crystals of the complex $\text{SbCl}_3 \cdot \text{C}_5\text{H}_5\text{N}$.

Fig. 2 - LOW TEMPERATURE X-RAY APPARATUS.



CHAPTER III
Identification of the Air Stable Hydrolysis Product, Q,
of the SbCl_3 /Pyridine System.

Amongst the oxychlorides of antimony another product has been identified in the presence of pyridine which proved to be pyridinium tetrachloroantimonate.

Identification of one crystal was made by virtue of a partial structural analysis.

Determination of Cell Dimensions and Space Group.

The cell dimensions were measured from X-ray film data collected using zirconium-filtered $\text{MoK}\alpha$ radiation. c was measured from a 15° oscillation photograph. a , b , were measured (using the axial reflections only) from a zero level Weissenberg photograph about c . A film measuring device, incorporating a sliding Vernier millimetre scale, was used. The angle β was measured from a zero layer Weissenberg photograph about b . The cell dimensions are summarised in Table 5.

The oscillation photograph about a showed no symmetry above and below the zero layer, but that about b did show such symmetry. The zero level Weissenberg about a showed symmetry across the axes. The combined symmetry of the oscillation photographs showed that the system was monoclinic, and this was confirmed by the symmetry of the $0kl$ and lkl Weissenberg photographs.

The following systematic absences were noted:

hkl , when $(h+k) = 2n+1$, indicating centring on the C face.

$h0l$, when $l = 2n+1$, indicating a c glide perpendicular to b .

TABLE 5

From 15° Oscn. Photo about c:

n	Sn (mm.)	Sn	ξ_c
±2	11.15±0.1	$S_2=0.1911\pm0.0017$	0.0955 ± 0.0008
±4	23.65±0.1	$S_4=0.3816\pm0.0017$	0.0954 ± 0.0004

Jacobson's &
Porter's (Å)

C (Å)

Mean ξ_c
 0.0955 ± 0.0006
 0.0954 ± 0.0003
7.44±0.04
7.48±0.01

From hko Weissenberg Photo:

n	Sn (mm.)	Θ_n°	$\xi_n (=2 \sin \Theta_n)$
±2	7.35±0.1	3.67±0.05	$\xi_2=0.1279\pm0.0018$
±4	14.80±0.1	7.40±0.05	$\xi_4=0.2576\pm0.0018$
±6	22.20±0.1	11.10±0.05	$\xi_6=0.3850\pm0.0018$
±8	29.65±0.1	14.82±0.05	$\xi_8=0.5115\pm0.0016$
±2	6.25±0.1	3.12±0.05	$\xi_2=0.1087\pm0.0018$
±4	12.50±0.1	6.25±0.05	$\xi_4=0.2177\pm0.0018$
±6	18.80±0.1	9.40±0.05	$\xi_6=0.3267\pm0.0018$
±8	25.20±0.1	12.60±0.05	$\xi_8=0.4363\pm0.0016$

 ξ Mean ξ

Axes a, b (Å)

J. & P. (Å)

 $\xi_a=0.0639\pm0.0009$ $\xi_a=0.0644\pm0.0005$ $\xi_a=0.0642\pm0.0003$ $\xi_a=0.0639\pm0.0002$ $\xi_a=0.0641$ $\xi_a \pm 0.0005$

a=12.92±0.02

a=13.12

±0.07

 $\xi_b=0.0544\pm0.0009$ $\xi_b=0.0544\pm0.0005$ $\xi_b=0.0544\pm0.0003$ $\xi_b=0.0545\pm0.0002$ $\xi_b=0.0544$ $\xi_b \pm 0.0005$

b=13.07

±0.10

b=12.83±0.02

From h0l Weissenberg Photo (β^*)

Mean Sn" (⊥ dist. between axes) (mm.)	Angular Dist. (Sn $\sqrt{5}/2$) (mm.)	β^*	β	J. & P.
25.78±0.1	28.94±0.11	57°41'±13'	122°19'±13'	$\beta=122^\circ 24' \pm 12'$

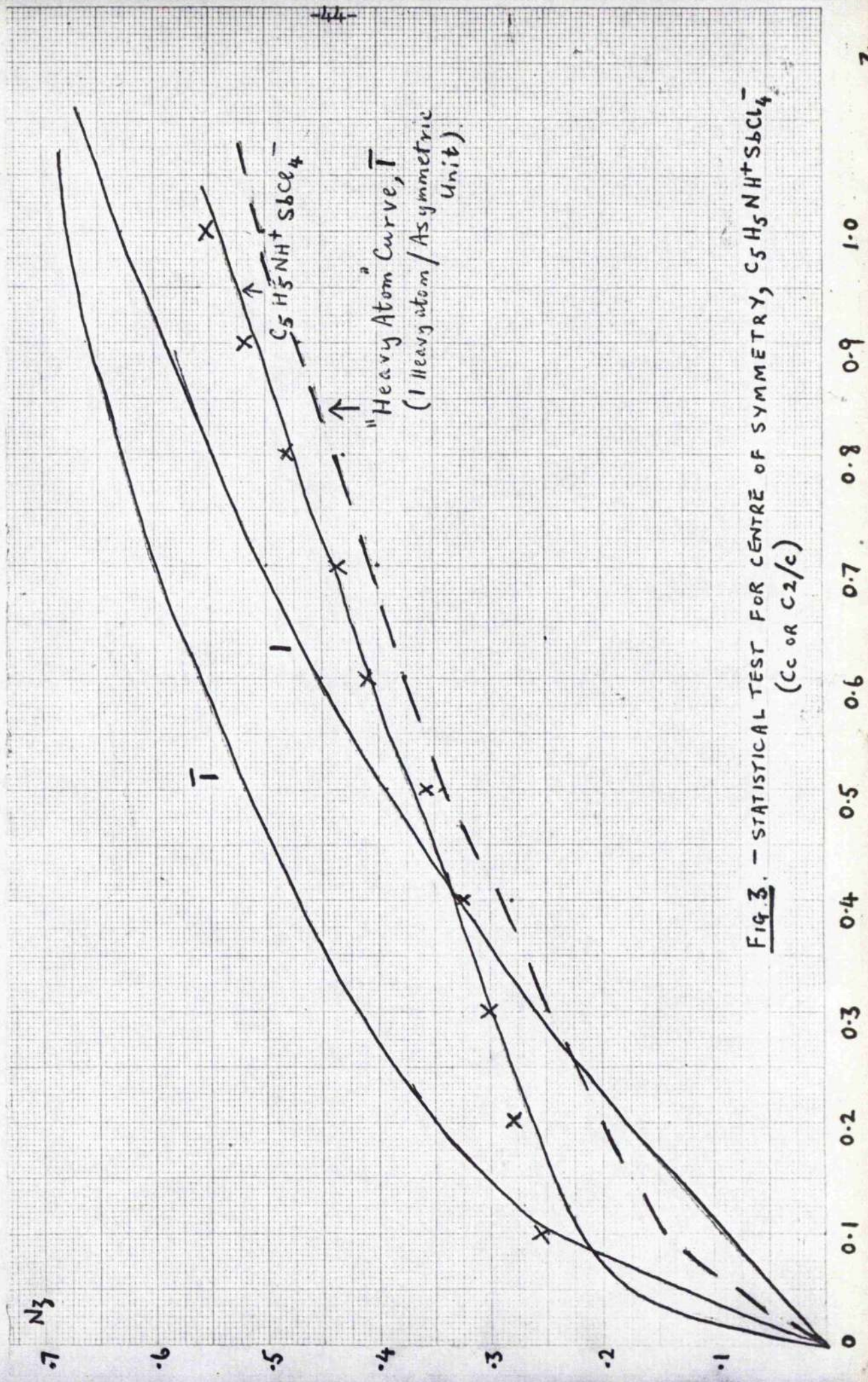


FIG. 3. - STATISTICAL TEST FOR CENTRE OF SYMMETRY, $C_5H_5NH^+SbCl_4^-$
(C_c OR $C_{2/c}$)

From these absences it was deduced that the space group was either Cc or C2/c. A statistical test for a centre of symmetry using a programme written for the purpose and calculating Nz at values of z from 0 to 1 suggested that a centre was probably present.

The result is summarised in a graph (fig.3). A curve for the 'heavy atom' case is also given⁸⁶.

Partial Determination of the Structure.

Three-dimensional intensity data (layers h0l to h8l) was collected using Zirconium-filtered MoK α radiation. A two-film pack was employed, and a total of 355 independent reflections was obtained. Intensity measurements were made from the films using a calibrated intensity wedge. After Lorentz and Polarisation corrections had been applied, the layers were placed on an arbitrary relative scale by reference to cross-level (0kl, lkl) data. No absorption corrections were applied. A three-dimensional Patterson map was computed.

The Patterson map was initially interpreted in terms of space group C2/c with antimony in a general 8 fold position. An electron density map (C2/c) phased on this antimony position revealed an unacceptable configuration of chlorine atoms about the "heavy" atom. At this stage the R-factor was 33%, and no reduction occurred on inclusion of these "chlorine positions".

A model revealed that eight antimony atoms in the unit cell gave rise to untenable intermolecular vectors on inclusion of the

indicated chlorine atoms. It was then found possible to interpret the three-dimensional Patterson map in terms of four antimony atoms per unit cell by considering previously supposed Sb-Sb vectors as Sb-Cl vectors. Accordingly, the space group Cc was adopted to accommodate this situation and to avoid recourse to the placing of antimony in a special position in the space group C2/c.

A three-dimensional electron density map phased on antimony alone (in space group Cc) revealed two possible chlorine positions. Inclusion of the two chlorine atoms resulted in an acceptable R-factor (20%), and indicated two further possibilities for chlorine positions. Inclusion of these further atoms resulted in an R-factor of 19% and revealed a possible position for a pyridine ring. In these initial stages, the atoms co-ordinated to antimony were considered to be chlorine atoms primarily on the basis of the Sb-X bond distances and on the basis of relative peak heights in the electron density map.

At this stage the identity of the hydrolysis product emerged as $C_5H_5NH^+SbCl_4^-$. Further least squares refinement of the structure was abandoned since it was discovered that the X-ray structure analysis of the compound had been performed by Porter and Jacobson (Porter S.K., Jacobson R.A., J. Chem. Soc., 1358, 1970). The above authors had obtained the best refinement in terms of the space group C2/c with antimony in a special position on the two-fold axis. This two-fold symmetry about antimony was emerging in the

electron density maps phased in space group Cc, both in terms of the chlorine peak heights and in terms of the Sb-Cl distances and chlorine positions.

The cell dimensions obtained by Porter and Jacobson are given and compared in Table 5.

The R-factor for limited film data (355 reflections) using the final co-ordinates of Porter and Jacobson in space group C2/c is 9.5% (cf. Porter's and Jacobson's diffractometer data which gave 3.8%). Comparison of the above authors' diffractometer data with the present film data gave an R-factor ($= \sum |F_{\text{film}} - F_{\text{diff}}| / \sum F_{\text{film}}$) of 9.9%. This is of the order of magnitude to be expected for such a comparison. A listing of the relevant structure factors is to be found in Appendix II.

Three independent Sb-Cl distances are found in the SbCl_4^- anion, 2.38 Å, 2.64 Å and 3.13 Å. The latter two distances are associated with bridging halogen atoms. By virtue of this bridging, antimony achieves octahedral co-ordination and the anion takes the form of an infinite chain. All angles Cl-Sb-Cl are close to 90° . The essential features of the structure are illustrated in figure 4. (taken from Porter and Jacobson).

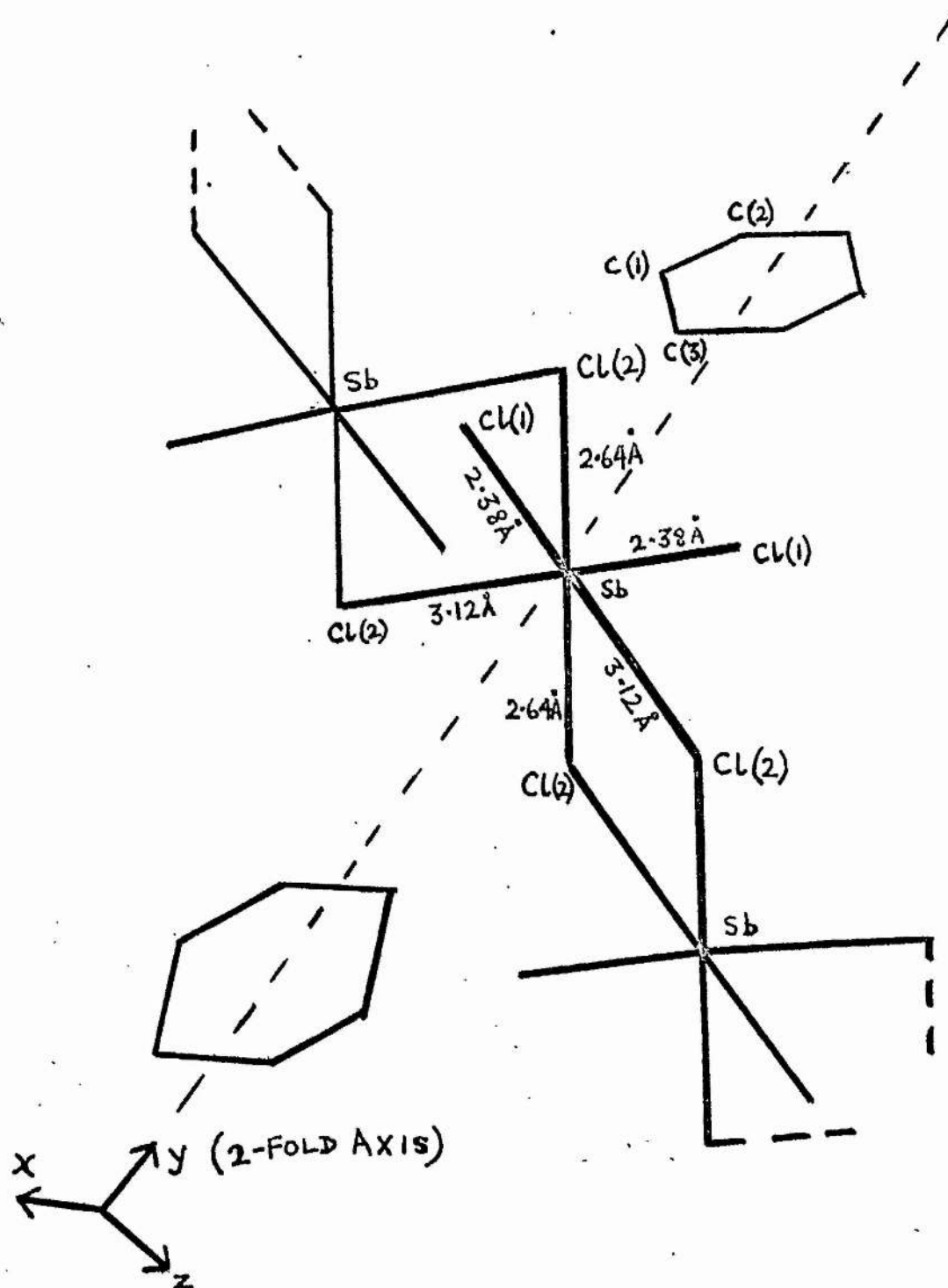


Fig. 4 - Structure of SbCl_4^- anion in pyridinium tetrachloroantimonate.

CHAPTER IV

The Structure of the Complex $2\text{SbCl}_3 \cdot \text{p-xylene}$ at -110°C

Determination of Cell Dimensions and Space Group

A 15° oscillation photograph (zirconium-filtered $\text{MoK}\alpha$ radiation) about the a axis showed no symmetry above and below the zero layer-line, indicating that the crystal belonged either to the triclinic or the monoclinic system. A zero-layer $\text{MoK}\alpha$ Weissenberg photograph about a showed symmetry across each of two possible axes which were 90° apart. In the first level Weissenberg photograph about this same axis there is symmetry across only one of these (c) axes. The combined symmetry of the oscillation and Weissenberg photographs indicated that the lattice was 'monoclinic.

The systematic absences in the intensity data were as follows:

hkl: no conditions, indicating a primitive cell;

h0l when $l = 2n + 1$, indicating a c glide perpendicular to b;

oko when $k = 2n + 1$, indicating a 2_1 screw axis parallel to b.

The space group is thus $\text{P}2_1/\text{c}$ (No.14). There are two units of $2\text{SbCl}_3 \cdot \text{p-xylene}$ per unit cell, with the p-xylene necessarily lying around a special two-fold position (at a centre of symmetry).

Low temperature ($-110 \pm 10^\circ\text{C}$) cell dimensions were measured from photographs taken using zirconium-filtered $\text{MoK}\alpha$ radiation. The measurements were made using a film measuring device incorporating a sliding millimetre vernier scale. ζ_a and β^* were measured from an hol Weissenberg photograph, while ζ_b, ζ_c were measured from an okl photograph. Room temperature cell dimensions were also measured from Mo data. ζ_a was obtained from a 15° oscillation photograph about a , and ζ_b, ζ_c from an Okl Weissenberg photograph. β^* was obtained by the method of angular lag⁸⁵ applied to the lkl layer. Both sets of cell data are summarised below, and detailed measurements are given in Table 6.

	Room Temperature Cell Data	Low Temperature Cell Data
a	$9.18 \pm .07 \text{ \AA}$	$9.13 \pm .08 \text{ \AA}$
b	$8.54 \pm .04 \text{ \AA}$	$8.44 \pm .04 \text{ \AA}$
c	$13.06 \pm .13 \text{ \AA}$	$12.79 \pm .08 \text{ \AA}$
β	$124^\circ 43' \pm 1^\circ$	$125^\circ 21' \pm 13'$
V	1180 \AA^3	1131 \AA^3

TABLE 6(a)

ROOM TEMPERATURE CELL DATA 2SbCl₃ p-XYLENE

From 15° Osm. Photo about a axis

n	Sn (mm)	Sn (r.l.u.)	\bar{S}_n (r.l.u.)	Mean \bar{S}_a (r.l.u.)	a(Å)
± 1	4.45 \pm 0.1	0.0776 \pm 0.0018	0.0776 \pm 0.0018		
± 2	8.95 \pm 0.1	0.1544 \pm 0.0018	0.0772 \pm 0.0009		
± 3	13.70 \pm 0.1	0.2326 \pm 0.0018	0.0775 \pm 0.0005	0.0774 \pm 0.0007	9.18 \pm 0.07
± 4	18.65 \pm 0.1	0.3096 \pm 0.0018	0.0774 \pm 0.0004		
± 5	24.05 \pm 0.1	0.3869 \pm 0.0015	0.0774 \pm 0.0003		
± 6	30.05 \pm 0.1	0.4643 \pm 0.0015	0.0774 \pm 0.0003		

-51-

From Okl Weissenberg Photograph

n	Sn (mm)	Θ_n°	\bar{S}_n n (r.l.u.)	\bar{S}_n (r.l.u.)	Mean \bar{S}_n (r.l.u.)	Axes b, c(Å)
± 4	19.15 \pm 0.1	9.58 \pm 0.05	0.3330 \pm 0.0016	$\bar{S}_n = 0.0833 \pm 0.0004$	$\bar{S}_n = 0.0833 \pm 0.0004$	b = 8.54 \pm 0.04
± 6	28.90 \pm 0.1	14.45 \pm 0.05	0.4990 \pm 0.0015	$\bar{S}_n = 0.0833 \pm 0.0003$		
± 2	7.75 \pm 0.1	3.88 \pm 0.05	0.1354 \pm 0.0018	$\bar{S}_n = 0.0677 \pm 0.0009$		
± 4	15.55 \pm 0.1	7.78 \pm 0.05	0.2708 \pm 0.0016	$\bar{S}_n = 0.0677 \pm 0.0004$		
± 6	23.40 \pm 0.1	11.70 \pm 0.05	0.4056 \pm 0.0016	$\bar{S}_n = 0.0676 \pm 0.0003$	$\bar{S}_n = 0.0677 \pm 0.0004$	c = 13.06 \pm 0.13
± 10	39.50 \pm 0.1	19.75 \pm 0.05	0.6758 \pm 0.0014	$\bar{S}_n = 0.0676 \pm 0.0001$		

From 1kl Weissenberg Photo: Angular log for β

Dist. across c axis (x) mm	ψ°	δ_n	δ (Mean)	β^*	β
114 114 21.05 \pm 1	68.95 \pm 0.1	0.0542 \pm 0.0011			
115 115 16.30 \pm 0.1	73.70 \pm 0.1	0.0535 \pm 0.0011			
116 116 13.30 \pm 0.1	76.70 \pm 0.1	0.0536 \pm 0.0010			
117 117 11.20 \pm 0.1	78.80 \pm 0.1	0.0530 \pm 0.0010			
			0.0536 \pm 0.0011	55°17'±1°	124°43'±1°

TABLE 6(b)

LOW TEMPERATURE CELL DIMENSIONS (SbCl₃ p-XYLENE)

h01 Weissenberg Photograph:				Mean ζ (r.l.u.)	Axes a, b, c (Å)
n	Sn (mm)	θ_n°	ζ_n (r.l.u.)		
+1	5.46 \pm 0.1	2.73 \pm 0.05	$\zeta_a = 0.0954 \pm 0.0018$		
+2	11.10 \pm 0.1	5.55 \pm 0.05	$\zeta_a = 0.097 \pm 0.0009$	0.0955 \pm 0.0011	a=9.13 \pm 0.08
+3	16.28 \pm 0.1	8.14 \pm 0.05	$\zeta_a = 0.0943 \pm 0.0005$		
From Ok1 Weissenberg Photograph:					
+4	19.40 \pm 0.1	9.70 \pm 0.05	$\zeta_b = 0.0843 \pm 0.0005$		
+6	29.25 \pm 0.1	14.63 \pm 0.05	$\zeta_b = 0.0842 \pm 0.0003$	0.0842 \pm 0.0004	b=8.44 \pm 0.04
+2	7.80 \pm 0.1	3.90 \pm 0.05	$\zeta_c = 0.0680 \pm 0.0009$		
+4	15.65 \pm 0.1	7.83 \pm 0.05	$\zeta_c = 0.0681 \pm 0.0005$		
+6	23.55 \pm 0.1	11.78 \pm 0.05	$\zeta_c = 0.0681 \pm 0.0003$	0.0681 \pm 0.0005	c=12.79 \pm 0.08
+10	39.90 \pm 0.1	19.95 \pm 0.05	$\zeta_c = 0.0682 \pm 0.0002$		
From h01 Weissenberg Photograph:					
Perp ^{ar}	Dist. between Axes (x) mm	Angular Dist. (mm)	β°	Mean β°	
127.40	71.35 = 56.05 \pm 0.1	62.67 \pm 0.11	125 $^\circ$ 20' \pm 13'	125 $^\circ$ 21' \pm 13'	
127.35	71.30 = 56.05 \pm 0.1	62.67 \pm 0.11	125 $^\circ$ 20' \pm 13'		
127.35	71.35 = 56.00 \pm 0.1	62.61 \pm 0.11	125 $^\circ$ 14' \pm 13'		
105.35	49.80 = 56.05 \pm 0.1	62.67 \pm 0.11	125 $^\circ$ 20' \pm 13'		
105	49.75 = 56.10 \pm 0.1	62.72 \pm 0.11	125 $^\circ$ 26' \pm 13'		
105.85	49.75 = 56.10 \pm 0.1	62.72 \pm 0.11	125 $^\circ$ 26' \pm 13'		

Determination of the Structure

Weissenberg photographs about the a axis ($0kl - 6kl$) were taken at -110°C using zirconium filtered $\text{MoK}\alpha$ radiation, and a total of 920 independent observable reflections were obtained. A two film pack was used and long and short duration exposures taken in order to achieve a more accurate estimate of very strong and very weak intensities, and to increase the amount of data. Two b axis cross-levels were also obtained for layer scaling purposes ($h0l, h1l$).

During the collection of the low temperature data, the crystals split and broke up, and slow cooling from room temperature did not overcome this problem. Several attempts had to be made to obtain the data because of this problem. An integration camera was used to compensate for variability in spot shape with θ .

After indexing, the intensities were estimated by using a standard, calibrated intensity wedge. A factor was calculated between the two films (fast and medium, Ilford Industrial G and B) in order to put the intensities measured from both films on the same scale. Lorentz and polarisation corrections were applied to the measured intensities, but no absorption corrections were applied. (L.P. Correction programme written for I.B.M. 1620 computer by E.J. Gabe).

Nor were corrections made for differing spot shape in different areas of the film. Cross-level photographs allow the various layers to be put on a relative arbitrary scale.

A Patterson projection down a based on room temperature (Ok1) data revealed the Sb atom and a subsequent electron density projection based on structure factors which were phased on the ("heavy") antimony atom alone revealed two chlorine positions.

A three-dimensional Patterson map based on the ~~stronger~~ ^{stronger} ~~higher~~ two-thirds of the low-temperature intensities confirmed the y, z coordinates for antimony and gave the x coordinate. The subsequent three-dimensional electron density map, based on the antimony position only, revealed all three chlorine positions and resolved the p-xylene molecule around the centre of symmetry. The R-factor, with antimony alone used to calculate structure factors, was 38%.

Refinement of the Structure

Refinement was carried out by using a structure factor/least squares programme written by G.A. Mair at the Royal Institution. Inclusion of the three chlorine atoms followed by rescaling of the layers dropped the R-factor to 15.0%. Inclusion of all the atoms (four independent carbon atoms in addition to Sb, Cl) and using about 800 of the 920 reflections (i.e. omitting the very low value

reflections) gave an R-factor of 12.9% after five rounds of least squares refinement (i.e. minimising $\sum w |\Delta F|^2$, where ΔF is the difference between F_o and F_c , the observed and calculated structure factors, and w is the weight assigned to each reflection).

The weighting scheme used throughout was as follows:

$$w = F_{av}/F_o, \text{ if } F_o \gg F_{av};$$

$$w = F_o/F_{av}, \text{ if } F_o < F_{av},$$

where F_{av} is the mean observed structure factor. This gives a weighting which falls off for high and low intensities and has a maximum value of unity for average intensities, reflecting the variability in certainty of measurement using a calibrated film wedge.

After a further rescaling of the layers and inclusion of all 920 reflections, the R-factor dropped to 11.8%.

The above refinement of the positional parameters, x_i , y_i , z_i , and of the isotropic thermal parameters B_i was carried out with all the atoms free to move independently. At this point, an examination of the p-xylene ring in terms of C-C bond distances and C-C-C bond angles showed some slight distortion from an expected ideal molecule in two respects. Firstly, the molecule was not completely planar, in that the substituent methyl groups were

bent slightly out of the plane of the benzene ring. Secondly, the ring C-C bond lengths had deviated from the ideal value of 1.395 Å expected for a benzenoid aromatic bond.

The p-xylene molecule was idealised and a set of orthogonal coordinates calculated. The position of the idealised molecule was defined by three angles and three distances from the ring centre to the origin of an orthogonal cell, these angles and distances being defined with respect to the orthogonal cell axes. This was carried out by using a "mean plane" programme (IBM 360/44, Fortran IV) which allows the aromatic molecule to be defined in terms of the above six parameters. Keeping the antimony and chlorine atoms free and the ring rigid, the parameters x_i, y_i, z_i, B_i , for the free atoms, and $\Theta, \phi, \psi, x', y', z', B_i$ for the rigid ring were refined using a rigid body least squares programme written by R. Hulme (I.B.M. 360/44, Fortran IV, "PARIBLES"), and embodying a block-diagonal approximation. Θ, ϕ, ψ are the angles which the plane of the rigid ring make with the x, y, and z orthogonal axes respectively, and x', y', z' the corresponding distances from the ring centre to the origin of the cell.

After three rounds of refinement (using the weighting scheme which has already been outlined) the R-factor dropped

to 10.9%. The "Paribles" programme also had facilities for layer scale refinement on each round as B_i values were isotropic⁸⁷.

On freeing all the atoms for a final two rounds of least squares refinement, it was found that the resulting parameter shifts were less than the corresponding standard deviations, although the same lengthening of one C-C bond and shortening of two others in the aromatic ring was found, as has been reported above. The departures from ideality in the aromatic ring are smaller than the standard deviations of the bonds and angles involved.

The final R-factor for 920 observed reflections was 11.3%. 12 unobserved reflections had calculated structure factors (F_c) which were greater than their allocated F-observed values of a half the local minimum, and all of these were within twice their local minimum. The relatively low R-factor found for the rigid body system compared with the refinement in which all of the atoms were free is explained by the fact that while four independent carbon atoms are defined rigidly by six parameters, this loss in the number of degrees of freedom is compensated by the introduction of several new parameters in

the form of layer scales, (for 0kl-6kl layers).

The variation of the R-factor with sine θ and over various ranges of the observed structure factors (F_o) is given below; *for free atom refinement.*

Sine Ranges	0.250	0.354	0.434	0.501	0.560
R. Factors	9.91	10.21	13.65	16.66	20.54
No. of Reflns.	243	313	209	123	32
Fobs. Ranges	192	384	576	768	960
R. Factors	18.28	11.69	8.05	8.42	10.30
No. of Reflns.	317	400	162	39	2

For F_o , F_e see Appendix I. The final atomic coordinates and temperature factors are listed in Table 7.

Description of the Structure

The essential feature of the structure is the layer-like nature of the molecular arrangements, with layers of antimony trichloride alternating with layers of p-xylene. This is shown in figure 6, which is a general view of the unit cell. The system of numbering of the atoms is given in figure 5(b).

The antimony trichloride molecules are oriented with their dipoles antiparallel, but they are too far apart for halogen

bridging to occur. (The distance from a chlorine atom of one of the Sb atoms to the other Sb atom is $3.24 \pm 0.01 \text{ \AA}$). The term "incipient dimer" has been coined to describe this orientation, ~~which occurs in antimony trichloride itself.~~

The distance from the antimony atom to the nearest carbon atom is 3.18 \AA , much shorter than the Van der Waals distance of 3.5 \AA . The carbon atom in question (C(4)) is the ring atom bonded to the substituent methyl group. A projection down the Cl(3) - Sb bond shows that the atoms Cl(3)-Sb-C(4) are almost co-linear. The Cl(3)-Sb distance is slightly longer than the other two Sb-Cl distances ($2.369 \pm 0.014 \text{ \AA}$ compared with $2.303 \pm 0.011 \text{ \AA}$ and $2.319 \pm 0.013 \text{ \AA}$). This Sb-aromatic interaction is shown diagrammatically in the projection down the Cl(3)-Sb bond in figure 5(a), p. 63.

The aromatic ring shows certain deviations from ideality, but none of these are significant, the greatest deviation being only 1.5 times the standard deviation. The bonds C(4)-C(2) ($1.37 \pm 0.07 \text{ \AA}$) and C(4)-C(3) ($1.37 \pm 0.05 \text{ \AA}$) are shortened and the bond C(2)-C(3) ($1.48 \pm 0.06 \text{ \AA}$) is lengthened compared with an ideal C-C aromatic bond length of 1.395 \AA . The bond C(4)-C(1)

is bent slightly out of plane, and away from the Sb atom.

These deviations from the isolated SbCl_3 and p-xylene molecular geometry, taken together, are suggestive of a weak Sb-aromatic interaction involving some tendency to localisation of the π -aromatic system.

Intermolecular and intramolecular distances and bond angles are to be found in Table 8.

TABLE 7

Fractional Coordinates and Isotropic Temperature Factors
(e.s.d. (in brackets) refer to least significant digits).

	x	y	z	B
Sb	0.3899(04)	0.1072(03)	0.0995(02)	1.06(02)
Cl(1)	0.3320(15)	0.3457(11)	-0.053(09)	2.92(20)
Cl(2)	0.4991(13)	0.2233(10)	0.2962(08)	2.02(16)
Cl(3)	0.6793(13)	0.0874(12)	0.1432(08)	2.60(18)
C(1)	0.0105(65)	0.3137(47)	0.1080(38)	3.2(8)
C(2)	0.0652(58)	0.0172(46)	0.1276(36)	2.8(8)
C(3)	0.0557(48)	-0.1393(43)	0.0709(29)	2.2(7)
C(4)	0.0125(56)	0.1538(46)	0.0560(34)	2.9(8)

TABLE 8

Bond Distances and Angles

(standard Deviations in brackets)

a). Intramolecular Bond Distances and Bond Angles.

Sb	-Cl(1)	2.303(11) Å
Sb	-Cl(2)	2.319(13) Å
Sb	-Cl(3)	2.369(14) Å
Cl(1)	-Cl(2)	3.38(2) Å
Cl(1)	-Cl(3)	3.38(2) Å
Cl(2)	-Cl(3)	3.40(2) Å
C(1)	-C(4)	1.51(6) Å
C(2)	-C(3)	1.48(6) Å
C(2)	-C(4)	1.37(7) Å
C'(3)	-C(4)	1.37(5) Å

Cl(1) - Sb - Cl(2)	94.1(4) ^o
Cl(1) - Sb - Cl(3)	92.8(5) ^o
Cl(2) - Sb - Cl(3)	93.1(5) ^o
C(1) - C(4) - C(2)	123.0(4.8) ^o
C(1) - C(4) - C [†] (3)	119.3(3.9) ^o
C(2) - C(4) - C [†] (3)	117.2(2.7) ^o
C(3) - C(2) - C(4)	121.4(5.0) ^o
C [†] (4) - C(3) - C(2)	117.4(2.7) ^o

b). Some Intermolecular Distances and Angles.

(standard deviations in brackets)

Sb - C(2)	3.28(5) ^o _A
Sb - C(4)	3.18(6) ^o _A
Sb - C [†] (3)	3.33(4) ^o _A
Sb - Sb [†]	4.440(6) ^o _A
Sb - Cl [†] (3)	3.235(14) ^o _A
Cl(3) - Sb - C(4)	175.5(9) ^o

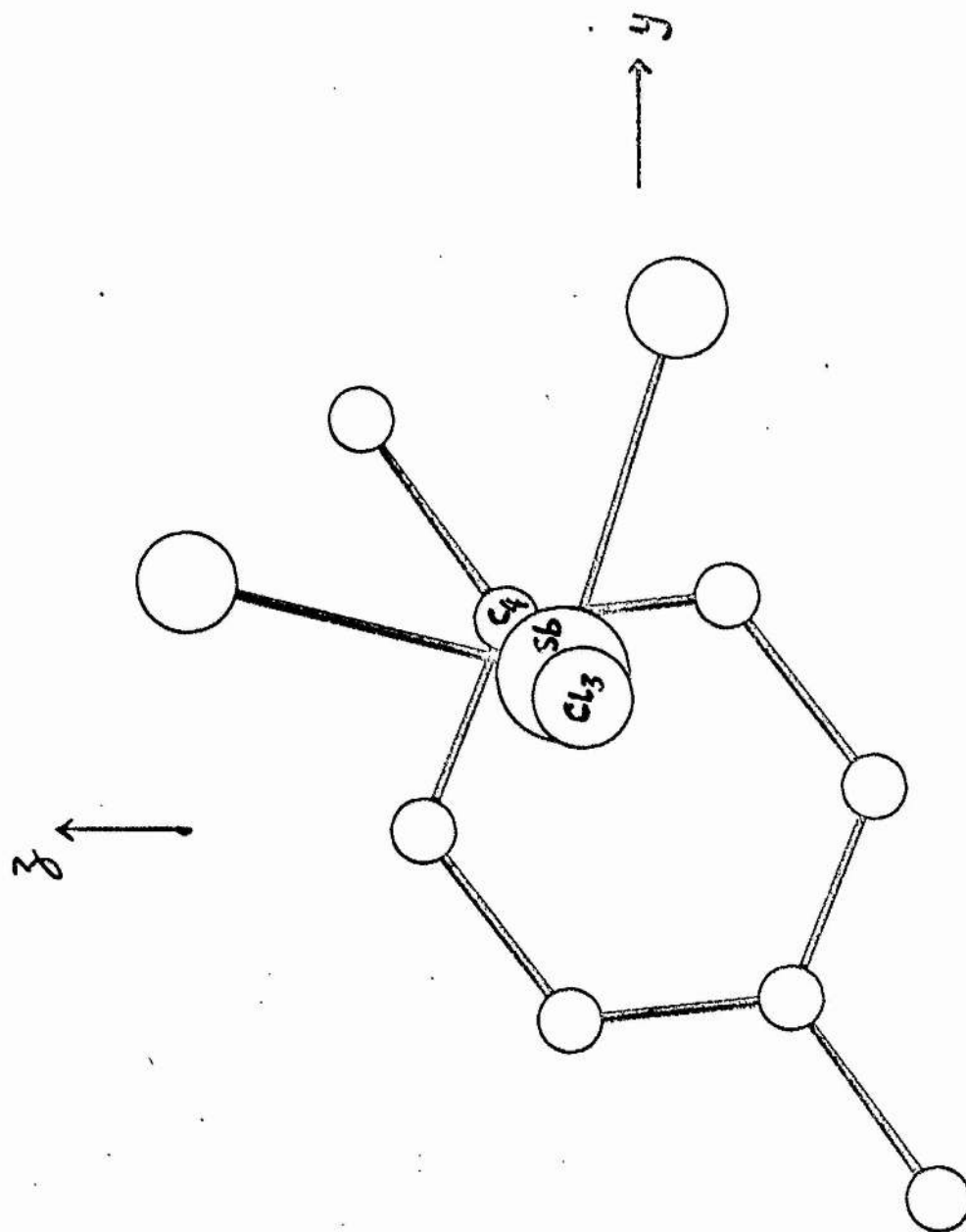


Fig. 5(a) - The SbCl_3 - p-xylene Interaction.

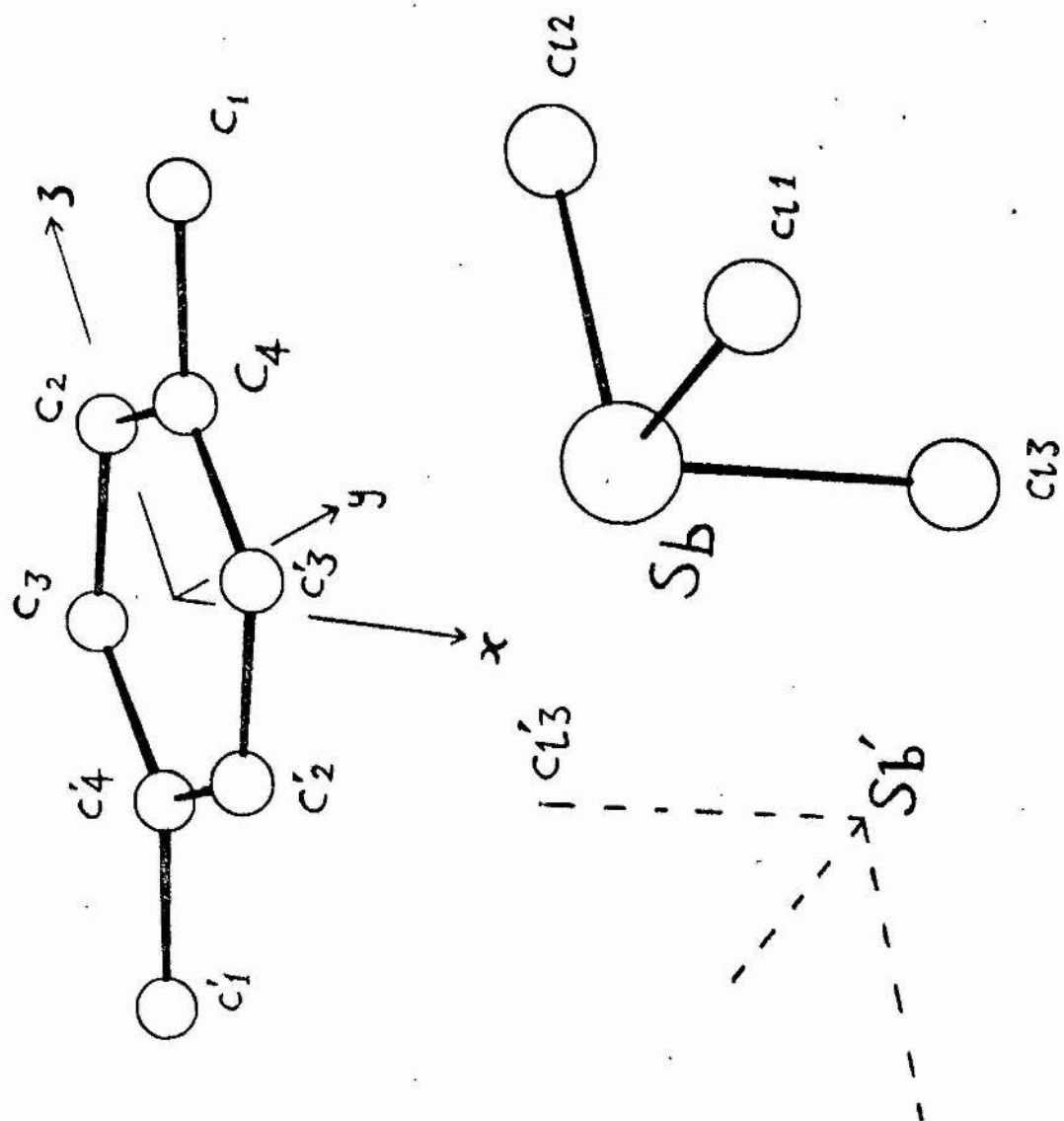


Fig. 5(b) - Numbering Scheme for 2SbCl₃·p-xylene.

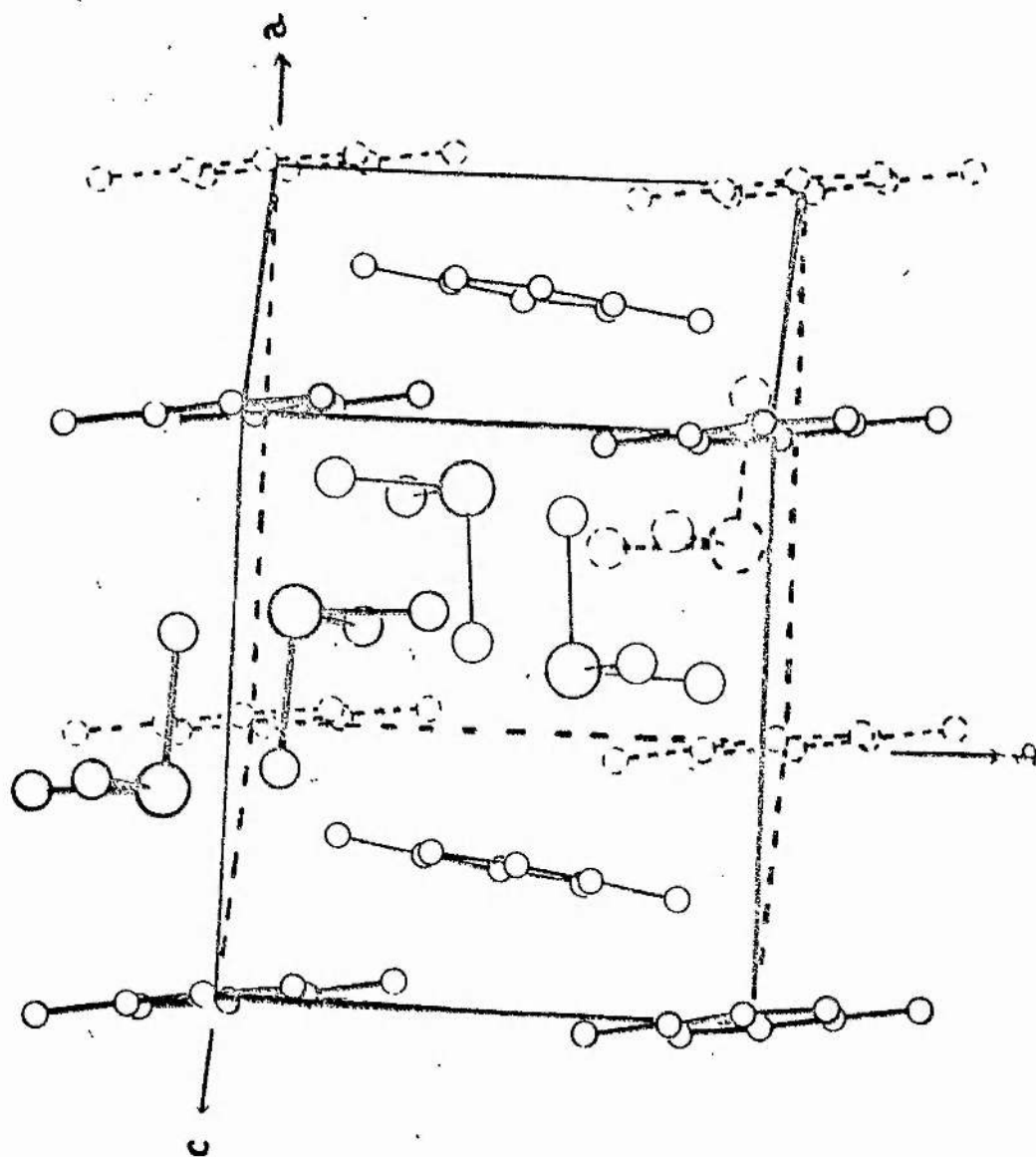


Fig. 6 - The Structure of the Complex 2SbCl₃.p-xylene.

CHAPTER V

The Structure of the Complex $2\text{SbCl}_3 \cdot 3\text{C}_5\text{H}_5\text{N}$

Determination of Cell Dimensions, Space Group & Composition.

A 15° oscillation photograph (zirconium-filtered $\text{MoK}\alpha$ radiation) showed symmetry above and below the zero layer-line, indicating that the crystal belonged either to the monoclinic system and was being rotated about the unique (b) axis, or else to the orthorhombic system.

A zero layer Weissenberg about this same axis showed symmetry across both remaining axes, which were 90° apart. This symmetry was preserved in upper levels indicating that the relevant system was orthorhombic. This was confirmed by cross-levels about another axis which showed a 90° angle and cross-axis symmetry.

The systematic absences in the intensity data were as follows:

hkl : no conditions, indicating a primitive cell.

hol : $h=2n+1$, indicating an a glide plane perpendicular to b.

$Ok1$: $l=2n+1$, indicating a c glide plane perpendicular to a.

$[00l: l=2n+1]$, either as a sub-set of $Ok1$ or indicating a two-fold screw axis along c.

Two possible space groups arise from these absences, a non-centrosymmetric one ($\text{Pca}2_1$, No.29) or a centrosymmetric one

TABLE 9

CELL DIMENSIONS $2\text{SbCl}_3 \cdot 3 \text{ pyridine}$

From hko Weissenberg Photograph:

n	Sn (mm)	θ_n°	ζ_n	ζ	Mean ζ (in r.l.m.)	Axes a, b, c (in Å)
± 14	21.90 ± 0.1	10.95 ± 0.05	$\zeta_{14} = 0.3799 \pm 0.0018$	$\zeta_a = 0.0271 \pm 0.00013$	0.0272 \pm 0.0001	26.14 ± 0.08
± 16	25.15 ± 0.1	12.58 ± 0.05	$\zeta_{16} = 0.4357 \pm 0.0018$	$\zeta_a = 0.0272 \pm 0.00011$		
± 3	16.25 ± 0.1	5.13 ± 0.05	$\zeta_3 = 0.1789 \pm 0.0018$	$\zeta_b = 0.0596 \pm 0.0006$	0.0595 \pm 0.0004	11.93 ± 0.07
± 6	20.55 ± 0.1	10.28 ± 0.05	$\zeta_6 = 0.3570 \pm 0.0018$	$\zeta_b = 0.0595 \pm 0.0003$		
± 7	24.00 ± 0.1	12.00 ± 0.05	$\zeta_7 = 0.4158 \pm 0.0018$	$\zeta_b = 0.0594 \pm 0.0003$		
± 8	27.60 ± 0.1	13.80 ± 0.05	$\zeta_8 = 0.4771 \pm 0.0016$	$\zeta_b = 0.0596 \pm 0.0002$		

-67-

From 15° Oscm. Photograph about c axis:

n	Sn (mm)	θ_n°	ζ_c	Mean ζ_c (in r.l.u.)
± 2	11.00 ± 0.1	0.1885 ± 0.0018	0.0943 ± 0.0009	0.0946 ± 0.0005
± 3	16.95 ± 0.1	0.2837 ± 0.0016	0.0946 ± 0.0005	
± 4	23.50 ± 0.1	0.3795 ± 0.0016	0.0949 ± 0.0004	
± 5	30.80 ± 0.1	0.4736 ± 0.0016	0.0947 ± 0.0003	

 7.51 ± 0.04

(Pcam, No.57, interchanging a and b axes).

The cell dimensions were determined from photographs taken using zirconium filtered $\text{MoK}\alpha$ radiation. Measurements on the film were made with a film measuring device incorporating a sliding vernier mm scale. ℓ_c was measured from a 15° oscillation photograph about the c axis. ℓ_a , ℓ_b were measured from a zero-layer Weissenberg photograph (hk0) about c. These measurements, and the cell dimensions derived from them, are given in Table 9.

The cell volume is 2342 \AA^3 . With the measured density (2.30), this implies a cell weight of 3257. On the basis of a volume of 120 \AA^3 for a pyridine molecule and 120 \AA^3 for a SbCl_3 molecule, the composition is limited to four units of 4:1, 3:2, 2:3 or 1:4 (SbCl_3 : pyridine), i.e. a total of five molecules per asymmetric unit. The cell weight favours the ratio 3:2.

Determination of the Structure

Three-dimensional room temperature data was collected about the c axis (layers hk0-hk6, 329 independent reflections) using zirconium-filtered $\text{MoK}\alpha$ radiation. A "Nonius" X-ray camera was used, intensity data being recorded on a two-film pack. The intensities were estimated by means of a calibrated intensity

wedge. Lorentz and polarisation corrections, but no absorption corrections, were applied to the intensities. The layers were put on an arbitrary relative scale by means of $h0l$ and $h1l$ cross-level correlation of the L.P. corrected intensities, prior to the computation of a three-dimensional Patterson map.

When the three-dimensional Patterson map was computed the composition of the complex was not fully known. The most satisfactory interpretation of the Patterson map involved two independent antimony atoms. $hk0$ and $h0l$ electron density projections based on space group $Pca2_1$ confirmed that these two positions for antimony were possibilities, but revealed no further atomic positions.

A three-dimensional electron density map phased on the two independent antimony atoms alone in space group $Pcam$ gave an initial R-factor of 95.0%. This R-factor did not diminish on the inclusion of possible chlorine positions. The three-dimensional electron density map phased on the antimony atoms alone in space group $Pca2_1$ gave an R-factor of 32%. The map revealed six possible chlorine positions, but these were not positions which gave the expected pyramidal geometry for the two independent nominal antimony trichloride molecules. It became necessary to accept that one of the antimony trichloride

"molecules" was planar on the basis of the possible positions revealed in the preliminary maps, and to accept a bridging halogen with an associated Sb-Cl bond length far in excess of anything hitherto encountered in SbCl_3 - aromatic complexes.

The correctness of these chlorine positions was confirmed by the drop in the R-factor (to 22%) and the appearance of two pyridine molecules bonded to an antimony atom in the electron density map phased on antimony and chlorine atoms only. The drop in the magnitude of the R-factor on the inclusion of these chlorine positions suggested that $\text{Pca}2_1$ was thus more probably the correct space group.

Inclusion of the two pyridine molecules lowered the R-factor to 15%. As required by the 2:3 molecular ratio, an additional pyridine molecule in a non-bonding position was suggested in the map, although it was poorly resolved. The electron density map phased by the inclusion of the bonded rings did not show significant improvement in the resolution of this additional non-bonded molecule. However, when a pyridine molecule, centred at this non-bonded position and satisfying the observable peaks as best possible, was included in the set of parameters used to compute structure factors, the R-factor

dropped to 12.4%.

Refinement of the Structure

After five rounds of least squares refinement (based on a total of 329 independent reflections out of a possible 5,600 up to $\sin \theta = 0.5$) with all atoms free and with isotropic temperature factors throughout, the R-factor dropped to 10.0%. (Structure factor/least squares programme written by G.A. Mair for an I.B.M. 1620 computer).

Some distortion was found in the bonded pyridine molecules, and severe distortion occurred in the unbonded pyridine molecule. This was attributed, for the most part, to the lack of high angle (θ) data. To compensate for this, the total number of parameters was reduced by describing the rings as rigid bodies, using the "PARIBLES" programme described in a previous section, p 56. The molecular dimensions used in the idealisation of the pyridine rings are those given by Bak and coworkers⁸⁴.

The first few rounds of least squares treatment in this manner led to a satisfactory refinement for the bonded rings. Two apparently unsatisfactory aspects existed at this point in the refinement. The bonded molecules did not settle in an ideal position, with the twofold ring axis through C-N colinear with

the antimony atom. Secondly, the unbonded molecule showed no tendency to refine in the normally expected manner, i.e. with the magnitude of parameter shifts decreasing with successive rounds. This molecule was idealised on the basis of bond lengths which were the mean of the three pyridine bond lengths⁸⁴, and all the atoms were given carbon scattering factors, the nitrogen position being unknown. The first problem was overcome by re-idealising the pyridine molecules with their twofold axes colinear with the antimony atom, whereupon after three rounds of refinement using the "PARIBLES" rigid body programme the colinearity was maintained and the R-factor dropped from 11.8% to 11.0%. The higher R-factor obtained in the rigid body refinement compared with the free-atom method is due to a decrease in the total number of degrees of freedom (i.e. of the number of parameters being refined). It was initially thought that the unbonded pyridine molecule was attempting to oscillate into a new position and was introduced in a grossly incorrect orientation. An orientation apparently compatible with the angular shifts indicated was tried, but this was to no avail and it proved again unsuccessful in bringing about a refinement of the ring parameters (i.e. the angles θ , ϕ , ψ defining the ring orientation).

The possibility that the ring was rotating about an axis perpendicular to its plane (a thermal effect) was next considered. To simulate more closely a rotating ring, twelve atoms were introduced to constitute the ring, each atom being given half the weight of a carbon atom in terms of a scattering factor. No significant difference was found: the angles θ , ϕ , ψ and the temperature factors, B_i , did not refine to an essentially fixed value. The angular shifts remained large and the temperature factors, in general, continued to increase, even after ten rounds of rigid-body refinement.

It was decided that the limited intensity data did not warrant further pursuit of the refinement process. The nature of this unbonded molecule is discussed further in the next section.

The final R-factor for 329 observed reflections was 11.0%. 17% unobserved reflections had calculated structure factors (F_c) which were greater than their allocated F-observed values of a half the local minimum, and all of these were within 1.5 times their local minimum. A breakdown of the R-factor for various ranges of $\sin \theta$ and of F-observed is given below. For F_o , F_c listing, see Appendix III.

The temperature factor is defined as $\exp(-B \sin^2 \theta / \lambda^2)$.

Intramolecular and intermolecular bond lengths and angles are given in Table 11. The atomic scattering factors used were taken from "International Tables", Vol. III (Kynoch Press, 1962), the appropriate H₀nl corrections being applied.

The numbering scheme used for the atoms is given in Fig. 7.

Sine Ranges	0.174	0.247	0.302	0.349	0.390
R Factors	11.39	10.07	13.59	12.57	21.51
No. of Reflms.	100	131	73	21	4
F obs. Ranges	660	1320	1980	2640	3300
R. Factors	16.60	11.01	9.10	7.71	9.22
No. of Reflms.	108	167	44	8	2

Description of the Structure

The general features of the structure are illustrated in Fig. 7. Fig. 8 shows a projection down the c axis. The asymmetric unit consists of a unit $(\text{Cl}_3\text{Sb} \cdots \text{Cl-SbCl}_2\text{py})\text{py}$, where py represents a pyridine molecule. There are four such units per unit cell. The "antimony trichloride" unit

which is not coordinated to pyridine shows an essentially similar geometry to antimony trichloride itself⁴⁵. The bond distances and angles are similar, and these can be found in Table 9. This antimony atom, Sb(1) (fractional coordinates: 0.2122, 0.1539, -0.0117) is linked through halogen bridging to symmetry related antimony trichloride units ²Sb'(1) (0.2878, 0.1538, -0.5117) and ²Sb(1) (0.2878, 0.1539, 0.4883). The bridging halogen atom is additional to the three halogen atoms initially nominally attached to Sb(1) and is derived (nominally) from the other independent antimony atom, ³Sb'(2) (0.3466, -0.1208, 0.0250). Sb(1) is thus involved in an infinite halogen-bridged chain extending down the c direction. This is shown in Fig. 7. Sb(1) is thus octahedrally coordinated, with an axial lone pair of electrons. The halogen bridge is asymmetric with a Sb(1) - ³Cl'(6) (bridging) length of 2.990 ± 0.033 Å and a ²Sb(1) - ³Cl'(6) (bridging) length of 2.748 ± 0.033 Å.

The other SbCl₃ entity (Sb(2)) is unrecognisable in terms of the normally expected geometry for this molecule. The chlorine atoms have become coplanar with the Sb(2) atom, and

the two pyridine ligands are bonded trans to each other. One of the chlorine atoms nominally associated with Sb(2) is involved as the bridging atom in the (Sb(1)Cl₄) chain. The distance ³Sb'(2)-³Cl'(6) (bridging) is 3.003 ± 0.033 Å, and the complex is thus tending to the ionic situation (SbCl₂py₂)⁺ SbCl₄⁻.

Another approach, considering 3.00 Å as a possible Sb-Cl covalent distance, invokes a three-coordinate chlorine atom. This is more fully discussed in chapter VIII.

The angles Sb(1) - bridging Cl-³Sb'(2) and Sb(1) - bridging Cl-²Sb(1) are $106.7 \pm 1.3^\circ$ and $95.2 \pm 1.3^\circ$ respectively. The antimony nitrogen bonds ³Sb'(2) - ³N'(1) and ³Sb'(2) - ³N'(2) are 2.27 ± 0.10 Å and 2.49 ± 0.09 Å respectively, and the angle ³N'(1) - ³Sb'(2) - ³N'(2) is $170 \pm 3^\circ$. Sb(2) is thus octahedrally coordinated and has an equatorial lone pair of electrons. The nitrogen-antimony bonds are approximately perpendicular to the plane of the Sb(2) and chlorine atoms.

The α-pyridine molecules (Fig. 7 gives the numbering of atoms and rings) are stacked in columns with plane-to-plane separation of 3.75 Å. The β-pyridine molecules are also stacked in columns, but the rings are not as closely superposed

(viewed down the c axis) as in the case of the α -pyridine rings. (Fig. 8). The β - and γ -pyridine molecules are situated near zero and a half in the 'a' direction, so that together they form layers of the organic component lying perpendicular to the 'a' axis. The planes of the β - and γ -pyridine molecules are approximately mutually perpendicular.

The γ -pyridine molecule is 3.21 ± 0.26 Å away from the nearest chlorine atom ($^3\text{Cl}'(5)$) and 2.99 ± 0.24 Å away from the nearest carbon atom of another molecule (β -pyridine molecule). This rather low intermolecular C-C distance is to be given small significance because of the difficulties involved in defining precisely the unbonded pyridine molecule. These were discussed earlier in the chapter.

The layers of pyridine together with the columns of pyridine totally surround the chains of (SbCl_4) units as well as the $(\text{SbCl}_2\text{py}_2)$ units. These chains lie in "channels" of the organic component running parallel to the c-axis. Through coordinated pyridine molecules they are bound to the walls of these channels.

The problem of refinement of the free pyridine molecule is believed to be due to the large thermal motions of the ring.

The molecule occupies a large hole in the lattice and is more free to move than are the bonded molecules. While there is no unambiguous evidence for rotation about an axis perpendicular to the plane of the molecule, the failure of the ring parameters to refine, and the very high temperature factors (of the order of 10.0 compared with 5.0 on average for the bonded rings), point to very large thermal vibrations. It has thus been necessary to define the ring in terms of the location of its centre.

TABLE 10(a)

Fractional Coordinates & Isotropic Temperature Factors (e.s.d. in brackets)

(for numbering see Fig. 7)

	x	y	z	B
Sb(1)	0.2122(4)	0.1539(8)	-0.0117(22)	4.85(19)
Sb(2)	0.8466(4)	0.1208(8)	0.0250(22)	6.03(26)
Cl(1)	0.1410(15)	0.0521(33)	0.0416(70)	7.3(1.2)
Cl(2)	0.1706(19)	0.2612(40)	0.2175(71)	7.2(1.4)
Cl(3)	0.1902(19)	0.2784(40)	-0.2503(76)	7.8(1.4)
Cl(4)	0.8905(17)	0.1945(34)	0.2352(66)	6.0(1.2)
Cl(5)	0.8890(23)	0.2214(47)	-0.2292(80)	10.7(1.9)
Cl(6)	0.7646(10)	0.0054(22)	0.2367(51)	2.2(0.8)
N(1)	0.795(5)	0.273(6)	0.019(11)	8.4(3.3)
C(1)	0.744(4)	0.264(6)	0.034(9)	2.6(3.0)
C(2)	0.710(3)	0.354(7)	0.038(11)	0.2(2.2)
C(3)	0.731(4)	0.462(6)	0.026(10)	1.8(2.9)
C(4)	0.784(4)	0.474(7)	0.011(11)	8.1(3.3)
C(5)	0.813(3)	0.377(7)	0.008(10)	3.1(2.6)
N(2)	0.914(3)	-0.025(6)	0.008(10)	3.7(2.5)
C(6)	0.910(3)	-0.129(6)	0.074(10)	6.4(3.1)
C(7)	0.950(3)	-0.206(5)	0.081(9)	9.0(3.6)
C(8)	0.998(3)	-0.173(6)	0.016(11)	4.9(2.9)
C(9)	0.003(3)	-0.064(6)	-0.053(9)	2.2(3.0)
C(10)	0.961(3)	0.005(6)	-0.053(10)	1.0(2.8)
C(11)	0.059(5)	0.348(10)	0.057(22)	8.5(5.6)
C(12)	0.053(4)	0.373(10)	-0.121(21)	13.0(8.6)
C(13)	0.064(4)	0.478(12)	-0.184(18)	5.2(5.0)
C(14)	0.082(5)	0.559(10)	-0.068(22)	10.8(7.1)
C(15)	0.088(4)	0.534(10)	0.110(20)	8.7(6.6)
C(16)	0.076(5)	0.429(13)	0.172(20)	4.7(4.5)

TABLE 10(b)

Orientational Angles and Centres of Pyridine Rings.

(Angles in degrees, coordinates fractional, e.s.d. in brackets)

	α -Pyridine	β -Pyridine	γ -Pyridine
θ	12.1(2.0)	-3.0(2.0)	-80.2(5.2)
ϕ	-84.9(2.5)	-65.2(2.5)	10.0(3.6)
ψ	24.5(2.7)	53.9(2.4)	-17.3(3.5)
x	0.7627(22)	0.9561(20)	0.0701(20)
y	0.3674(42)	-0.0988(42)	0.4534(61)
z	0.0225(71)	0.0123(72)	-0.0057(152)

TABLE 11

Bond Distances & Angles

(e.s.d. in brackets, least significant digits)

a) Intramolecular Bond Distances & Angles

Sb(1)-Cl(1)	2.258(40) Å
Sb(1)-Cl(2)	2.405(51) Å
Sb(1)-Cl(3)	2.397(55) Å
Sb(1)- ⁴ Cl ¹ (6)	2.748(33) Å
Sb(1)- ³ Cl ¹ (6)	2.990(33) Å
³ Sb ¹ (2)- ³ Cl ¹ (4)	2.141(49) Å
³ Sb ¹ (2)- ³ Cl ¹ (5)	2.513(68) Å
³ Sb ¹ (2)- ³ Cl ¹ (6)	3.003(33) Å
³ Sb ¹ (2)- ³ N ¹ (1)	2.270(103) Å
³ Sb ¹ (2)- ³ N ¹ (2)	2.487(92) Å
³ N ¹ (1)- ³ C ¹ (1)	1.340(220) Å
³ C ¹ (1)- ³ C ¹ (2)	1.390(220) Å
³ C ¹ (2)- ³ C ¹ (3)	1.400(220) Å
³ N ¹ (2)- ³ C ¹ (6)	1.340(210) Å
³ C ¹ (6)- ³ C ¹ (7)	1.390(210) Å
³ C ¹ (7)- ³ C ¹ (8)	1.400(210) Å
³ C ¹ (11)- ³ C ¹ (12)	1.377(330) Å
Cl(1)-Sb(1)-Cl(2)	77.7(1.7)°
Cl(2)-Sb(1)-Cl(3)	95.6(1.7)°
Cl(1)-Sb(1)-Cl(3)	105.5(1.8)°
Cl(1)-Sb(1)- ³ Cl ¹ (6)	85.7(1.7)°
Cl(2)-Sb(1)- ³ Cl ¹ (6)	95.7(1.9)°
Cl(3)-Sb(1)- ³ Cl ¹ (6)	165.6(1.8)°
³ Cl ¹ (6)-Sb(1)- ⁴ Cl ¹ (6)	83.6(1.5)°
³ Cl ¹ (4)- ³ Sb ¹ (2)- ³ Cl ¹ (5)	97.3(1.9)°
³ Cl ¹ (5)- ³ Sb ¹ (2)- ³ Cl ¹ (6)	159.4(1.7)°
³ Cl ¹ (4)- ³ Sb ¹ (2)- ³ Cl ¹ (6)	100.4(1.5)°

Idealised
Ring Parameters

$^2\text{Sb}(1)-^3\text{Cl}^1(6)-^3\text{Sb}^1(2)$	121.6(1.3) ^o
$\text{Sb}(1)-^3\text{Cl}^1(6)-^2\text{Sb}(1)$	95.2(1.3) ^o
$\text{Sb}(1)-^3\text{Cl}^1(6)-^3\text{Sb}^1(2)$	106.7(1.3) ^o
$^3\text{N}^1(1)-^3\text{Sb}^1(2)-^3\text{N}^1(2)$	170.4(3.1) ^o
$^3\text{N}^1(1)-^3\text{Sb}^1(2)-^3\text{Cl}^1(4)$	90.4(2.9) ^o
$^3\text{N}^1(1)-^3\text{Sb}^1(2)-^3\text{Cl}^1(5)$	82.4(3.0) ^o
$^3\text{N}^1(1)-^3\text{Sb}^1(2)-^3\text{Cl}^1(6)$	87.1(2.7) ^o
$^3\text{N}^1(2)-^3\text{Sb}^1(2)-^3\text{Cl}^1(4)$	86.7(2.9) ^o
$^3\text{N}^1(2)-^3\text{Sb}^1(2)-^3\text{Cl}^1(5)$	88.9(3.2) ^o
$^3\text{N}^1(2)-^3\text{Sb}^1(2)-^3\text{Cl}^1(6)$	102.4(2.5) ^o
$^3\text{Sb}^1(2)-^3\text{N}^1(1)-^3\text{C}^1(1)$	122(9) ^o
$^3\text{Sb}^1(2)-^3\text{N}^1(1)-^3\text{C}^1(5)$	122(9) ^o
$^3\text{Sb}^1(2)-^3\text{N}^1(2)-^3\text{C}^1(6)$	125(8) ^o
$^3\text{Sb}^1(2)-^3\text{N}^1(2)-^3\text{C}^1(10)$	118(8) ^o
$^3\text{C}^1(5)-^3\text{N}^1(1)-^3\text{C}^1(1)$	116.7(14.0) ^o
$^3\text{N}^1(1)-^3\text{C}^1(1)-^3\text{C}^1(2)$	124.0(14.0) ^o
$^3\text{C}^1(1)-^3\text{C}^1(2)-^3\text{C}^1(3)$	118.6(14.0) ^o
$^3\text{C}^1(2)-^3\text{C}^1(3)-^3\text{C}^1(4)$	118.1(14.0) ^o
$^3\text{C}^1(10)-^3\text{N}^1(2)-^3\text{C}^1(6)$	116.7(13.0) ^o
$^3\text{N}^1(2)-^3\text{C}^1(6)-^3\text{C}^1(7)$	124.0(13.0) ^o
$^3\text{C}^1(6)-^3\text{C}^1(7)-^3\text{C}^1(8)$	118.6(13.0) ^o
$^3\text{C}^1(7)-^3\text{C}^1(8)-^3\text{C}^1(9)$	118.1(13.0) ^o
$^3\text{C}^1(11)-^3\text{C}^1(12)-^3\text{C}^1(13)$	120.0(24.0) ^o

b) Intermolecular Bond Distances less than 3.4 Å

$^3\text{C}^1(12)-^3\text{C}^1(7)$	2.99(24) Å
$^3\text{C}^1(15)-^3\text{Cl}^1(5)$	3.21(26) Å

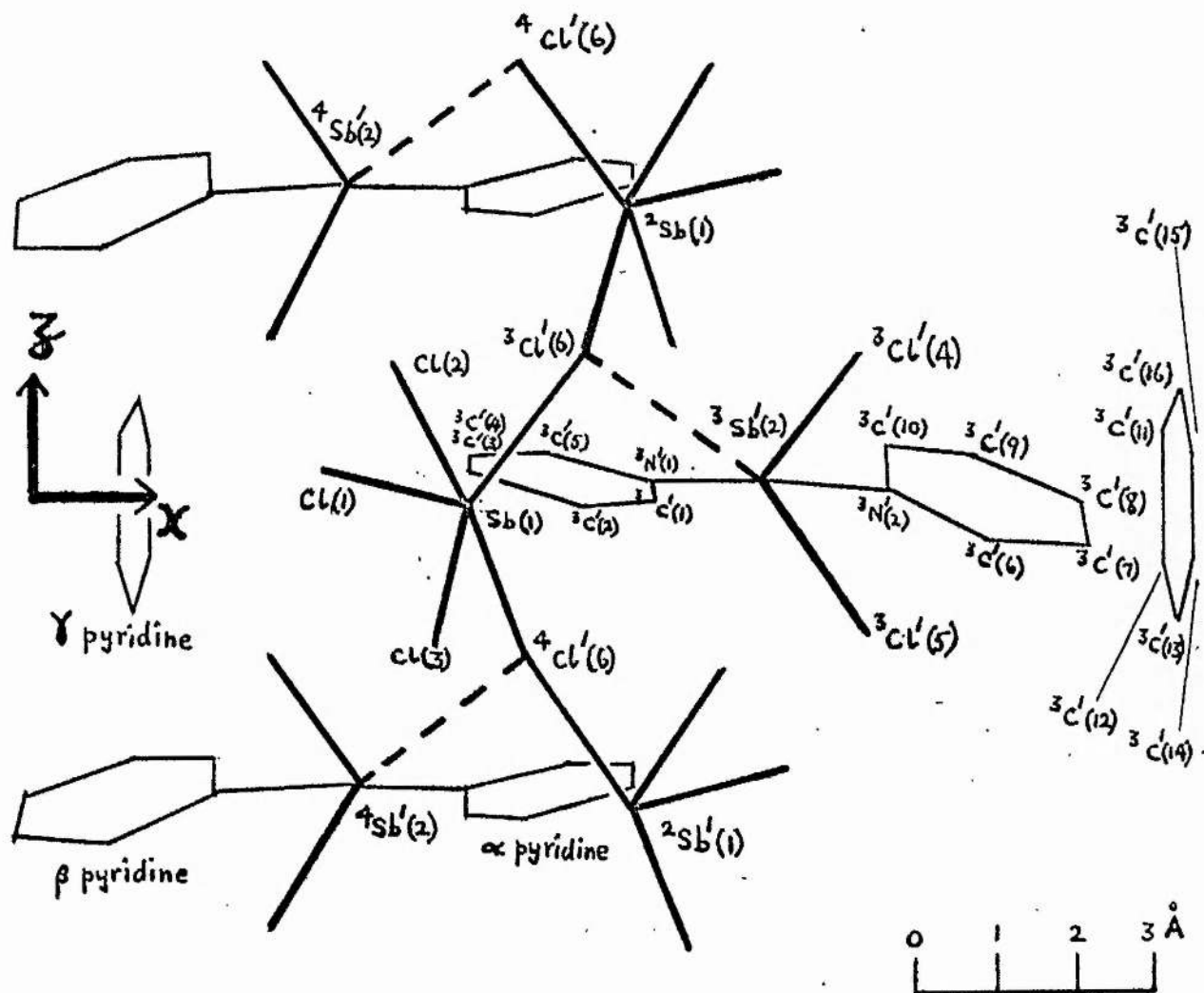


Fig. 7 - Numbering of Atoms in the Asymmetric Unit
and Arrangement of (SbCl_4) Chain in the Structure.

(Legend for Numbering:

- (a) pre-superscript indicates symmetry-related atom:
 $x, y, z; \frac{1}{2}-x, y, \frac{1}{2}+z; \frac{1}{2}+x, -y, z; -x, -y, \frac{1}{2}+z;$
- (b) dashed superscript following atom symbol indicates cell-shifted atom;
- (c) number in brackets following atom symbol is atom number in asymmetric unit).

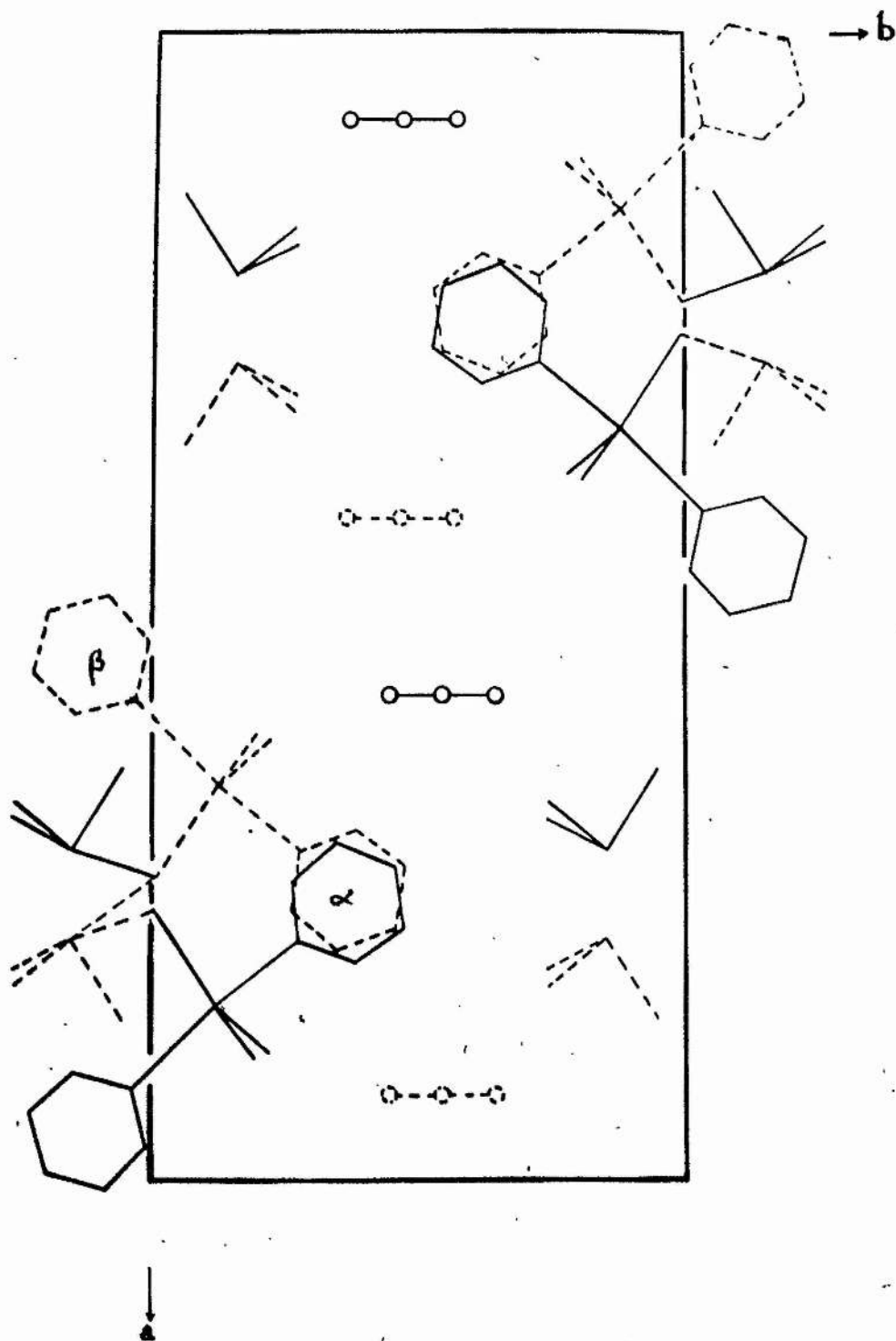


Fig. 8 - $2\text{SbCl}_3 \cdot 30\text{H}_5\text{N}$, $hk0$ Projection.

CHAPTER VI.

The Complex $\text{SbCl}_3 \cdot \text{C}_5\text{H}_5\text{N}$.

Determination of Cell Dimensions and Space Group.

A 15° oscillation photograph about the a axis taken at room temperature using MoK_α radiation showed no symmetry above and below the zero-layer line. A zero layer Weissenberg photograph (Ok1) about a showed symmetry across both axes. A first layer Weissenberg photograph (1kl) about a showed symmetry across only one (c) axis. The symmetry of the Weissenberg and oscillation photographs indicated that the crystal belonged to the monoclinic system.

The systematic absences were as follows:

hkl : no conditions, indicating a primitive cell;

h0l : when $l = 2n + 1$, indicating a c glide plane perpendicular to b;

Ok0 : when $k = 2n + 1$, indicating a 2_1 screw axis parallel with the b axis.

The space group is thus $\text{P}2_1/\text{c}$.

Room temperature cell dimensions were measured from films taken with MoK_α radiation. ξ_b was measured from a 15° oscillation photograph about the b axis and ξ_a , ξ_c and β were measured from a 180° zero level Weissenberg photograph about the b axis. Low temperature cell dimensions (at -110°C) were measured from MoK_α data as follows: ξ_a from a zero layer Weissenberg

TABLE 42(a) - ROOM TEMPERATURE CELL DIMENSIONS, $\text{SbCl}_3\text{O}_5\text{H}_5\text{N}$.

From 15° oscillation photo about a:

n	Sn(mm)	Σ_n (r.l.u.)	Σ_a (r.l.u.)	Mean Σ_a (r.l.u.)	a(Å)
± 3	9.70±0.10	0.1668±0.0012	0.05556±0.0006		
± 4	13.10±0.10	0.2230±0.0016	0.0557±0.0004		
± 5	16.60±0.10	0.2782±0.0016	0.0556±0.0003		
± 6	20.20±0.10	0.3324±0.0016	0.0554±0.0003	0.0555±0.0003	13.00±0.06
± 7	24.10±0.10	0.3878±0.0016	0.0554±0.0002		
± 8	28.30±0.10	0.4428±0.0016	0.0554±0.0002		
± 9	32.80±0.10	0.4967±0.0014	0.0552±0.0002		

From 15° oscillation photo about b:

n	Sn(mm)	Σ_n (r.l.u.)	Σ_b (r.l.u.)	Mean Σ_b (r.l.u.)	b(Å)
± 4	9.20±0.10	0.1585±0.0018	0.0396±0.0005		
± 5	11.60±0.10	0.1985±0.0018	0.0397±0.0004		
± 6	14.00±0.10	0.2374±0.0016	0.0396±0.0003		
± 7	16.70±0.10	0.2798±0.0016	0.0400±0.0003	0.0398±0.0003	17.87±0.10
± 8	19.30±0.10	0.3192±0.0016	0.0399±0.0002		
± 9	22.00±0.10	0.3584±0.0016	0.0398±0.0002		

TABLE 12(a) (continued)

From h01 Weissenberg about b:

n	Sn(mm)	θ_n (deg.)	ζ_n (r.l.u.)	ζ_c (r.l.u.)	Mean ζ_c (r.l.u.)	$c(\text{\AA})$
± 4	14.65 ± 0.10	7.33 ± 0.05	0.2553 ± 0.0018	0.0638 ± 0.0005		
± 5	18.40 ± 0.10	9.20 ± 0.05	0.3198 ± 0.0018	0.0639 ± 0.0004	0.0639 ± 0.0004	12.17 ± 0.06
± 6	22.10 ± 0.10	11.05 ± 0.05	0.3833 ± 0.0018	0.0639 ± 0.0003		

L Dist. between axes (mm)

Mean Ang. Dist. (mm)

 β^* (deg.) β (deg.) $49.30 \rightarrow 75.60 = 26.30 \pm 0.10$ $49.50 \rightarrow 75.65 = 26.35 \pm 0.10$ $49.35 \rightarrow 75.65 = 26.30 \pm 0.10$ 29.41 ± 0.11 $58^\circ 14' \pm 14'$ $121^\circ 11' \pm 14'$

TABLE 12(b)

LOW TEMPERATURE CELL DIMENSIONS, SbCl₃ PYRIDINE (-110°C)

From Okl Weissenberg Photo about a.

n	Sn (mm)	En (deg)	ζ_n (r.l.n.)	ζ (r.l.n.)	Mean ζ (r.l.n.)	Axes, c(Å)
± 8	18.20 \pm 0.10	9.10 \pm 0.05	0.3163 \pm 0.0018	$\zeta_b = 0.0395 \pm 0.0002$		
± 10	22.85 \pm 0.10	11.43 \pm 0.05	0.3965 \pm 0.0018	$\zeta_b = 0.0396 \pm 0.0002$	$\zeta_b = 0.0396 \pm 0.0002$	$b = 17.95 \pm 0.07$
± 14	32.20 \pm 0.10	16.10 \pm 0.05	0.5546 \pm 0.0016	$\zeta_b = 0.0396 \pm 0.0001$		
± 16	36.95 \pm 0.10	18.48 \pm 0.05	0.6341 \pm 0.0016	$\zeta_b = 0.0396 \pm 0.0001$		

± 2	7.90 \pm 0.10	3.95 \pm 0.05	0.1378 \pm 0.0018	$\zeta_c = 0.0689 \pm 0.0009$		
± 4	15.80 \pm 0.10	7.90 \pm 0.05	0.2749 \pm 0.0018	$\zeta_c = 0.0687 \pm 0.0005$	$\zeta_c = 0.0688 \pm 0.0006$	$c = 12.05 \pm 0.10$
± 6	23.75 \pm 0.10	11.88 \pm 0.05	0.4119 \pm 0.0018	$\zeta_c = 0.0686 \pm 0.0003$		

From hko Weissenberg about c

n	Sn (mm)	En (deg)	ζ_n (r.l.n.)	ζ (r.l.n.)	Mean ζ (r.l.n.)	a(Å)
± 4	14.55 \pm 0.10	7.28 \pm 0.05	0.2534 \pm 0.0018	$\zeta_a = 0.0634 \pm 0.0005$		
± 6	22.00 \pm 0.10	11.00 \pm 0.05	0.3816 \pm 0.0018	$\zeta_a = 0.0636 \pm 0.0003$	$\zeta_a = 0.0635 \pm 0.0004$	13.06 \pm 0.10
± 7	25.65 \pm 0.10	12.83 \pm 0.05	0.4442 \pm 0.0018	$\zeta_a = 0.0635 \pm 0.0003$		

From lkl Weissenberg Photo about a: Angular log for β .

L Dist.	between reflns. (mm)	Angle at Origin (deg)	S(r.l.n.)	Mean S(r.l.n.)	β (deg)
$\overline{115}$	$\overline{115} = 27.30 \pm 0.10$	14.60 \pm 0.20	0.0360 \pm 0.0035		
$\overline{116}$	$\overline{116} = 6.00 \pm 0.10$	12.00 \pm 0.20	0.0349 \pm 0.0044	0.0347 \pm 0.0042	122 $^\circ$ 1'1 $''$
$\overline{117}$	$\overline{117} = 5.05 \pm 0.10$	10.10 \pm 0.20	0.0332 \pm 0.0048		

photograph about the a axis. β^* was computed by means of an angular lag method⁸⁵, the relevant measurements for which were made from a first level Weissenberg photograph about the a axis. All measurements from films were made with a film measuring device incorporating a sliding vernier millimetre scale. Room temperature and low temperature cell dimensions are summarised in Tables 12(a), 12(b).

Interpretation of the Patterson Vector Map.

The following three dimensional data, taken using zirconium-filtered MoK_α radiation, was collected: at room temperature, Weissenberg levels (h0l) to (h8l) about b and cross-level (2kl) about a; and at low temperature, levels (hk0) to (hk4) about c and cross-levels (0kl) and (1kl) about a. In all cases a two-film pack was used to record the data (Ilford Industrial G and B films).

The intensities were estimated by means of a calibrated intensity wedge. The estimated intensities were corrected for Lorentz and polarisation effects, but no absorption corrections were applied. The corrected intensities were put on a relative arbitrary scale with reference to cross-levels. For F_0 see Appendix IV.

A Patterson projection down the a axis was computed using low temperature (0kl) data, and the best interpretation of this map was in terms of two independent antimony atoms. This interpretation was supported by a further Patterson projection down b, using (h0l) room temperature data.

A three dimensional Patterson map computed using room

temperature b axis data (h01 - h81) was best interpreted in terms of two independent antimony atoms, and the coordinates of these were in agreement with those obtained from the two projections. The fractional coordinates of the antimony atoms were :- x: 0.1440, y: 0.0362, z: 0.2143; and 0.4475, 0.1001, 0.4571.

CHAPTER VII.

The Structure of the Complex $2\text{SbCl}_3 \cdot \text{C}_5\text{H}_5\text{N}$.

Determination of Cell Dimensions and Space Group.

A 15° oscillation photograph about the b axis was taken at room temperature using zirconium-filtered $\text{MoK}\alpha$ radiation, and it was found to have no symmetry above and below the zero-layer line. A 180° zero layer Weissenberg photograph ($\text{MoK}\alpha$) showed symmetry above and below the line $\theta = 0^\circ$, but no symmetry across any possible axes. The combined symmetry of the oscillation and Weissenberg photographs indicated that the crystal belonged to the triclinic system. This was confirmed by the nature of the first layer Weissenberg photograph which showed no symmetry across the axes. There were no systematic absences, and the space group was therefore either $P1$ or $P\bar{1}$, the latter being adopted.

The cell dimensions were all determined from room temperature $\text{MoK}\alpha$ data. ζ_b was measured from a 15° oscillation photograph about the b axis. ζ_a , ζ_c and β^* were measured from a zero level $h0l$ Weissenberg photograph. α^* and γ^* were obtained by a graphical angular lag method described by Hulme⁸⁵, measurements being made from a first level ($h1l$) Weissenberg photograph about b. All measurements from films were made by means of a film measuring device incorporating a sliding millimetre scale. The details of the relevant measurements and the final cell

TABLE 13

From 15° Oscillation Photo about b.

n	sn (mm)	ξ_n (r.l.u.)	ξ_b (r.l.u.)	Mean ξ_b (r.l.u.)	b(Å)
± 1	4.55 \pm 0.10	0.0790 \pm 0.0018	0.0790 \pm 0.0018		
± 2	9.15 \pm 0.10	0.1576 \pm 0.0018	0.0788 \pm 0.0009		
± 3	14.15 \pm 0.10	0.2397 \pm 0.0016	0.0799 \pm 0.0005	0.0795 \pm 0.0009	8.92 \pm 0.07
± 4	19.40 \pm 0.10	0.3206 \pm 0.0016	0.0801 \pm 0.0004		

From hol Weissenberg Photo about b

n	Sn (mm)	Θ_n°	ξ_n (r.l.u.)	ξ (r.l.u.)	Mean ξ (r.l.u.)	Axes a, c(Å)
± 2	8.50 \pm 0.10	4.25 \pm 0.05	0.1482 \pm 0.0018	$\xi_a = 0.0741 \pm 0.0009$		
± 3	12.80 \pm 0.10	6.40 \pm 0.05	0.229 \pm 0.0018	$\xi_a = 0.0743 \pm 0.0006$		
± 4	17.10 \pm 0.10	8.55 \pm 0.05	0.2973 \pm 0.0018	$\xi_a = 0.0743 \pm 0.0005$		
± 5	21.45 \pm 0.10	10.73 \pm 0.05	0.3725 \pm 0.0018	$\xi_a = 0.0745 \pm 0.0004$		
± 6	25.70 \pm 0.10	12.85 \pm 0.05	0.4448 \pm 0.0018	$\xi_a = 0.0741 \pm 0.0003$		
± 7	30.10 \pm 0.10	15.05 \pm 0.05	0.5193 \pm 0.0016	$\xi_a = 0.0742 \pm 0.0002$		
± 8	34.65 \pm 0.10	17.33 \pm 0.05	0.5959 \pm 0.0016	$\xi_a = 0.0745 \pm 0.0002$		
± 2	9.35 \pm 0.10	4.68 \pm 0.05	0.1633 \pm 0.0018	$\xi_c = 0.0817 \pm 0.0009$		
± 3	14.05 \pm 0.10	7.03 \pm 0.05	0.2449 \pm 0.0018	$\xi_c = 0.0816 \pm 0.0006$		
± 5	23.50 \pm 0.10	11.75 \pm 0.05	0.4073 \pm 0.0018	$\xi_c = 0.0815 \pm 0.0004$		
					$\xi_a = 0.0743 \pm 0.0005$	a = 10.93 \pm 0.15
					$\xi_c = 0.0816 \pm 0.0006$	c = 9.30 \pm 0.15

TABLE 13 (continued)

From h01 Weissenberg Photo

\perp Dist. between Axes (mm)	Mean Dist. (mm)	Ang. Dist. (mm)	β^* (deg)
71.10	116.70 = 45.60 \pm 0.10		
71.10	116.75 = 45.65 \pm 0.10	51.00 \pm 0.11	78° 0' \pm 14' β = 92° 48' \pm 1°
71.10	116.70 = 45.60 \pm 0.10		

From h11 Weissenberg Photo (Angular lag for α ; γ Graphical Method)

	Dist. (mm)	Ang. Dist. (deg)	α, γ (deg)	α^*, γ^* (deg)
111	111	32.2 0.10		
112	112	28.90 0.10		
013	211	37.10 0.10		
112	211	42.10 84.20		
111	011	44.50 0.10		
211	112	34.10 0.10		
211	211	22.20 0.10		
210	112	21.6 0.10		
211	211	37.00 0.10		
210	212	30.00 0.10		
011	211	35.50 0.10		
211	310	21.70 0.10		
$\delta_{La} = 0.0240 \pm 0.0007$				
$\delta_{Lo} = 0.0400 \pm 0.0007$				
			$\alpha = 105^\circ 48' \pm 1^\circ$	$\alpha^* = 69^\circ 36' \pm 1^\circ$
			$\gamma = 116^\circ 36' \pm 1^\circ$	$\gamma^* = 61^\circ 6' \pm 1^\circ$

dimensions are summarised in Table 13.

Determination of the Structure.

Only a limited amount of data was collected because of the very hygroscopic nature of the material, in consequence of which only two suitable single crystals were obtained. 180° Weissenberg photographs were taken at room temperature about the b axis (h0l-h2l) using zirconium-filtered $\text{MoK}\alpha$ radiation. A two-film pack (Ilford Industrial G and B) was used to record the intensities. The intensities were estimated by using a calibrated intensity wedge. Lorentz and polarisation corrections were applied, but no absorption corrections. No cross-layer data was available for layer scaling, and an arbitrary relative scale based on layer exposure times was calculated.

The cell volume (762 \AA^3) together with the density (2.34) gave a cell weight of 1073. This corresponded to two units of $2\text{SbCl}_3 \cdot \text{C}_5\text{H}_5\text{N}$ per unit cell.

A Patterson projection down b was best interpreted in terms of two independent antimony atoms in the asymmetric unit, in agreement with the cell content found above.

An electron density projection (h0l) about b, phased on the two antimony atoms alone, revealed some of the chlorine positions and the pyridine molecule, but all six chlorines were not revealed unambiguously, subsequent refinement showing them to be apparently erroneous.

A three dimensional Patterson map (computed using h0l to h2l MoK α data) gave x, y and z coordinates for the two antimony atoms, and these were in agreement (for x and z) with those obtained from the h0l projection. A three dimensional electron density map, phased on the two antimony atoms alone, revealed six possible chlorine positions and also the pyridine molecule. The R-factor with all the atomic parameters included in the calculation of structure factors was 24.5%.

Refinement of the Structure

Attempts to refine the coordinates (x, z) using h0l data by the conventional least squares method was beset by the problem that ~~all~~^{none} of the chlorine positions were ~~not~~ known with certainty. In order to overcome the problem of grossly erroneous positional and thermal parameters, a different method

of refinement was attempted in the initial stages. This method, described by Stanley and Bhuija⁹⁹ consists of varying each parameter in turn by a specified distance over a specified area of the unit cell, and after each shift calculating structure factors and the residual $R (= \sum |\Delta F| / \sum |F_o|)$. The best coordinate is taken as that which minimises the residual, ~~$R^2 (= \sum w(\Delta F)^2)$~~ . The advantage of the Stanley method over the least squares method is that a greater initial error is allowed in the positioning of the atoms. The least-squares method applied to a grossly incorrect set of parameters will refine to a minimum value for the residual, R^2 , which may be a false minimum. By suitably choosing the value of the initial parameter shift, Δ , the residual R^2 may be allowed to refine to the best minimum within the range of the shifts, Δ , chosen.

The Stanley method, applied to the h0l data gave an R-factor of 18.7% after five rounds of refinement. Applied to the three dimensional data (304 reflections) five rounds of Stanley refinement gave an R-factor of 18.5%, with the pyridine molecule free. The initial shift value, Δ , was 0.05 Å with all atoms included in the refinement. This is reduced to a half of its starting value on each successive round of refinement.

At this stage, refinement was continued with a least squares method using the "PARIBLES" rigid body Programme described in Chapter IV. After five rounds with the pyridine molecule free, the R-factor was 15.3%. Severe distortion occurred in the pyridine molecule, and it was therefore idealised using the "Mean Plane" programme described in Appendix VI. The R-factor for structure factors calculated using a rigid pyridine molecule was 18.6% after five rounds of least squares refinement.

At this stage, it was found that there was very poor agreement for very high value observed structure factors. This was attributed to the fact that these particular reflections were too strong to be estimated by means of the available intensity wedge, i.e. they lay well beyond the highest value measurable and were given a value of the order of 1.5 times the maximum for the particular wedge. These intensities, a total of 18, were eliminated from the refinement process. Another feature of the refinement at this stage was the failure of the carbon atom temperature factors to refine to a fixed value. Five of the six ring atoms showed large shifts (increases) for B_i . This was interpreted in terms of large vibrations of the ring, and the one atom which had a much lower thermal parameter was thought to

be the nitrogen atom.

The least squares refinement was continued with the above modifications (i.e. elimination of high value intensities and inclusion of the nitrogen atom), and after five rounds (with the ring rigid) the R-factor dropped to 16.2%.

The R-factor after a further three rounds with the pyridine molecule free was 15.5%.

Using the final coordinates (with the ring ideal and rigid) and including the eliminated high value reflections in the computation of structure factors, the R-factor was 20%.

A break-down of the R-factor (rigid ring, high value F's eliminated) over sine θ and F_o ranges is given below. For F_o , see Appendix V. Coordinates are given in Table 14, and bond lengths and angles in Table 15.

Sine Ranges	0.192	0.272	0.333	0.385	0.430
R Factors	19.33	13.46	14.11	18.96	23.87
No. of Reflns.	88	104	61	33	6
Fobs Ranges	150	300	450	600	750
R Factors	32.22	19.27	13.86	13.39	15.90
No. of Reflns.	19	137	105	30	1

Description of the Structure

The structure of the 2:1 complex consists essentially of alternate layers of pyridine molecules and " $\text{Sb}_4\text{Cl}_{12}$ " tetramers. There is no bonding between the pyridine molecules and the antimony atoms, the closest intermolecular approach between pyridine and the tetramers being a distance of 3.31 \AA between $^1\text{C}(1)$ and $^1\text{Cl}'(5)$. These general features are evident in the projection down the b axis shown in Fig 9. Fig 10 shows the numbering scheme and the detailed structure of the " $\text{Sb}_4\text{Cl}_{12}$ " tetramer.

$^4\text{Sb}(1)$ has two short and one long Sb-Cl distance associated with it, $2.36(9) \text{ \AA}$, $2.37(8) \text{ \AA}$, and $2.68(8) \text{ \AA}$. The latter chlorine atom, $^4\text{Cl}(3)$, is involved in an asymmetric halogen bridge between $^4\text{Sb}(1)$ and $^2\text{Sb}(2)$, the distance $^2\text{Sb}(2)-^4\text{Cl}(3)$ being $3.44(8) \text{ \AA}$. A further halogen bridge, through $^2\text{Cl}(4)$, between $^4\text{Sb}(1)$ and $^2\text{Sb}(2)$ has a $^4\text{Sb}(1)-^2\text{Cl}(4)$ distance of $2.96(7) \text{ \AA}$, and a $^2\text{Sb}(2)-^2\text{Cl}(4)$ distance of $3.20(7) \text{ \AA}$. $^4\text{Sb}(1)$ is also linked, through $^4\text{Cl}'(4)$ to $^4\text{Sb}'(2)$, with a distance $^4\text{Sb}(1)-^4\text{Cl}'(4)$ of $2.37(7) \text{ \AA}$.

$^4\text{Sb}'(2)$ has associated with it two short Sb-Cl distances, $2.33(9) \text{ \AA}$ and $2.34(8) \text{ \AA}$, and one exceptionally long one, $^4\text{Sb}'(2)-^4\text{Cl}'(4)$ of $3.20(7) \text{ \AA}$. $^4\text{Cl}'(4)$ is however involved in a Sb-Cl-Sb

bridge between $^4\text{Sb}(1)$ and $^2\text{Sb}^*(1)$ with Sb-Cl distances of $2.17(7)$ Å respectively.

The three Cl-Sb-Cl angles associated with $^1\text{Sb}(1)$ are $93.0(3.5)^\circ$, $97.0(3.5)^\circ$, and $91.2(3.4)^\circ$, and with $^1\text{Sb}^*(2)$, $76.0(3.5)^\circ$, $93.7(3.5)^\circ$, and $87.7(3.4)^\circ$.

$^4\text{Cl}^*(4)$ is a bridging atom which approaches closely (3.20 Å) to a third ($^1\text{Sb}^*(2)$) antimony atom. In this environment, it may be compared with the "three coordinate" chlorine atom in the $2\text{SbCl}_3 \cdot 3\text{pyridine}$ complex (Chapter V).

The coordination about $^4\text{Sb}(1)$ is octahedral, with chlorine atoms occupying the sub-set square planar. $^1\text{Sb}^*(2)$ has a trigonal bipyramidal coordination with an equatorial lone-pair.

The closest approach between tetrameric units is a distance of $3.31(8)$ Å between $^4\text{Cl}(2)$ and $^4\text{Sb}(2)$.

The tetramer " $\text{Sb}_4\text{Cl}_{12}$ ", in terms of the various Sb-Cl distances, is tending to the extreme $(2\text{SbCl}_2^+)(\text{Sb}_2\text{Cl}_8^-)$.

Regarding the structure as ionic favours the short Sb - Cl bonds (2.33°\AA and 2.31°\AA) in the SbCl_2^+ units.

Alternatively the whole antimony/chlorine system may be regarded as an infinite chain, extending along the c axis direction, with the "tetrameric units" linked through $^1\text{Cl}(2)$ in $^1\text{Sb}(1) - ^1\text{Cl}(2) - ^1\text{Sb}(2)$ bridges with Sb-Cl distances of 2.31°\AA and 3.34°\AA . This is illustrated in Fig. 9.

The close C - Cl contact of 3.34°\AA between $^1\text{C}(1)$ and $^1\text{Cl}(1)$ may be compared with the C - Cl contact of 3.24°\AA in the complex $2\text{SbCl}_3 \cdot 3\text{C}_5\text{H}_5\text{N}$.

TABLE 14

(a) Fractional Coordinates for the Complex $2\text{SbCl}_3 \cdot \text{C}_5\text{H}_5\text{N}$

(e.s.d. in brackets; see Fig. 10 for numbering scheme.)

Sb(1)	0.3771(18)	0.0435(29)	0.1539(16)	3.10(44)
Sb(2)	0.3717(18)	0.2734(30)	0.7656(17)	3.07(44)
Cl(1)	0.1467(74)	-0.0050(117)	0.1522(70)	5.4(1.6)
Cl(2)	0.4283(71)	0.1103(118)	0.4230(67)	4.9(1.4)
Cl(3)	0.3197(71)	-0.2953(112)	0.0992(63)	4.6(1.3)
Cl(4)	0.3406(62)	-0.0761(97)	0.8256(57)	2.8(1.0)
Cl(5)	0.3185(73)	0.3576(100)	0.0024(65)	4.8(1.6)
Cl(6)	0.1406(80)	0.0579(110)	0.6475(73)	6.4(1.8)
C (1)	0.196	0.513	0.294	10.9(4.0)
C (2)	0.259	0.671	0.326	13.5(4.0)
C (3)	0.181	0.743	0.362	12.4(4.1)
C (4)	-0.023	0.499	0.335	12.3(3.9)
C (5)	0.055	0.427	0.299	11.5(4.3)
N (1)	0.040	0.656	0.367	8.4(3.7)

(b) Rigid Ring Coordinates (orientational angles and centre of ring)

(angles in degrees, coordinates fractional)

θ	ϕ	ψ
-66.7(0.9)	-75.2(1.1)	-54.0(1.0)
x'	y'	z'
0.118(16)	0.585(21)	0.331(15)

TABLE 15

Bond Distances and Angles.

(e.s.d. in brackets; for numbering scheme see Fig. 10)

$^1\text{Sb}(1) - ^1\text{Cl}(1)$	2.36(9)Å	
$^1\text{Sb}(1) - ^1\text{Cl}(2)$	2.37(8)Å	
$^1\text{Sb}(1) - ^1\text{Cl}(3)$	2.68(8)Å	
$^1\text{Sb}(1) - ^1\text{Cl}'(4)$	2.87(7)Å	
$^1\text{Sb}(1) - ^2\text{Cl}(4)$	2.96(7)Å	
$^1\text{Sb}'(2) - ^1\text{Cl}'(4)$	3.20(7)Å	
$^1\text{Sb}'(2) - ^1\text{Cl}'(5)$	2.31(8)Å	
$^1\text{Sb}'(2) - ^1\text{Cl}'(6)$	2.33(9)Å	
$^1\text{Sb}'(2) - ^2\text{Cl}'(3)$	3.44(8)Å	
$^1\text{C}(1) - ^1\text{C}(2)$	1.377Å	Ideal ring parameter.
$^1\text{Sb}(2) - ^1\text{Cl}(2)$	3.31(8)Å	
$^1\text{C}(1) - ^1\text{Cl}'(5)$	3.31 Å	
$^1\text{Cl}(1) - ^1\text{Sb}(1) - ^1\text{Cl}(2)$	93.0(3.5)°	
$^1\text{Cl}(1) - ^1\text{Sb}(1) - ^1\text{Cl}(3)$	97.0(3.5)°	
$^1\text{Cl}(2) - ^1\text{Sb}(1) - ^1\text{Cl}(3)$	91.2(3.4)°	
$^1\text{Cl}(1) - ^1\text{Sb}(1) - ^1\text{Cl}'(4)$	94.5(3.3)°	
$^1\text{Cl}(1) - ^1\text{Sb}(1) - ^2\text{Cl}(4)$	173.6(3.3)°	
$^1\text{Cl}(2) - ^1\text{Sb}(1) - ^2\text{Cl}(4)$	83.0(3.3)°	
$^1\text{Cl}(3) - ^1\text{Sb}(1) - ^1\text{Cl}'(4)$	80.5(3.4)°	
$^1\text{Cl}(3) - ^1\text{Sb}(1) - ^2\text{Cl}(4)$	78.1(3.4)°	

${}^1\text{Cl}'(4) - {}^1\text{Sb}'(2) - {}^1\text{Cl}'(5)$	87.7(3.4) ^o	
${}^1\text{Cl}'(4) - {}^1\text{Sb}'(2) - {}^1\text{Cl}'(6)$	76.0(3.5) ^o	
${}^1\text{Cl}'(5) - {}^1\text{Sb}'(2) - {}^1\text{Cl}'(6)$	93.7(3.5) ^o	
${}^1\text{Cl}'(5) - {}^1\text{Sb}'(2) - {}^2\text{Cl}'(3)$	96.2(3.4) ^o	
${}^1\text{Cl}'(6) - {}^1\text{Sb}'(2) - {}^2\text{Cl}'(3)$	138.8(3.5) ^o	
${}^1\text{Cl}'(4) - {}^1\text{Sb}'(2) - {}^2\text{Cl}'(3)$	64.6(3.3) ^o	
${}^1\text{Sb}'(2) - {}^1\text{Cl}'(4) - {}^2\text{Sb}'(1)$	105.7(3.4) ^o	
${}^1\text{Sb}'(2) - {}^1\text{Cl}'(4) - {}^1\text{Sb}(1)$	99.8(3.4) ^o	
${}^1\text{Sb}(1) - {}^1\text{Cl}'(4) - {}^2\text{Sb}'(1)$	91.2(3.4) ^o	
${}^1\text{Sb}'(2) - {}^2\text{Cl}'(3) - {}^2\text{Sb}'(1)$	105.9(3.3) ^o	
${}^1\text{Sb}(2) - {}^1\text{Cl}(2) - {}^1\text{Sb}(1)$	148.3(3.5) ^o	
${}^1\text{C}(1) - {}^1\text{C}(2) - {}^1\text{C}(3)$	120 ^o	Ideal ring parameter.

(Legend for numbering (Fig. 10):

(a) pre-superscript indicates symmetry related positions,

$x, y, z; -x, -y, -z.$

(b) dashed superscript indicates shift of cell;

(c) number in brackets following atom symbol is

number of atom in asymmetric unit.)

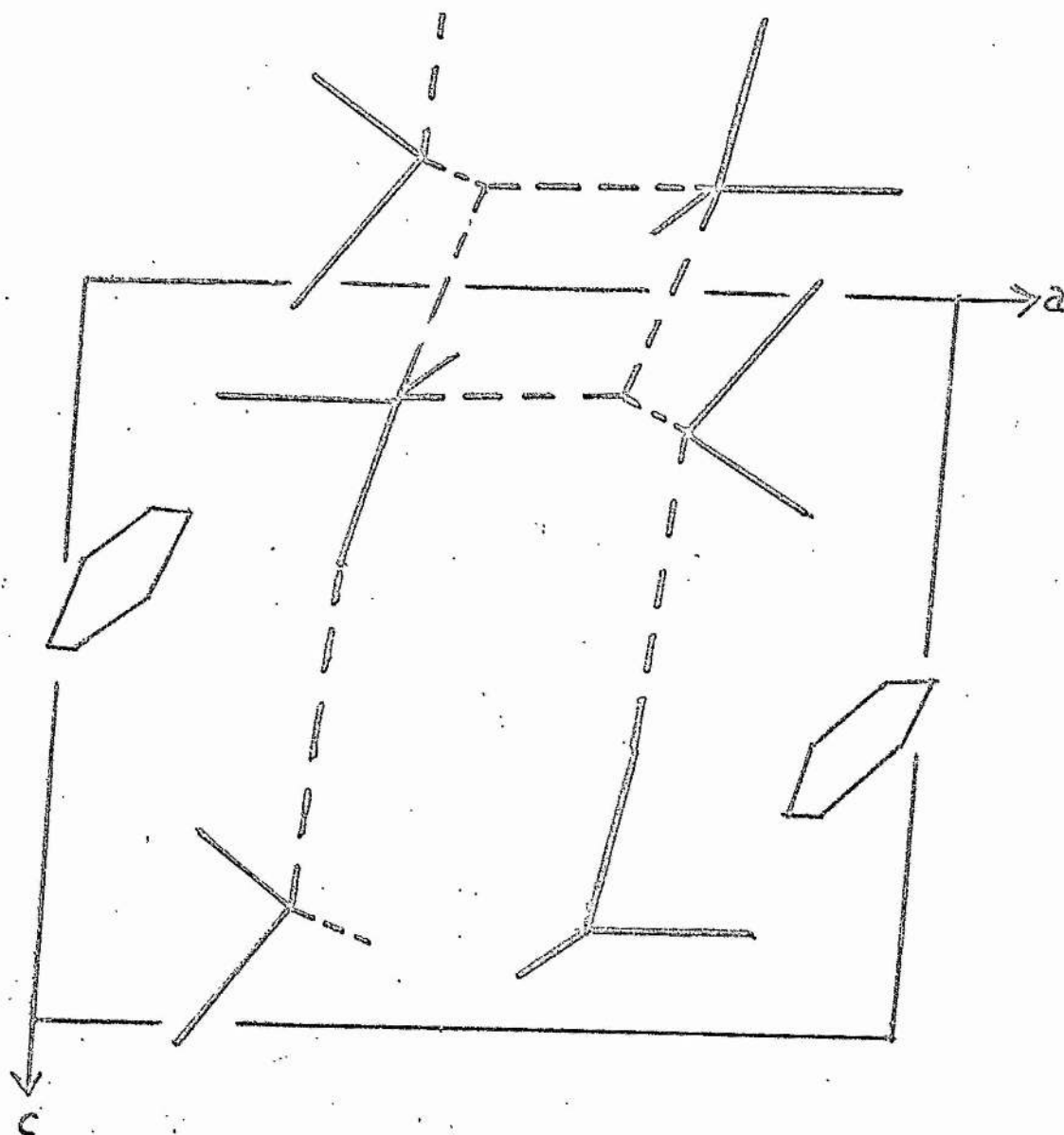


Fig. 9 - h01 Projection, $2\text{SbCl}_3 \cdot 5\text{C}_5\text{H}_5\text{N}$.

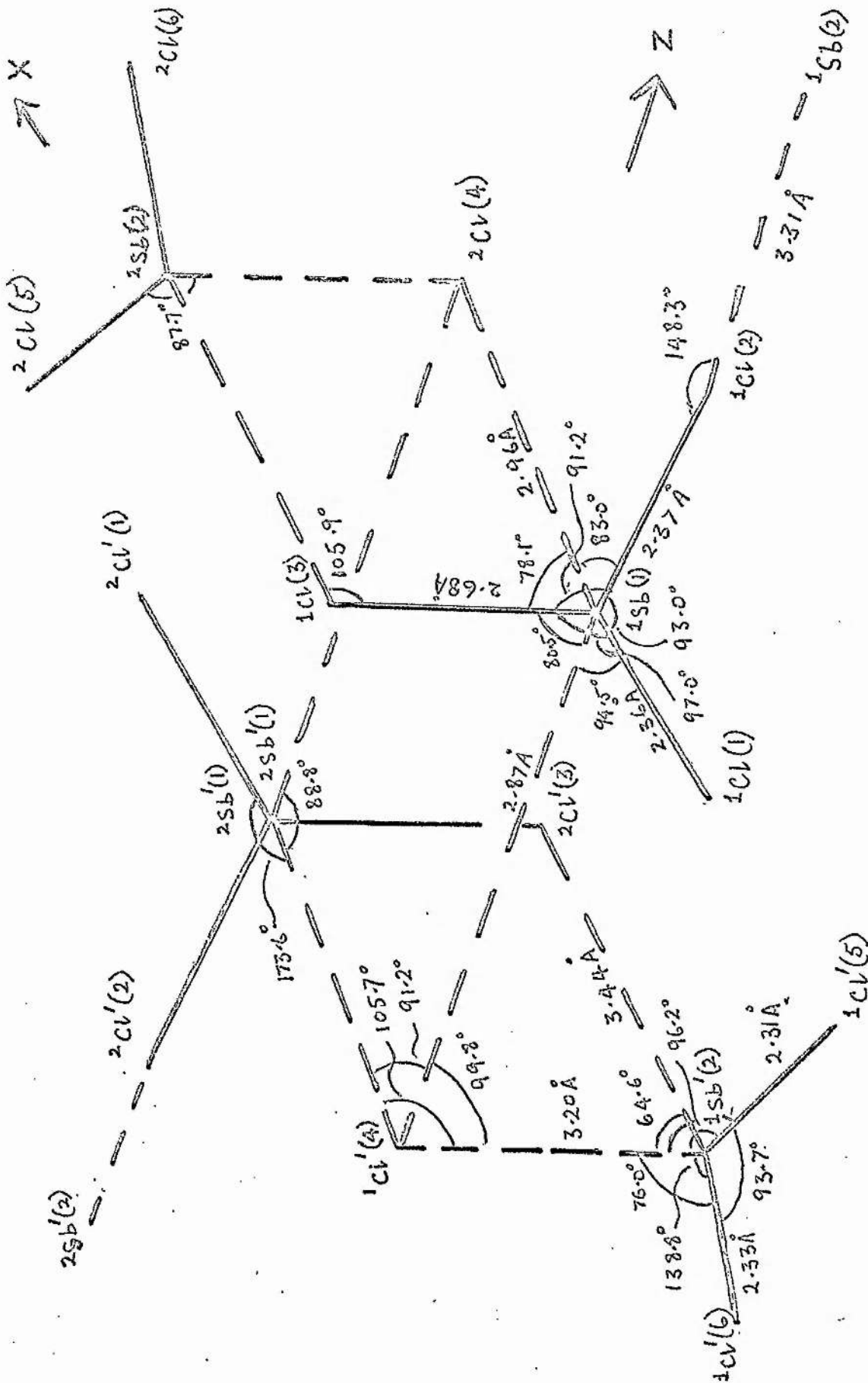


Fig. 10 - Structure of the $\text{Sb}_4\text{Cl}_{12}$ Tetramer in the Complex $2\text{SbCl}_3 \cdot \text{C}_5\text{H}_5\text{N}$

CHAPTER VIII.DISCUSSION AND COMPARISONDiscussion of the complex 2SbCl_3 .p-xylene

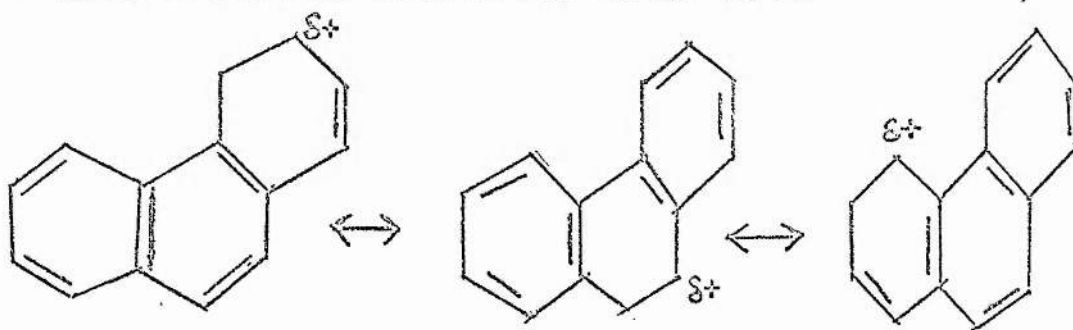
The complex 2SbCl_3 .p-xylene is one of a very large group of antimony trichloride aromatic complexes (summarised in Table 1) which has as a basic structural feature a layer-like lattice with Van der Waals interactions between the SbCl_3 and aromatic molecules.

The antimony trichloride is sp^3 hybridised. The closest Sb-Sb approach (in an "incipient dimer" configuration, see p.59) is 4.24 \AA , and the closest Sb-carbon approach is 3.18 \AA .

The relative orientation of the interacting aromatic and SbCl_3 molecules is illustrated in Fig. 11. A vacant lobe of the SbCl_3 sp^3 orbital is directed towards an aromatic π -orbital which is acting as an "incipient donor". There is a close similarity between the nature of the bonding in the complex 2SbCl_3 .p-xylene and that of the bonding in the complex 2SbCl_3 .naphthalene. Fig. 11 shows the bonding situation for the latter complex for the sake of comparison.

The complex 2SbCl_3 .phenanthrene has recently been investigated by Nardelli⁸⁹, and it affords an interesting comparison with the above mentioned complexes in terms of the nature of the intermolecular interactions. The basic structural feature of alternate layers of

the components is preserved. The antimony trichloride molecules are again found in the "incipient dimer" orientation. However, the closest distance of approach Sb-C is very much less (2.94 \AA) than an accepted Van der Waals distance of 3.5 \AA . The Sb-Cl distances are similar to those found for the p-xylene complex (see p. 61). The short Sb-C distances are interpreted in terms of a greater degree of SbCl_3 -aromatic interaction. The polycyclic aromatic phenanthrene, has a lower ionisation potential than simpler aromatics such as benzene and p-xylene, and consequently acts as a better electron donor. The donor state (D^+) is more highly stabilised for phenanthrene than for p-xylene because of the more extensive conjugation in the polycyclic molecule and the greater delocalisation of the charge (S^+):



Within the p-xylene/ SbCl_3 system itself, two complexes are known, the complex $2\text{SbCl}_3 \cdot \text{p-xylene}$ which is being discussed, and

the complex SbCl_3 p-xylene, investigated by Szymanski⁴¹. These complexes are structurally very similar, and both belong to the space group $P2_1/c$. The p-xylene molecules are situated in the unit cell of the 1:1 complex in fourfold general positions. To accommodate the additional p-xylene molecules, the z axis is longer in the 1:1 unit cell by an amount corresponding to the length of one p-xylene molecule. The cell dimensions of both complexes (at room temperature) are given below for comparison.

	$2\text{SbCl}_3 \cdot \text{p-xylene}$	$\text{SbCl}_3 \cdot \text{p-xylene}$
a	$9.18 \pm 0.07 \text{ \AA}$	$9.45 \pm 0.01 \text{ \AA}$
b	$8.54 \pm 0.04 \text{ \AA}$	$8.63 \pm 0.01 \text{ \AA}$
c	$13.06 \pm 0.13 \text{ \AA}$	$17.65 \pm 0.02 \text{ \AA}$
β	$124^\circ 43' \pm 1^\circ$	$127^\circ \pm 15'$

Fig. 12 shows projections down the b axis (h0l) for both complexes for the sake of comparison.

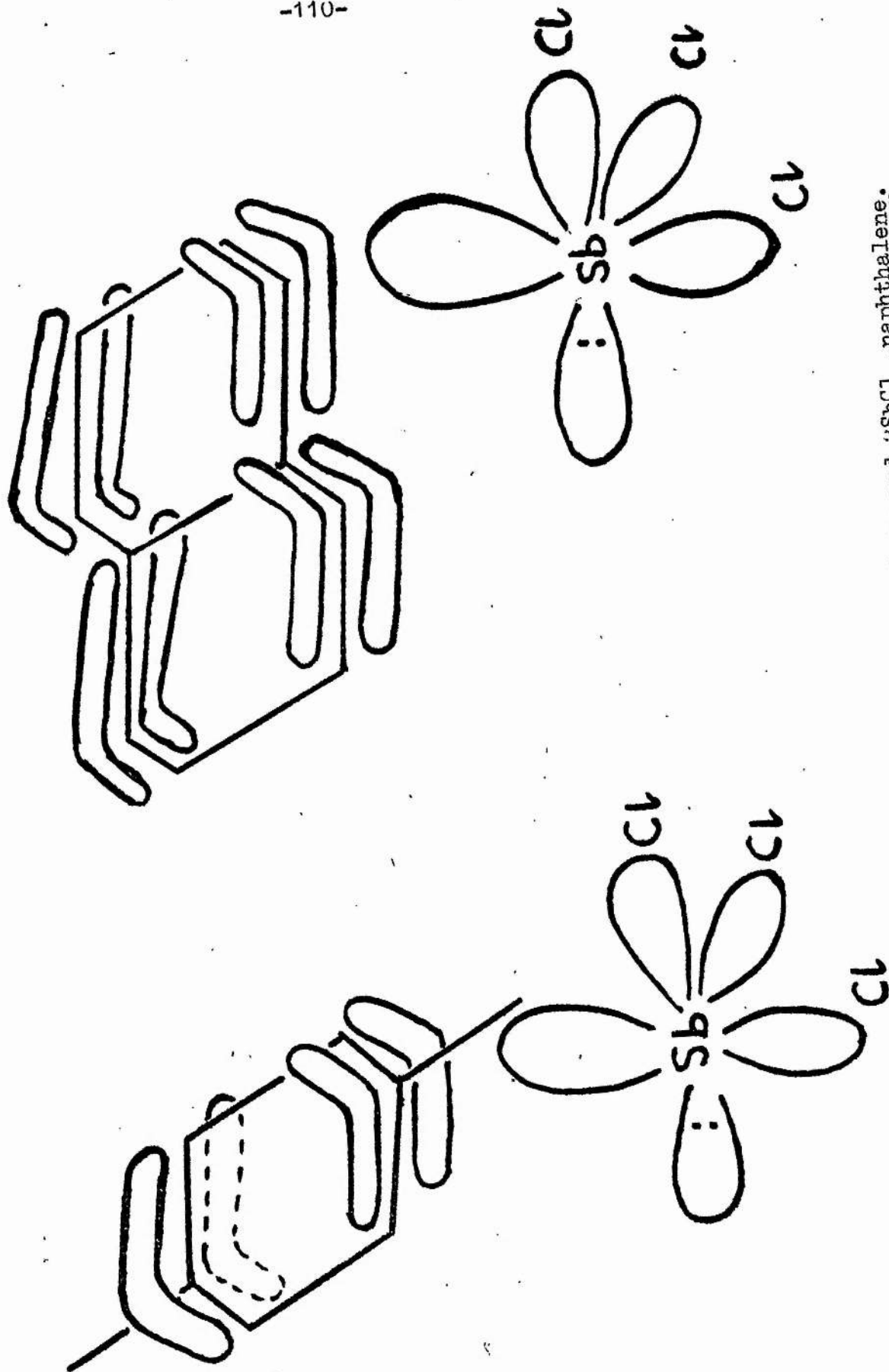


Fig. 11 - Orientation of orbitals in $2\text{SbCl}_3 \cdot \text{p-xylene}$ and $2\text{SbCl}_3 \cdot \text{naphthalene}$.

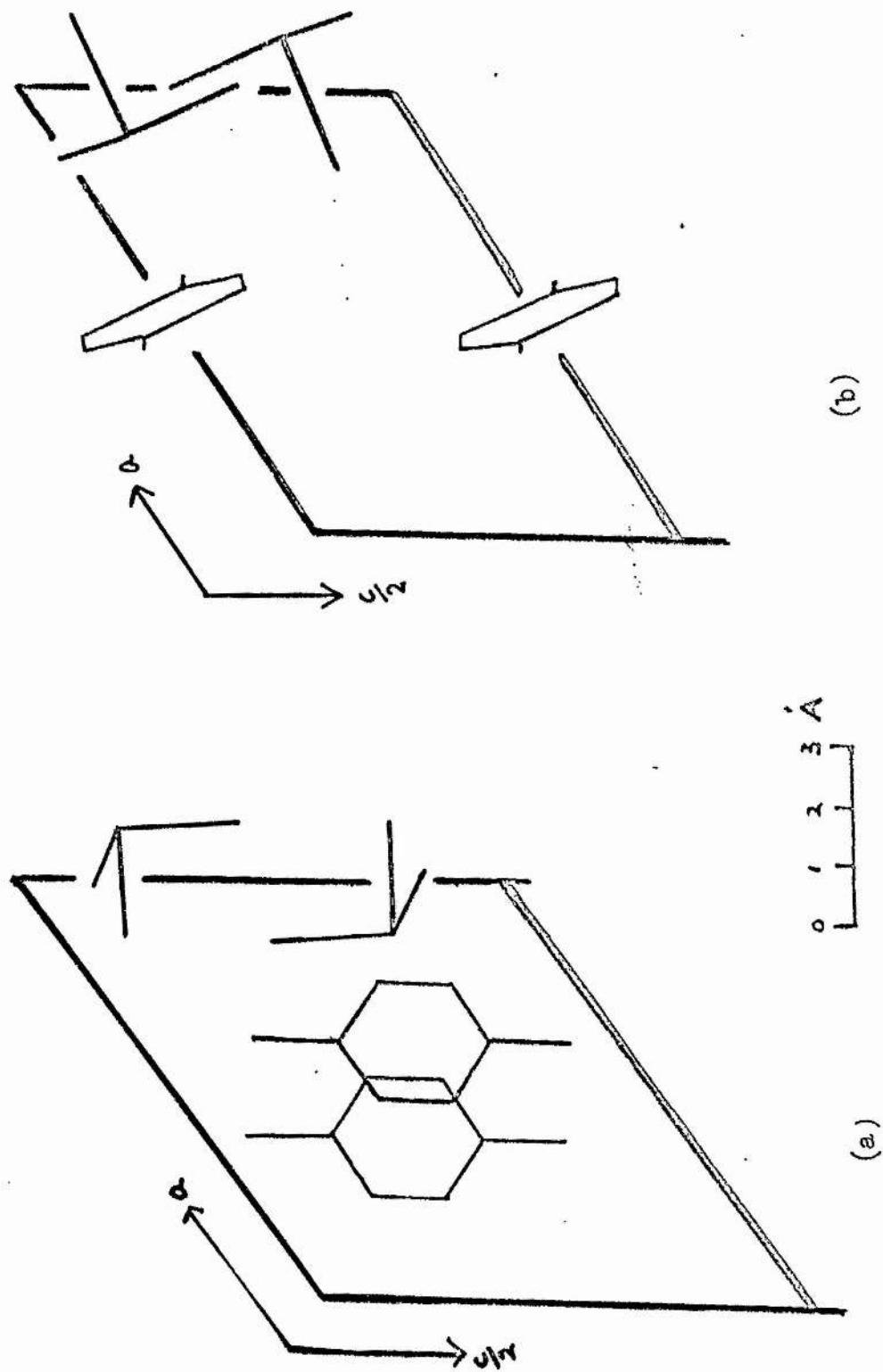


Fig. 12 - $h0l$ Projections of (a) $SbCl_3 \cdot p\text{-xylene}$ and (b) $2SbCl_3 \cdot p\text{-xylene}$.

Discussion of the Complexes $2\text{SbCl}_3 \cdot 3\text{C}_5\text{H}_5\text{N}$ and $2\text{SbCl}_3 \cdot \text{C}_5\text{H}_5\text{N}$

The prominent feature of the 2:3 complex, in terms of the bonding of the pyridine molecules, is the dual role which these molecules play in the structure, i.e. as a donor species bound to the antimony atom and as a free "solvating" molecule. Other examples of this type of complex have been outlined in the "Introduction", (see p. 19).

Another feature worthy of note is the nature of the halogen bridge. In the 2:3 complex this is an asymmetric bridge involving the Sb atom which is not bound to pyridine, and having Sb-Cl bond lengths of 2.75 Å and 2.99 Å and a Sb-Cl-Sb angle of 95.2°. However, the Sb atom bound to pyridine is only 3.00 Å away from the bridging chlorine atom. The coordination about this chlorine atom is therefore 3-fold.

If we consider the simple 2-fold bridge, close comparison in terms of bond length and Sb-Cl-Sb angle can be made with the compound $\text{C}_5\text{H}_5\text{NH}^+\text{SbCl}_4^-$ (see Chapter III). This latter compound also has a chain-like anion with an asymmetric halogen bridge with Sb-Cl bond lengths of 2.64 Å and 3.12 Å and a Sb-Cl-Sb angle of

95.6°. This is in line with the idea of regarding the complex $2\text{SbCl}_3 \cdot 3\text{pyridine}$ as essentially ionic (or tending to ionic), in terms of such units as $(\text{SbCl}_2\text{py}_2^+ \text{SbCl}_4^-)$, py.

Viewing the chlorine as three-coordinate, we have for comparison such examples as the Cadmium chloride structure and the mercuric bromide structure. In the CdCl_2 layer lattice, each chlorine atom is 2.74 Å away from three cadmium atoms at the base of a trigonal pyramid⁹⁰. In HgBr_2 the three relevant HgBr bond lengths are 2.48 Å, 3.23 Å and 3.23 Å⁹¹. In the compound NH_4HgCl_3 , we have a Cl coordination which is tending to an ionic Cl^- species. Here the Cl atom has four Hg nearest neighbours at distances of 2.96 Å away and situated at the corners of a square of which the Cl atom is the centre⁹². Certain features of the complex $2\text{SbCl}_3 \cdot 3$ pyridine allow us to draw limited comparisons with other molecular complexes, in the sense that the α -pyridine molecules are stacked plane-to-plane after the fashion of "polarisation bonded" complexes, and the SbCl_4 chains are surrounded by pyridine molecules in the form of "channels" running down the c axis (like the "channel" type complexes outlined in the "Introduction".)

The complex $2\text{SbCl}_3 \cdot \text{pyridine}$ shows two basic features in common with the 2:3 complex. One of these features is the existence

of a pyridine molecule in a packing role in both the structures. The other common feature is the extensive halogen bridging within the SbCl_3 system, in the 2:3 complex leading to an infinite chain, and in the 2:1 to a bridged tetramer, $\text{Sb}_4\text{Cl}_{12}$.

Two features of interest remain: the geometry of the " SbCl_3 molecules" and the Sb-pyridine bonding. These are discussed with reference to the SbCl_3 /p-xylene⁴¹ and SbCl_3 /aniline^{77,93} systems.

Comparison of the Systems SbCl_3 /pyridine, SbCl_3 /aniline, and SbCl_3 /p-xylene.

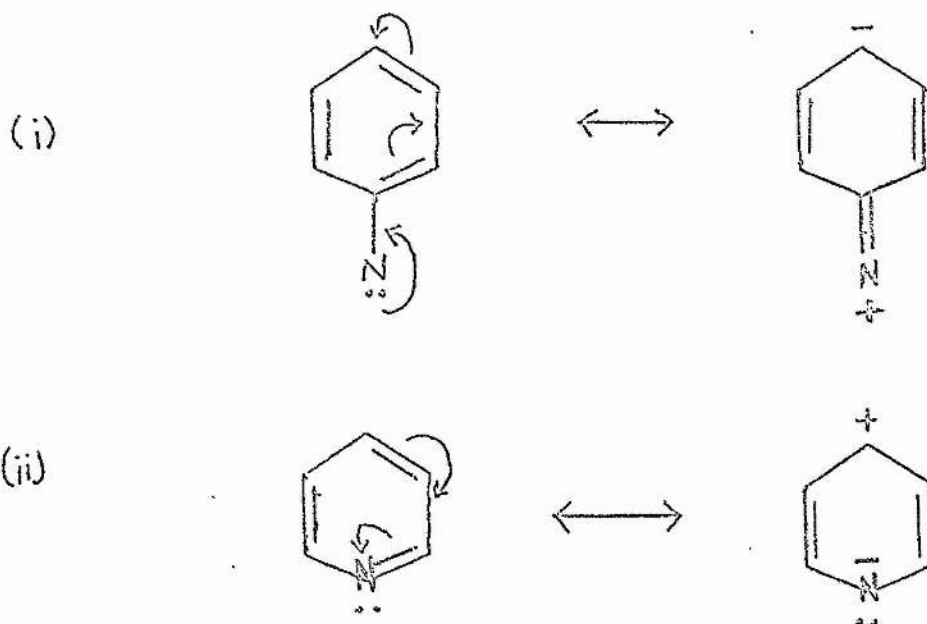
A closer comparison can be made between the two nitrogen containing aromatics than between these and the p-xylene system, because of the existence of lone-pair interactions in the first two systems.

In particular, reference is made to the compounds $2\text{SbCl}_3 \cdot 3$ pyridine, $2\text{SbCl}_3 \cdot \text{pyridine}$, $\text{SbCl}_3 \cdot \text{aniline}$, and $\text{SbCl}_3 \cdot 2$ aniline.

The Sb-N bond lengths in the 2:3 pyridine complex are 2.27 (10) Å and 2.49 (9) Å, while in the 1:1 aniline complex it is 2.53 (5) Å and in the 1:2 aniline complex it is 2.64 (5) Å. The aniline-Sb bond length is thus rather longer than one of the pyridine-

Sb bond lengths, but of the same order of magnitude as the other. In general, pyridine is a stronger donor than aniline because of the possibility of π -back bonding involving low-energy 3d orbitals of the antimony atom and π^* anti-bonding orbitals of the pyridine molecule. This π contribution would therefore be expected to lead to a shorter bond for pyridine. All of the Sb-N bonds, however, are much longer than the sum of the single-bond covalent radii⁹⁴ of the two atoms Sb, N, which has a value of 2.10 Å. Lengthening of the Sb-N bond beyond this value would be expected because of such effects as an ionic contribution and higher coordination about the antimony atom. An example for comparison, where the nitrogen donor atom is not part of an aromatic molecule, is found in the octahedral antimony complex $\text{SbCl}_5 \cdot \text{S}_4\text{N}_4$ ⁹⁵, which has a Sb-N bond length of 2.17 Å.

The availability of the lone pair for donation at the pyridine nitrogen appears to be greater than for the aniline nitrogen, in terms of calculated electron densities at atomic sites within the molecules⁹⁶. This may be accounted for by the resonance effects:



A point of contrast is the stereochemistry of the ligand coordination in the two cases. In the 2:3 pyridine complex we find trans coordination of the pyridine molecules, while in the 1:2 aniline complex the coordination of the aromatic is cis. It would be expected that cis bonding for pyridine would be less favoured than for the aniline case because of the greater stereochemical hindrance of the former. This greater hindrance arises for two reasons. Firstly, the aniline nitrogen atom is further from the aromatic ring than in the pyridine case. Secondly the sp^3 orbital of the $-NH_2$ group which is occupied by the lone-pair is directed at an angle to the plane of the molecule.

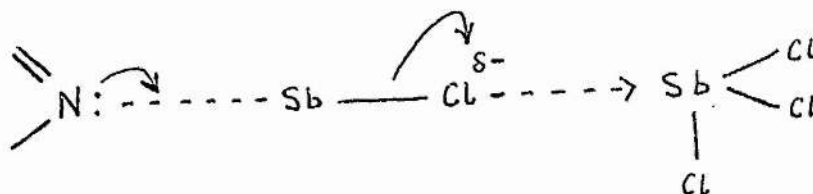
The antimony atoms in the 2:3 pyridine complex both have octahedral coordination. For one antimony atom, chlorine atoms

occupy the sub-set square pyramidal. This compares with the situation in the 1:2 aniline complex where the coordination for antimony is similar, two of the positions being occupied by nitrogen instead of chlorine. The other antimony atom in the 2:3 pyridine complex has trans bonded pyridine molecules. The lone-pair and chlorine atoms are in a plane perpendicular to the N-Sb-N direction. In contrast, the 1:1 aniline complex has a trigonal bipyramidal coordination about antimony with an equatorial lone-pair. In the Sb_4 tetramer of the 2:1 pyridine complex, one antimony atom has an octahedral coordination with the lone-pair occupying one of the apices of the distorted octahedron. The other antimony atom has a trigonal bipyramidal arrangement of chlorine atoms, with an equatorial lone-pair.

The promotion energy required to involve d orbitals in Sb-N bonding (i.e. in sp^3d^2 hybridisation) is offset by the energy gained from the formation of the Sb-N bond, and the additional lattice energy due to pyridine occurring in the solid state.

A further point of contrast between the two systems is the occurrence of extensive halogen bridging in both the 2:3 and 2:1 pyridine complexes, a feature not observed with the aniline complexes. This effect may also be explained, for the 2:3 complex, in terms of

the much greater donor strength of pyridine compared with aniline, leading to a greater lengthening (weakening) of Sb-Cl bonds, and hence to a tendency to bridge, represented schematically as:



Scruton⁹³ reports short N-Cl intramolecular distances (3.26 Å and 3.25 Å) and intermolecular distances (3.21 Å) in the 1:1 aniline complex, and this situation is found in the 2:3 pyridine complex where a "C-Cl" distance of 3.21 Å occurs. This "carbon" atom occurs in the non-bonding pyridine molecule and it is possible that it is in fact the nitrogen atom. However, such N-Cl bonds have previously been interpreted in terms of hydrogen bonding⁹⁷, whereas a pyridine N-Cl bond cannot obviously be due to such hydrogen bonding. Any pyridine N-Cl interaction would probably involve a donor-acceptor nature with Cl d orbitals being utilised to accept electrons. Such donor-acceptor interactions would be weak and of the charge-transfer type as in pyridine/halogen complexes

(see "Introduction", p.23). However, short C-Cl distances are also possible⁹⁸ and are explained in terms of hydrogen bonding.

In the p-xylene/SbCl₃ system, the aromatic molecule is acting more as a solvating molecule than as a ligand, such interaction as there is being weak, and intermolecular distances being of the order of a Van der Waals distance. A feature in common for p-xylene, aniline and pyridine systems is that a layer-like nature can be discerned in all of them. It is an obvious feature in the p-xylene system because of the lack of intermolecular bonding, but it nevertheless exists in the latter two systems.

In contrast to the p-xylene system, the aniline and pyridine systems have two possible functional groups for interaction with SbCl₃: a lone pair of electrons as well as the aromatic π -system. The aniline molecule appears to behave as a ligand, utilising its lone-pair. The pyridine molecule behaves like the aniline molecule in that it forms lone-pair bonds to antimony, as in the 2:3 complex with pyridine, and like the p-xylene in that it can act as a solvating molecule with only Van der Waals interaction, as in both the 2:1 and 2:3 pyridine complexes.

REFERENCES.

- (1) Addison W. E., "Structural Principles in Inorganic Chemistry",
Longmans, 1961, p. 51.
- (2) London F, Trans. Farad. Soc., 1937, 33, 8.
- (3) Keesom W. H., Physik. Z., 1922, 23, 225.
Ibid., 1921, 22, 643.
- (4) Debye P., Physik Z., 1920, 21, 178.
Ibid., 1921, 22, 302.
- (5) Mulliken R., J.A.C.S., 1952, 74, 811.
J. Phys. Chem., 1952, 56, 801.
J. Chem. Phys., 1955, 23, 397.
- (6) Briegleb G., Z. Physikal. Chem., 1936, B31, 58.
Ibid., 1937, B32, 305.
- (7) Pauling L., Proc. Nat. Acad. Sc. U.S., 1939, 25, 581.
- (8) Weiss J., J.Chem. Soc., 1942, 245.
- (9) Brackman W., Rec. Trav. Chim., 1949, 68, 147.
- (10) Chatt J., Nature, 1950, 165, 637.
- (11) Craig D.P., Maccoll A., Nyholm R.S., Orgel L.E., Sutton L.E.,
J. Chem.Soc., 1954, 332.
- (12) Craig D.P., Nyholm R.S., "Chelating Agents and Metal Chelates",
Ed. Dwyer and Mellor, 1968, p. 83.
- (13) von Stackelberg M., Muller H.R., J. Chem. Phys., 1951, 19, 1319.
- (14) Powell H.M., Research, 1948, 1, 353.
- (15) Powell H.M. , J. Chem. Soc., 1948, 61.
- (16) Powell H.M., J. Chem. Soc., 1950, pp. 298, 300, 468.

- (17) Powell H.M., J. Chem. Soc., 1954, 2658.
- (18) Palin D.E., Powell H.M., J. Chem. Soc., 1947, 208.
- (19) Palin D.E., Powell H.M., J. Chem. Soc., 1948, pp. 571, 815.
- (20) Newman A.C.D., Powell H.M., J. Chem. Soc., 1952, 3747.
Lawton D., Powell H.M., J. Chem. Soc., 1958, 2339.
- (21) Powell H.M., Rayner J.H., Nature, 1949, 163, 566.
- (22) Rayner J.H., Powell H.M., J. Chem. Soc., 1952, 319.
- (23) Robertson J.M., "Organic Crystals and Molecules",
Cornell Univ. Press, 1953, pp. 254, 255.
- (24) Schlenk W., Annalen, 1949, 565, 204.
- (25) Smith A.E., Acta Cryst., 1952, 5, 224.
- (26) Powell H.M., Huse G., Cooke P.W., J. Chem. Soc., 1943, 153.
- (27) Powell H.M., Huse G., J. Chem. Soc., 1943, 435.
- (28) Saunder D.H., Proc. Roy. Soc., 1946, A188, 31.
- (29) Saunder D.H., Proc. Roy. Soc., 1947, A190, 508.
- (30) Van Niekerk J.N., Saunder D.H., Acta Cryst., 1948, 1, 44.
- (31) Menshutkin B.N., Chem. Zentr., 1910, 578.
- (32) Menshutkin B.N., J. Chim. Phys., 1912, 9, 314.
- (33) Menshutkin B.N., J. Russ. Phys. Chem. Soc., 1912, 43, 1805.
- (34) Menshutkin B.N., Ibid., , 1329.
- (35) Menshutkin B.N., Chem. Zentr., 1912, 806.
- (36) Menshutkin B.N., J. Russ. Phys. Chem. Soc., 1913, 44, 1079.
- (37) Ewell R.H., J. Chem. Phys., 1937, 5, 967.

- (38) Shinomiya C., J. Chem. Soc. Japan, 1938, 29, 1165.
- (39) Ashkanazi M.S., Kornosova P.V., Finkelstein V.S.,
J. Phys. Chem. U.S.S.R., 1936, 7, 438.
- (40) Raskin S.S., Doklady Akad. Nauk. S.S.S.R., 1955, 100, 485.
Optika i Spectroscopiya, 1956, 1, 576.
Fiz. Sbornik Lvov Univ., 1957, 3, 203.
Doklady Akad. Nauk. S.S.S.R., 1958, 123, 645.
- (41) Szymanski J.T., Ph.D. Thesis, University of London, 1963.
- (42) Jayaweera S.A.A., M.Sc. Thesis, University of London, 1964.
- (43) Hursthouse M.B., Ph.D. Thesis, University of London, 1965.
- (44) Moss D.S., Ph.D. Thesis, University of London, 1967.
- (45) Lindqvist I., Niggli A., J. Inorg. and Nucl. Chem.,
1956, 2, 345.
- (46) Perkampus H.H., Baumgarten E., Z. Phys. Chem., 1963, 32, 1.
Z. Phys. Chem., 1964, 40, 144.
- (47) Grechischkin V.S., Kyuntsel I.A., Sov. Phys. Solid State,
1963, 5, 694.
Optics and Spectr., 1963, 15, 453.
- (48) Grechischkin V.S., Kyuntsel I.A., Chem. Abs., 67, 77742j(1967)
- (49) Atkinson J.R., Jones T.P., Baughan E.C.,
J. Chem. Soc., 1964, 5808.
- (50) Gerbier J., Compt. Rend., 1966, 262B, 685.
- (51) Borodin P.M., Kondratenkov G.P., Yad. Magn. Rezonans,
1968, Leningrad. Gos. Univ., 2, 76.

- (52) Cameron A.F., Forrest K.P., Nuttall R.H., Taylor D.W.,
Chem. Comm., 1970, 210.
- (53) Rogers D., et al., Chem. Comm., 1969, 1383.
- (54) Stalick J.K., Ibers J.A., Inorg. Chem., 1970, 9, 453.
- (55) Powell H.M., Yasin Y.M.G., Hodder O.J.R.,
Chem. Comm., 1966, 705.
- (56) Lever A.B.P., Lewis J., Nyholm R.S., J. Chem. Soc., 1963, 5042.
- (57) Hanotier J., de Radzitzky P., Nature, 1966, 210, 944.
- (58) Drew M.G.B., Lewis D.F., Walton R.A., Inorg. Nucl. Chem. Letters,
1970, 6, 163.
- (59) Benezi H.A., Hildebrand J.H., J.A.C.S., 1948, 70, 2832.
Ibid., 1949, 71, 2703.
- (60) Mulliken R.S., J.A.C.S., 1950, 72, 600.
- (61) Ferguson E.E., J. Chem. Phys., 1956, 25, 577.
- (62) Hanna M.W., Williams D.E., J.A.C.S., 1968, 90, 5358.
- (63) Yagi Y., Popov A.I., Person W.B., J. Phys. Chem.,
1967, 71, 2439.
- (64) Mulliken R.S., Person W.B., Ann. Rev. Phys. Chem.,
1962, 13, 107.
- (65) Hassel O., Hope H., Acta Chem. Scand., 1961, 15, 407.
- (66) Strieter F.J., Templeton D.H., J. Chem. Phys., 1962, 37, 161.
- (67) Hassel O., Strømme K., Acta Chem. Scand., 1959, 13, 1781.
- (68) Hassel O., Acta Chem. Scand., 1954, 8, 873.
- (69) Hassel O., Strømme K., Acta Chem. Scand., 1959, 13, 215.
- (70) Wallwork S.C., J. Chem. Soc., 1961, 494.

- (71) Wallwork S.C., Acta Cryst., 1954, 7, 648.
- (72) Wallwork S.C., Harding M., Acta Cryst., 1955, 8, 787.
Jones N.D., Marsh R.E., Acta Cryst., 1962, 15, 809.
- (73) Wallwork S.C., Harding M., Nature, 1953, 171, 40.
Acta Cryst., 1953, 6, 791.
- (74) de Santis F., et al., Nature, 1961, 191, 900.
- (75) Kinell P., Lindqvist I., Zackrisson M., Acta Chem. Scand.,
1959, 13, 1159.
- (76) Zackrisson M., Alden K.I., Acta Chem. Scand., 1960, 14, 994.
- (77) Scruton J., Ph.D. Thesis, University of London, 1968.
- (78) Holmes R.R., Bertaut E.F., J.A.C.S., 1960, 80, 2980.
- (79) Prasad S., J. Indian Chem. Soc., 1959, 36, 129.
- (80) Funk H., Koehler H., J. Prakt. Chem., 1961, 14, 226.
- (81) Watori F., Sci. Repts. Res. Inst., Tohoku Univ.,
1961, 13A, 330.
- (82) Kijima I., Takahashi N., Kogyo Kagaku Zasshi, 1964, 67, 1092.
- (83) Markman A.L., Agzamov K.A., Tr. Tashkent Politekh. Inst.,
1968, 42, 70.
- (84) Bak B., et al., J. Chem. Phys., 1954, 22, 2013.
- (85) Hulme R., Acta Cryst., 1966, 21, 898.
- (86) Hargreaves A., Acta Cryst., 1955, 8, 12.
- (87) Lingafelter E.C., Acta Cryst., 1966, 20, 321.
- (88) Altona C., Acta Cryst., 1964, 17, 1282.
- (89) Nardelli M., et al., private communication, 1970.

- (90) Wells A.F., "Structural Inorganic Chemistry",
Oxford Univ. Press, 3rd. edn., 1967, p. 346.
- (91) Verweel H.J., Bijvoet J.M., Z. Krist., 1931, 77, 122.
- (92) Wells A.F., "Structural Inorganic Chemistry", O.U.P.,
3rd. edn., 1967, p. 893.
- (93) Hulme R., Scruton J.C., J. Chem. Soc., 1968, 2448.
- (94) Pauling L., "The Nature of the Chemical Bond",
Cornell Univ. Press, 3rd. edn., 1960.
- (95) Neubauer D., Weiss J., Z. anorg. Chem., 1960, 303, 28.
- (96) Coulson C.A., "Valence", Oxford Univ. Press,
2nd. edn., 1961, pp. 258, 262.
- (97) Sakurai K., Tomiie Y., Acta Cryst., 1952, 5, 293.
- (98) Huckerby T.N., Wilson J.W., Worrall I.J., Chem. Comm., 1967, 1190.
- (99) Bhuiya A.K., Stanley E., Acta Cryst., 1963, 16, 981.

APPENDIX I

Structure Factors, $2\text{SbCl}_3 \cdot \text{p-xylene}$.

(Low Temperature, -110°C)

$h, k, l, F_o, F_c \quad (\times 10)$

h k l				F _o	F _c	h k l				F _o	F _c	h k l				F _o	F _c	h k l				F _o	F _c
0	10	6	168.3	-199.3		1	8	6	160.9	218.3		1	0	-14	172.9	199.5		2	3	-7	-278.0	-270.3	
0	8	6	228.5	-165.4		1	10	6	181.7	219.9		1	2	-6	157.9	154.6		2	4	-7	217.2	-202.1	
0	9	9	225.4	199.0		1	1	7	378.4	302.2		1	6	-11	166.8	163.1		2	5	-7	315.7	-268.8	
0	8	7	237.5	-221.0		1	5	7	318.7	-354.1		2	0	-1	391.	464.9		2	6	-7	269.1	-263.3	
0	7	6	282.5	-273.5		1	6	7	149.0	149.9		2	0	2	350.4	311.9		2	4	-8	437.3	-447.1	
0	9	5	348.7	-350.5		1	7	7	178.6	178.6		2	3	4	315.7	274.7		2	6	-8	257.8	-263.4	
0	10	4	312.6	-284.1		1	1	8	187.7	-224.0		2	0	0	428.6	-442.2		2	10	-8	202.7	256.0	
0	8	4	141.3	-157.4		1	3	8	426.1	-379.4		2	0	-4	495.3	-579.1		2	5	-9	393.9	-400.0	
0	7	4	264.5	259.5		1	5	8	229.5	215.2		2	0	12	199.8	219.2		2	6	-9	234.6	-227.6	
0	6	4	456.9	369.8		1	7	8	166.8	221.7		2	1	0	515.5	617.4		2	7	-10	257.8	-290.2	
0	6	3	240.4	295.7		1	2	9	321.8	-353.3		2	1	1	376.5	355.5		2	0	-4	553.0	-623.4	
0	6	3	486.9	457.6		1	4	9	151.9	-140.6		2	1	2	344.1	344.9		2	0	-8	475.0	-466.3	
0	5	3	399.8	340.2		1	6	9	163.9	175.2		2	1	3	559.0	551.7		2	0	-10	321.5	274.0	
0	4	3	432.9	-425.4		1	8	9	277.1	246.7		2	1	4	431.6	-492.2		2	0	-12	454.7	-494.3	
0	3	3	139.2	119.7		1	1	12	289.0	-262.5		2	1	6	136.2	-99.2		2	0	-14	185.3	-233.3	
0	4	2	568.1	-480.1		1	3	10	286.0	-252.6		2	1	7	408.4	-361.5		2	0	-16	402.6	-404.0	
0	5	2	147.3	112.3		1	4	10	160.9	152.9		2	1	7	168.0	-162.2		2	3	-1	92.7	63.4	
0	6	2	162.3	114.1		1	7	10	178.6	169.2		2	2	1	231.7	264.7		2	4	-1	173.8	132.6	
0	7	2	471.4	441.3		1	5	11	268.2	259.0		2	2	2	252.0	-253.1		2	5	-1	197.0	196.5	
0	4	1	246.5	-274.6		1	4	12	274.1	249.8		2	2	1	127.3	376.5		2	6	-1	266.5	-238.2	
0	5	1	637.3	-693.2		1	6	13	-196.7	-175.0		2	2	2	252.0	241.7		2	7	-1	147.7	114.7	
0	6	1	174.4	154.4		1	1	11	208.6	-267.7		2	2	3	246.2	-222.7		2	8	-1	356.2	-355.5	
0	8	1	303.6	325.7		1	0	2	280.1	-293.8		2	2	5	677.7	-691.3		2	9	-1	173.8	-186.6	
0	9	1	327.7	317.5		1	0	4	92.4	-99.2		2	2	9	746.2	-237.6		3	0	-1	185.3	233.3	
0	3	2	820.6	-952.4		1	0	6	327.7	333.9		2	2	9	327.3	335.5		3	6	2	273.4	250.3	
0	2	1	664.3	-750.0		1	0	6	294.9	271.4		2	3	0	501.1	539.7		3	7	2	347.8	332.0	
0	2	0	87.1	-68.0		1	0	10	312.8	-328.7		2	3	1	336.0	-316.6		3	6	1	374.4	452.5	
0	4	0	724.4	-741.0		1	1	0	375.4	-442.2		2	3	2	208.5	180.0		3	8	1	237.7	258.0	
0	6	0	405.4	-342.5		1	2	0	95.3	78.1		2	3	3	428.6	-433.7		3	4	0	638.9	-602.1	
0	8	0	291.5	277.8		1	3	0	335.7	-289.1		2	3	4	289.9	-261.5		3	7	1	306.1	373.7	
0	10	0	240.4	268.6		1	4	0	464.8	410.1		2	3	6	486.6	-484.4		3	1	2	534.9	-494.8	
0	12	0	183.3	-230.3		1	5	0	292.0	251.0		2	3	8	231.7	213.5		3	1	3	722.2	-711.9	
0	8	9	165.4	-160.2		1	6	0	452.9	416.9		2	3	10	301.3	317.1		3	1	4	312.0	301.6	
0	7	7	222.5	-187.4		1	7	0	199.6	198.2		2	4	0	110.1	108.3		3	2	5	416.1	467.9	
0	7	8	231.5	-253.3		1	8	0	217.5	-205.9		2	4	1	353.4	326.2		3	3	6	401.2	563.1	
0	6	6	201.4	202.8		1	10	0	166.8	-223.2		2	4	2	553.2	-579.0		3	1	5	196.2	-232.7	
0	6	7	405.8	-327.8		1	8	-11	280.1	276.9		2	4	4	220.1	-171.2		3	1	6	208.0	221.1	
0	5	5	475.1	440.0		1	9	-7	232.4	-239.1		2	4	5	202.7	-155.5		3	1	7	225.9	275.7	
0	5	7	129.2	133.8		1	7	-3	238.3	-213.5		2	4	6	338.3	379.5		3	2	3	169.4	-166.6	
0	5	9	211.4	-171.9		1	8	-8	163.9	-150.2		2	4	6	379.5	348.6		3	4	5	306.1	268.3	
0	5	9	312.6	-315.1		1	7	-7	149.0	-111.4		2	5	0	367.3	-316.0		3	1	-0	410.1	-423.0	
0	5	11	243.5	-226.2		1	8	-7	157.9	-229.3		2	5	1	376.5	-327.0		3	2	0	267.5	237.0	
0	4	4	475.0	439.4		1	5	-7	169.8	-172.1		2	5	3	402.6	-356.4		3	3	0	523.1	-559.0	
0	4	5	198.4	156.1		1	6	-6	232.4	-188.4		2	5	7	501.1	478.2		3	2	1	653.9	-714.1	
0	4	6	360.7	326.4		1	7	-6	441.0	-513.5		2	6	1	347.6	-351.4		3	2	2	371.9	-353.2	
0	4	7	309.6	281.9		1	9	-6	163.9	-137.7		2	6	2	272.2	-234.2		3	3	2	493.4	-426.4	
0	4	8	318.6	-210.4		1	11	-6	241.3	216.0		2	6	3	240.4	254.3		3	4	2	347.8	342.0	
0	4	10	279.6	-265.1		1	5	-5	414.2	-412.4		2	6	4	292.4	-255.9		3	3	3	374.4	378.9	
0	4	12	231.5	-167.7		1	6	-5	289.0	-280.2		2	6	5	307.0	343.7		3	5	3	392.3	463.3	
0	3	4	132.3	-117.6		1	7	-5	140.1	-134.7		2	7	0	443.1	-383.8		3	4	4	389.4	346.1	
0	3	5	492.9	464.2		1	8	-5	149.0	-142.8		2	7	1	150.6	169.2		3	6	4	350.7	337.6	
0	3	6	345.6	287.1		1	9	-5	262.2	296.2		2	7	4	367.8	382.7		3	5	5	225.9	273.5	
0	3	7	213.4	165.0		1	6	-4	435.0	-460.6		2	7	6	228.0	272.9		3	5	7	252.7	-319.3	
0	3	8	432.9	391.2		1	8	-4	223.4	219.6		2	8	1	211.4	-195.4		3	0	2	751.9	745.7	
0	3	12	243.5	-223.7		1	10	-4	259.2	300.1		2	8	2	214.4	223.1		3	0	2	279.3	-254.0	
0	2	2	129.2	98.1		1	4	-3	432.0	-412.9		2	8	5	179.6	242.1		3	0	4	641.9	-615.2	
0	2	3	679.3	-751.4		1	5	-3	545.2	-572.0		2	9	1	176.6	181.4		3	0	8	413.1	502.9	
0	2	4	444.8	-370.2		1	6	-3	274.1	277.6		2	9	3	234.6	291.6		3	3	-1	208.0	-140.2	
0	2	5	135.2	101.5		1	7	-3	134.0	137.4		2	10	2	191.2	245.9		3	5	-1	636.0	-580.4	
0	2	6	171.3	-113.2		1	8	-3	265.2	262.9		2	9	7	202.7	-206.7		3	1	-2	398.2	437.3	
0	2	7	475.0	430.9		1	9	-3	202.6	193.9		2	6	8	182.5	216.1		3	3	-2	255.6	203.4	
0	2	8	210.4	129.3		1	3	-2	893.9	-956.6		2	4	9	175.6	131.5		3	4	-2	677.7	-609.4	
0	2	9	225.4	168.4		1	5	-2	312.8	271.2		2	8	9	295.4	-291.6		3	8	-2	193.2	-210.5	
0	2	11	282.5	-216.5		1	7	-2	473.7	466.0		2	7	10	295.4	-248.5		3	8	-2	231.6	286.3	
0	2	13	252.5	-227.2		1	8	-2	143.0	144.0		2	8	-11	257.8	-295.1		3	1	-3	243.7	221.0	
0	1	1	538.1	743.0		1	6	-2	119.2	-94.1		2	6	-11	182.5	-167.9		3	2	-3	674.6	711.4	
0	1	2	574.1	-598.8		1	2	-2	619.8	-211.1		2	6	-12	191.2	195.7		3	4	-3	294.2	248.3	
0	1	3	501.9	-514.1		1	4	-1	256.2	-222.4		2	5	-10	165.1	-152.1		3	6	-3	273.4	-241.1	
0	1	4	486.9	-440.8		1	5	-1	405.3	326.5		2	5	-13	312.8	338.2		3	8	-3	231.0	-294.4	
0	1	5	694.4	-752.7		1	6	-1	265.2	259.0		2	4	-9	243.3	202.6		3	1	-1	668.7	708.2	
0	1	6	571.1	4																			

k	l	F ₀	F _c	k	l	F ₀	F _c	k	l	F ₀	F _c	k	l	F ₀	F _c				
4	9	195.4	-190.6	4	1	446.8	300.2	5	9	266.2	-292.5	6	4	421.4	-412.2				
4	7	390.6	-426.3	4	2	112.5	89.5	5	11	132.1	-134.0	6	6	93.5	-84.0				
4	11	210.1	221.8	4	3	455.7	431.2	5	1	67.6	-42.0	6	7	130.3	-141.2				
4	4	121.3	122.4	4	7	476.4	-424.4	5	2	147.5	-119.2	6	8	247.1	246.1				
4	4	174.6	206.3	4	11	192.4	209.2	5	3	516.2	-473.4	6	2	380.7	414.1				
4	5	272.3	-301.5	4	1	352.2	-391.3	5	4	387.1	327.1	6	1	153.6	120.7				
4	5	130.2	162.7	4	2	464.6	437.6	5	6	196.6	269.2	6	4	103.6	97.2				
4	6	174.6	176.2	4	3	201.2	161.2	5	8	107.5	-156.6	6	5	320.5	-264.2				
4	7	136.1	161.1	4	4	162.5	137.6	5	10	122.9	-169.3	6	6	290.5	-234.1				
4	8	136.1	175.1	4	5	349.2	263.3	5	11	132.1	-182.3	6	8	110.2	-192.5				
4	1	150.9	130.5	4	6	372.6	-343.4	5	1	172.0	-133.7	6	9	116.9	-116.2				
4	2	331.5	-316.6	4	9	159.4	-179.1	5	2	706.7	-772.8	6	1	170.3	143.0				
4	3	366.9	311.5	4	2	107.1	-167.6	5	4	252.0	-210.0	6	2	83.5	-69.4				
4	4	550.4	594.1	4	4	553.4	546.6	5	6	381.9	352.6	6	3	487.5	474.6				
4	1	171.7	-180.6	4	8	183.5	-169.4	5	8	252.0	274.2	6	4	106.8	-62.1				
4	2	615.5	685.2	4	1	331.5	-277.5	5	1	445.5	-401.8	6	5	217.0	-191.0				
4	3	115.5	71.1	4	3	227.7	179.0	5	3	427.2	-412.3	6	7	320.5	-288.4				
4	4	298.4	242.1	4	4	174.6	-156.2	5	4	122.9	-154.7	6	1	787.1	-247.2				
4	5	88.8	152.3	4	5	272.3	317.4	5	6	221.2	-212.8	6	2	447.4	422.7				
4	1	334.4	305.6	4	9	281.2	-233.2	5	7	427.2	378.7	6	3	176.9	147.9				
4	2	133.1	158.0	4	1	12	251.6	-248.7	5	10	193.6	147.1	6	5	190.3	232.1			
4	3	223.2	406.2	4	2	12	100.6	81.3	5	11	205.4	-183.4	6	6	197.3	-195.3			
4	4	2	407.1	-146.3	4	3	12	177.6	-241.3	5	1	534.7	482.7	6	7	146.9	-171.6		
4	6	2	100.6	-92.0	4	4	12	162.6	174.6	5	2	356.4	-303.4	6	8	157.1	-197.3		
4	1	3	364.9	335.6	4	5	12	109.5	73.6	5	3	184.4	-196.5	6	3	133.5	62.6		
4	2	3	378.4	432.4	4	7	12	263.4	223.3	4	9	132.1	-131.4	6	4	279.5	223.1		
4	3	3	207.1	-226.4	4	8	12	127.2	-140.0	5	5	485.5	-419.9	6	6	217.0	242.9		
4	5	3	287.5	-241.5	4	2	13	254.5	-295.7	5	6	236.4	204.6	6	7	146.9	-149.3		
4	6	3	180.5	-192.5	4	6	13	121.3	163.6	5	9	264.2	289.7	6	8	160.2	-218.6		
4	8	3	150.9	-144.7	4	8	13	186.5	219.6	5	1	13	184.4	230.5	6	10	183.7	-711.7	
4	9	3	153.9	194.8	4	3	14	201.2	-245.6	5	2	10	338.0	282.1	6	1	480.8	-446.9	
4	1	4	150.9	-169.9	4	5	14	121.3	121.3	5	3	10	165.9	132.3	6	2	103.6	-98.1	
4	4	4	251.6	-281.1	4	6	14	127.2	-124.2	5	4	10	479.3	-435.4	6	3	390.7	351.2	
4	6	4	233.6	-257.2	4	7	14	133.1	157.6	5	6	10	239.7	-254.1	6	5	357.2	465.3	
4	8	4	121.3	183.1	4	3	15	186.5	-138.2	5	8	10	116.8	136.0	6	9	173.7	-230.7	
4	10	4	136.1	201.7	4	4	16	186.5	-186.6	5	1	11	282.7	253.0	6	2	250.4	-264.4	
4	1	5	224.9	254.4	4	3	17	136.1	-112.1	5	2	11	365.7	294.2	6	3	327.2	-201.2	
4	2	5	165.7	-141.8	4	7	6	654.3	625.0	5	3	11	119.9	-73.4	6	4	347.3	718.5	
4	3	5	100.6	-117.6	4	0	9	411.4	-305.7	5	4	11	316.5	315.8	6	6	1	180.3	172.6
4	4	5	103.6	-96.0	4	2	10	485.3	-457.1	5	5	11	236.7	-237.5	6	7	10	230.3	236.3
4	6	5	112.5	76.3	5	9	5	135.2	-167.2	5	6	11	248.5	-250.0	6	1	10	293.0	-264.9
4	8	5	127.2	122.2	5	8	5	122.9	183.5	5	1	11	184.4	-190.6	6	1	11	173.7	-124.0
4	9	5	186.5	163.5	5	7	2	212.0	253.9	5	9	11	129.0	160.0	6	2	11	436.7	-392.0
4	1	6	174.6	-167.9	5	6	1	153.7	181.4	5	1	12	439.4	413.0	6	3	11	187.6	137.2
4	3	6	304.8	-346.4	5	9	1	172.0	236.4	5	2	12	135.2	-77.9	6	4	11	303.5	-221.3
4	5	6	174.6	181.3	5	5	7	169.4	-147.3	5	3	12	405.6	411.6	6	6	11	447.5	316.5
4	7	6	174.6	183.5	5	6	7	147.5	-146.5	5	7	12	273.5	-291.7	6	8	11	173.7	167.6
4	2	7	260.4	-274.6	5	8	7	169.4	175.4	5	4	12	101.4	91.7	6	1	12	352.6	-283.1
4	1	8	198.3	-229.9	5	1	8	150.6	157.6	5	5	12	107.5	-89.5	6	2	12	136.1	104.3
4	3	8	118.4	-157.6	5	1	1	322.6	319.0	5	1	13	230.4	-244.5	6	3	12	303.6	-315.1
4	1	9	186.5	-188.8	5	1	2	227.4	-222.1	5	2	13	236.7	274.6	6	4	12	227.1	-247.4
4	1	11	136.1	-122.6	5	1	4	107.5	-42.5	5	3	13	147.5	108.0	6	7	12	227.1	259.7
4	2	11	136.1	170.6	5	1	5	153.7	-188.3	5	4	13	107.5	150.0	6	1	13	310.6	260.0
4	3	12	145.0	147.1	5	1	7	175.2	-174.0	5	5	13	172.0	193.7	6	2	13	140.2	-169.4
4	0	0	432.1	-469.7	5	1	8	184.4	233.7	5	6	13	181.3	-139.3	6	3	13	103.6	-107.5
4	0	4	393.6	410.9	5	2	1	196.6	-195.3	5	8	13	184.4	-219.2	6	5	13	233.7	-777.7
4	9	6	174.6	132.4	5	3	1	331.9	-782.7	5	9	13	135.2	-146.4	6	9	13	193.7	239.6
4	0	8	198.3	-222.2	5	2	3	396.4	-444.4	5	3	14	110.7	129.9	6	1	14	120.2	125.1
4	0	10	127.2	-174.2	5	2	5	230.4	-223.6	5	4	14	245.6	254.2	6	4	14	253.8	-294.4
4	1	3	130.2	107.1	5	2	7	150.6	164.1	5	5	14	119.9	-108.3	6	6	14	173.7	-197.1
4	2	3	633.3	-725.3	5	2	7	196.6	181.2	5	6	14	107.4	183.7	6	1	15	110.2	139.1
4	3	3	221.9	-170.3	5	3	4	322.6	-372.6	5	6	14	135.2	-127.1	6	2	15	253.8	294.5
4	4	3	408.4	-358.8	5	3	8	193.5	209.3	5	1	15	175.2	-725.6	6	5	15	173.7	-221.4
4	5	3	216.0	159.7	5	4	4	156.7	132.1	5	2	15	132.1	-168.7	6	6	15	126.9	-120.3
4	6	3	322.6	280.3	5	4	6	264.2	274.6	5	5	15	215.1	279.5	6	3	16	273.8	327.5
4	8	3	441.0	475.5	5	5	5	261.7	324.2	5	3	16	190.5	-744.3	6	7	16	197.0	-218.6
4	10	3	121.3	-125.9	5	5	7	162.8	147.1	5	0	6	602.2	-676.6	6	2	17	263.8	243.1
4	12	3	195.4	-205.0	5	6	5	119.9	136.5	5	0	0	402.6	369.5	6	5	17	190.3	167.1
4	4	2	417.3	348.6	5	6	6	122.9	137.1	5	0	10	448.6	449.7	6	0	2	420.7	467.5
4	5	2	112.5	85.1	5	2	0	227.4	170.1	5	3	2	291.9	364.3	6	0	8	164.0	-624.3
4	6	2	366.7	340.1	5	3	9	113.7	107.7	6	8	3	183.7	-182.5	6	0	10	167.0	-132.7
4	7	2	355.2	350.8	5	4	3	430.2	-443.1	6	8	2	123.5	-166.7	6	0	12	200.4	164.1
4	8	2	106.6	-152.1	5	5	1	304.2	-311.5	6	8	1	120.2	164.7	6	1	4	297.2	305.4
4	10	2	186.5	-183.0	5	3	2	187.4	-168.7	6	9	1	180.3	-215.9	6	1	3	350.6	371.6
4	11	2	133.2	-144.1	5	4	2	141.3	-113.5	6	7	0	247.1	278.1	6	3	3	213.7	-171.6
4	4	1	201.2	-177.1	5	6	2	159.8	-184.4	6	6	0	103.6	79.1	6	2	2	143.6	140.4
4	5	1	521.8	557.0	5	6	3	248.9	256.4	6	8	0	116.9	-112.2	6	3	2	160.2	-187.4
4	6	1	91.8	101.7	5	8	3	122.9	163.0	6	1	9	233.7	-276.3	6	4	2	434.1	-425.0
4	7	1	171.7	153.2	5	7	4	181.3	222.5	6	1	1	387.3	-401.5	6	2	1	387.3	-405.0
4	9	1	298.9	-350.7	5	8	7	138.2	-146.7	6	1	3	303.6	-233.3	6	4	1	220.4	-230.7
4	11	1	133.1	-125.3	5	6	9	141.3	-142.1	6	1	4	146.9	171.0					
4	1	4	405.4	-347.0	5	4	10	141.3	-143.0	6	1	5							

APPENDIX II

Structure Factors, $C_5H_5NH.SbCl_4$.

(Room Temperature, $25^{\circ}C$)

$h, k, l, FDM^*, F_o^+, F_o^{\ddagger}$

(* Data collected on film;

+ Porter and Jacobson observed data;

‡ " " calculated data;

see Chapter III).

h	k	l	F _{AM}	F _o	F _c	h	k	l	F _{AM}	F _o	F _c	h	k	l	F _{AM}	F _o	F _c	h	k	l	F _{AM}	F _o	F _c	h	k	l	F _{AM}	F _o	F _c
12	C	-4	77	67	66	12	C	-4	77	67	66	12	C	-4	77	67	66	12	C	-4	77	67	66	12	C	-4	77	67	66
10	C	-4	78	68	67	10	C	-4	78	68	67	10	C	-4	78	68	67	10	C	-4	78	68	67	10	C	-4	78	68	67
8	C	-2	112	123	123	8	C	-2	112	123	123	8	C	-2	112	123	123	8	C	-2	112	123	123	8	C	-2	112	123	123
8	C	-4	76	70	71	8	C	-4	76	70	71	8	C	-4	76	70	71	8	C	-4	76	70	71	8	C	-4	76	70	71
8	C	-8	55	54	51	8	C	-8	55	54	51	8	C	-8	55	54	51	8	C	-8	55	54	51	8	C	-8	55	54	51
6	C	-4	124	144	146	6	C	-4	124	144	146	6	C	-4	124	144	146	6	C	-4	124	144	146	6	C	-4	124	144	146
6	C	-6	79	81	80	6	C	-6	79	81	80	6	C	-6	79	81	80	6	C	-6	79	81	80	6	C	-6	79	81	80
4	C	-2	115	137	136	4	C	-2	115	137	136	4	C	-2	115	137	136	4	C	-2	115	137	136	4	C	-2	115	137	136
4	C	-4	103	103	99	4	C	-4	103	103	99	4	C	-4	103	103	99	4	C	-4	103	103	99	4	C	-4	103	103	99
2	C	-4	108	108	95	2	C	-4	108	108	95	2	C	-4	108	108	95	2	C	-4	108	108	95	2	C	-4	108	108	95
0	C	-6	145	152	147	0	C	-6	145	152	147	0	C	-6	145	152	147	0	C	-6	145	152	147	0	C	-6	145	152	147
0	C	-6	66	57	57	0	C	-6	66	57	57	0	C	-6	66	57	57	0	C	-6	66	57	57	0	C	-6	66	57	57
2	C	-2	138	134	128	2	C	-2	138	134	128	2	C	-2	138	134	128	2	C	-2	138	134	128	2	C	-2	138	134	128
6	C	-6	124	145	145	6	C	-6	124	145	145	6	C	-6	124	145	145	6	C	-6	124	145	145	6	C	-6	124	145	145
6	C	-6	139	145	145	6	C	-6	139	145	145	6	C	-6	139	145	145	6	C	-6	139	145	145	6	C	-6	139	145	145
6	C	-6	107	108	107	6	C	-6	107	108	107	6	C	-6	107	108	107	6	C	-6	107	108	107	6	C	-6	107	108	107
11	1	-4	85	73	73	11	1	-4	85	73	73	11	1	-4	85	73	73	11	1	-4	85	73	73	11	1	-4	85	73	73
11	1	-6	77	55	55	11	1	-6	77	55	55	11	1	-6	77	55	55	11	1	-6	77	55	55	11	1	-6	77	55	55
9	1	-3	85	75	74	9	1	-3	85	75	74	9	1	-3	85	75	74	9	1	-3	85	75	74	9	1	-3	85	75	74
5	1	-4	70	60	60	5	1	-4	70	60	60	5	1	-4	70	60	60	5	1	-4	70	60	60	5	1	-4	70	60	60
5	1	-6	73	46	43	5	1	-6	73	46	43	5	1	-6	73	46	43	5	1	-6	73	46	43	5	1	-6	73	46	43
9	1	-6	73	46	43	9	1	-6	73	46	43	9	1	-6	73	46	43	9	1	-6	73	46	43	9	1	-6	73	46	43
7	1	-2	147	159	154	7	1	-2	147	159	154	7	1	-2	147	159	154	7	1	-2	147	159	154	7	1	-2	147	159	154
7	1	-2	106	114	110	7	1	-2	106	114	110	7	1	-2	106	114	110	7	1	-2	106	114	110	7	1	-2	106	114	110
7	1	-5	104	106	102	7	1	-5	104	106	102	7	1	-5	104	106	102	7	1	-5	104	106	102	7	1	-5	104	106	102
7	1	-5	97	100	100	7	1	-5	97	100	100	7	1	-5	97	100	100	7	1	-5	97	100	100	7	1	-5	97	100	100
7	1	-5	65	55	55	7	1	-5	65	55	55	7	1	-5	65	55	55	7	1	-5	65	55	55	7	1	-5	65	55	55
5	1	-7	188	150	150	5	1	-7	188	150	150	5	1	-7	188	150	150	5	1	-7	188	150	150	5	1	-7	188	150	150
5	1	-7	139	148	148	5	1	-7	139	148	148	5	1	-7	139	148	148	5	1	-7	139	148	148	5	1	-7	139	148	148
5	1	-6	81	65	65	5	1	-6	81	65	65	5	1	-6	81	65	65	5	1	-6	81	65	65	5	1	-6	81	65	65
3	1	-1	52	54	54	3	1	-1	52	54	54	3	1	-1	52	54	54	3	1	-1	52	54	54	3	1	-1	52	54	54
3	1	-4	64	68	68	3	1	-4	64	68	68	3	1	-4	64	68	68	3	1	-4	64	68	68	3	1	-4	64	68	68
3	1	-6	74	62	62	3	1	-6	74	62	62	3	1	-6	74	62	62	3	1	-6	74	62	62	3	1	-6	74	62	62
3	1	-6	84	70	70	3	1	-6	84	70	70	3	1	-6	84	70	70	3	1	-6	84	70	70	3	1	-6	84	70	70
1	1	-2	41	46	46	1	1	-2	41	46	46	1	1	-2	41	46	46	1	1	-2	41	46	46	1	1	-2	41	46	46
1	1	-5	92	56	56	1	1	-5	92	56	56	1	1	-5	92	56	56	1	1	-5	92	56	56	1	1	-5	92	56	56
1	1	-5	69	50	50	1	1	-5	69	50	50	1	1	-5	69	50	50	1	1	-5	69	50	50	1	1	-5	69	50	50
1	1	-1	184	182	182	1	1	-1	184	182	182	1	1	-1	184	182	182	1	1	-1	184	182	182	1	1	-1	184	182	182
1	1	-3	77	77	77	1	1	-3	77	77	77	1	1	-3	77	77	77	1	1	-3	77	77	77	1	1	-3	77	77	77
1	1	-4	102	94	94	1	1	-4	102	94	94	1	1	-4	102	94	94	1	1	-4	102	94	94	1	1	-4	102	94	94
3	1	-5	69	55	55	3	1	-5	69	55	55	3	1	-5	69	55	55	3	1	-5	69	55	55	3	1	-5	69	55	55
3	1	-5	94	105	105	3	1	-5	94	105	105	3	1	-5	94	105	105	3	1	-5	94	105	105	3	1	-5	94	105	105
3	1	-2	85	65	65	3	1	-2	85	65	65	3	1	-2	85	65	65	3	1	-2	85	65	65	3	1	-2	85	65	65
5	1	-0	87	115	115	5	1	-0	87	115	115	5	1	-0	87	115	115	5	1	-0	87	115	115	5	1	-0	87	115	115
5	1	-2	61	47	47	5	1	-2	61	47	47	5	1	-2	61	47	47	5	1	-2	61	47	47	5	1	-2	61	47	47
7	1	-0	143	151	151	7	1	-0	143	151	151	7	1	-0	143	151	151	7	1	-0	143	151	151	7	1	-0	143	151	151
7	1	-2	77	62	62	7	1	-2	77	62	62	7	1	-2	77	62	62	7	1	-2	77	62	62	7	1	-2	77	62	62
10	2	-1	56	80	80	10	2	-1	56	80	80	10	2	-1	56	80	80	10	2	-1	56	80	80	10	2	-1	56	80	80
10	2	-6	60	57	57	10	2	-6	60	57	57	10	2	-6	60	57	57	10	2	-6	60	57	57	10	2	-6	60	57	57
6	2	-1	54	55	55	6	2	-1	54	55	55	6	2	-1	54	55	55	6	2	-1	54	55	55	6	2	-1	54	55	55
6	2	-5	56	102	102	6	2	-5	56	102	102	6	2	-5	56	102	102	6	2	-5	56	102	102	6	2	-5	56	102	102
6	2	-7	59	99	99	6	2	-7	59	99	99	6	2	-7	59	99	99	6	2	-7	59	99	99	6	2	-7	59	99	99
6	2	-1	51	50	50	6	2	-1	51	50	50	6	2	-1	51	50	50	6	2	-1	51	50	50	6	2	-1	51	50	50
6	2	-2	71	68	68	6	2	-2	71	68	68	6	2	-2	71	68	68	6	2	-2	71	68	68	6	2	-2	71	68	68
6	2	-5	51	54	54	6	2	-5	51	54	54	6	2	-5	51	54	54	6	2	-5	51	54	54	6	2	-5	51	54	54
4	2	-1	105	127	127	4	2	-1	105	127	127	4	2	-1	105	127	127	4	2	-1	105	127	127	4	2	-1	105	127	127
4	2	-3	58	146	146	4	2	-3	58	146	146	4	2	-3	58	146	146	4	2	-3	58	146	146	4	2	-3	58	146	146
4	2	-6	109	127	127	4	2	-6	109	127	127	4	2	-6	109	127	127	4	2	-6	109	127	127	4	2	-6	109	127	127
4	2	-6	67	67	68	4	2	-6	67	67	68	4	2	-6	67	67	68	4	2	-6	67	67	68	4	2	-6	67	67	68
2	2	-1	201																										

APPENDIX III

Structure Factors, $2\text{SbCl}_3 \cdot 5\text{C}_5\text{H}_5\text{N}$.

(Room Temperature, 25°C)

$h, k, l, F_o, F_c, \text{PHASE}, (F's \times 10)$

[illegible]

APPENDIX IV(a)

Structure Factors, $\text{SbCl}_3 \cdot \text{C}_5\text{H}_5\text{N}$.

(Room Temperature, 25°C)

$h, k, l, F_o, \sin \theta$

[illegible]

h	k	l	Fo	SINθ	h	k	l	Fo	SINθ
3	5	3	4874	C.1994	3	8	-3	4436	C.1867
3	5	4	3327	C.2265	3	8	-7	5874	C.2607
2	5	5	4058	C.2333	4	8	-3	5062	C.1965
0	5	2	2127	C.1207	6	8	-5	3963	C.2395
0	5	3	3021	C.1428	7	8	-4	2526	C.2450
0	5	4	3653	C.1690	8	8	-4	2714	C.2705
0	5	6	1785	C.2278	8	8	-5	2235	C.2732
0	5	7	2388	C.2589	1	8	1	5928	C.1693
3	5	2	1802	C.1747	2	8	1	4652	C.1813
7	6	-3	4501	C.2259	4	8	1	5805	C.2176
3	6	-1	3660	C.1457	2	8	3	4167	C.2161
4	6	-1	1653	C.1650	0	8	3	6764	C.1853
5	6	-1	4197	C.1879	2	8	0	2009	C.1715
6	6	-1	3297	C.2131					
1	6	-2	3903	C.1330					
2	6	-2	3342	C.1360					
2	6	-3	2808	C.1465					
2	6	-4	7593	C.1672					
2	6	-5	3912	C.1703					
2	6	-7	2316	C.2443					
3	6	-2	4063	C.1460					
3	6	-3	5231	C.1542					
3	6	-4	3695	C.1690					
4	6	-3	4240	C.1659					
4	6	-4	3962	C.1760					
6	6	-5	3788	C.2151					
8	6	-4	2035	C.2452					
1	6	-3	1269	C.1496					
2	6	0	3586	C.1354					
3	6	0	1512	C.1531					
5	6	0	2795	C.1994					
6	6	0	2673	C.2258					
1	6	1	4126	C.1326					
3	6	1	3560	C.1673					
4	6	1	3799	C.1905					
3	6	2	2287	C.1868					
4	6	2	6281	C.2105					
2	6	3	4317	C.1887					
2	6	4	4061	C.2146					
3	6	4	4786	C.2359					
1	6	5	5197	C.2236					
1	6	6	3566	C.2531					
0	6	2	5582	C.1376					
0	6	3	4357	C.1573					
0	6	5	2710	C.2084					
8	7	-4	3230	C.2593					
6	7	-2	4094	C.2174					
1	7	-2	1321	C.1511					
1	7	-3	2014	C.1659					
1	7	-4	5956	C.1859					
2	7	-1	1563	C.1496					
2	7	-3	2441	C.1649					
3	7	-2	4450	C.1627					
3	7	-3	2569	C.1701					
3	7	-6	4208	C.2241					
4	7	-2	4260	C.1771					
4	7	-4	1722	C.1906					
4	7	-8	3879	C.2724					
5	7	-4	5085	C.2025					
5	7	-5	1939	C.2141					
7	7	-6	2585	C.2529					
2	7	-2	2310	C.1537					
2	7	0	4930	C.1533					
5	7	0	3507	C.2120					
6	7	0	2449	C.2370					
1	7	1	3340	C.1507					
5	7	1	2896	C.2275					
1	7	2	5362	C.1654					
2	7	2	3095	C.1808					
3	7	2	5544	C.2001					
1	7	4	4638	C.2086					
2	7	4	3721	C.2262					
0	7	2	4284	C.1551					
0	7	4	2659	C.1951					
0	7	6	2542	C.2478					
7	8	-3	4828	C.2493					
3	8	-1	6840	C.1797					
5	8	-1	4335	C.2154					
2	8	-3	4931	C.1821					
2	8	-5	5660	C.2175					

APPENDIX IV(b)

Structure Factors, $\text{SbCl}_3 \cdot \underset{5}{\text{C}} \underset{5}{\text{H}} \underset{5}{\text{N}}$.

(Low Temperature, -110°C)

$h, k, l, F_o, \sin \theta.$

h	k	l	F ₀	SINθ	h	k	l	F ₀	SINθ	h	k	l	F ₀	SINθ	h	k	l	F ₀	SINθ
3	C	0	842	C.0452	3	6	1	2525	0.1669	1	14	2	1379	0.2914	6	-2	-3	2819	0.1663
4	C	0	3486	C.1270	3	8	1	1272	0.1970	2	1	2	2515	C.1174	1	-3	-3	2049	C.1082
5	C	0	1557	C.1587	3	12	1	2509	C.2649	2	2	2	1857	0.1223	4	-3	-3	1245	C.1241
6	C	0	2328	C.1905	4	5	1	1803	C.1782	2	3	2	2108	0.1301	5	-3	-3	4002	C.1483
7	C	0	3423	C.2222	4	6	1	2066	C.1899	2	5	2	2777	0.1523	8	-3	-3	2458	C.2256
1	2	0	865	C.0508	4	7	1	1294	0.2029	2	7	2	1453	C.1806	1	-4	-3	4045	C.1252
1	3	0	3506	C.0674	4	8	1	3619	C.2169	2	11	2	1603	C.2466	3	-4	-3	2527	C.1249
1	4	0	1379	C.0853	4	10	1	2053	C.2473	2	13	2	1560	C.2822	4	-4	-3	3618	C.1384
1	5	0	1246	C.1040	5	7	1	1824	C.2267	3	1	2	1642	C.1454	5	-4	-3	1481	C.1773
1	10	0	2702	C.2005	5	11	1	1573	C.2822	3	3	2	1877	C.1558	6	-4	-3	4808	C.1799
1	12	0	1959	C.2397	3	2	1	2946	0.1237	3	7	2	2676	C.1999	1	-5	-3	5198	C.1341
2	4	0	3989	C.1015	3	3	1	2270	C.1314	3	9	2	2654	0.2292	2	-5	-3	4261	C.1324
2	5	0	2657	C.1176	4	2	1	2925	0.1533	4	2	2	1556	C.1780	3	-5	-3	5338	C.1382
2	6	0	2731	C.1347	4	3	1	1495	C.1596	4	4	2	4749	C.1908	4	-5	-3	4051	C.1506
2	7	0	3291	C.1525	5	3	1	2561	C.1893	4	6	2	2519	0.2103	8	-5	-3	3428	C.2391
2	9	0	4638	C.1892	5	5	1	2760	C.2349	4	10	2	2240	0.2633	2	-6	-3	1629	C.1478
3	1	0	5014	C.0973	6	1	1	3630	C.2117	5	1	2	1108	C.2047	3	-6	-3	4269	0.1530
3	3	0	3390	C.1123	10	-7	-1	1508	C.3311	6	3	2	2743	0.2418	4	-6	-3	2650	0.1643
3	4	0	1762	C.1239	7	-5	-1	2772	C.2286	5	-3	-2	3400	C.1479	7	-6	-3	3937	0.2232
3	5	0	1316	C.1374	9	-5	-1	2101	C.2967	7	-3	-2	2115	0.2036	2	-7	-3	1529	0.1641
3	10	0	1700	C.2157	5	-3	-1	2156	C.1553	9	-3	-2	1827	C.2628	3	-7	-3	2208	C.1688
3	11	0	2105	C.2377	4	-2	-1	2407	0.1194	4	-2	-2	4511	C.1147	2	-8	-3	3143	C.1812
3	13	0	2123	C.2745	8	-2	-1	2674	C.2408	6	-2	-2	3470	0.1694	3	-8	-3	3730	C.1854
4	1	0	2541	C.1285	3	-1	-1	2210	C.0847	8	-2	-2	1811	0.2287	4	-8	-3	3986	C.1946
4	2	0	3272	C.1330	4	-1	-1	2531	C.1143	5	-1	-2	2290	0.1369	1	-9	-3	1756	C.1998
4	4	0	2133	C.1457	5	-1	-1	4792	C.1449	3	0	-2	1322	C.0828	3	-10	-3	2863	C.2202
4	11	0	1427	C.2521	7	-1	-1	2534	0.2070	6	0	-2	3502	C.1647	1	-11	-3	1961	0.2358
4	3	0	2060	C.1402	1	-3	-1	1699	C.0675	8	0	-2	2955	0.2252	4	-11	-3	2014	C.2456
5	4	0	1786	C.1774	1	-4	-1	1784	C.0855	1	-2	-2	2281	C.0707	1	-7	-3	1539	C.1655
5	5	0	2085	C.1871	1	-5	-1	998	0.1041	1	-3	-2	2662	C.0834					
5	6	0	2486	C.1983	1	-6	-1	1095	0.1231	1	-4	-2	1777	C.0985					
5	7	0	2971	C.2107	1	-7	-1	1299	C.1423	1	-5	-2	2356	0.1150					
5	9	0	2393	C.2387	1	-11	-1	1516	C.2202	1	-6	-2	2634	C.1324					
5	10	0	2026	C.2538	1	-13	-1	1670	0.2594	1	-9	-2	2427	0.1876					
6	3	0	1610	C.1995	1	-15	-1	1596	C.2987	1	-10	-2	1575	0.2065					
6	4	0	2935	C.2063	2	-1	-1	1709	C.0574	2	-2	-2	1509	C.0755					
6	5	0	1678	C.2147	2	-2	-1	2151	C.0668	2	-3	-2	1483	C.0875					
6	6	0	1886	C.2245	2	-3	-1	3727	C.0802	2	-4	-2	1581	0.1020					
6	7	0	2094	C.2356	2	-4	-1	1277	C.0958	2	-5	-2	2482	C.1180					
6	9	0	1456	C.2609	2	-5	-1	2679	0.1127	2	-6	-2	2043	C.1351					
6	10	0	1939	C.2748	2	-7	-1	1537	0.1487	2	-7	-2	1197	C.1528					
7	3	0	1562	C.2301	2	-9	-1	1067	0.1862	2	-9	-2	1727	0.1894					
8	4	0	1473	C.2661	2	-11	-1	2471	0.2244	2	-11	-2	1669	C.2271					
1	7	0	1340	C.1422	3	-2	-1	1495	C.0914	3	-3	-2	3716	C.1019					
2	10	0	1277	C.2079	3	-6	-1	2072	C.1445	3	-4	-2	3076	C.1146					
3	6	0	1076	C.1523	3	-8	-1	4081	C.1785	3	-6	-2	2589	C.1448					
1	11	0	1522	0.2201	3	-10	-1	2003	C.2144	3	-7	-2	2931	C.1615					
7	2	0	1545	C.2258	4	-4	-1	3168	C.1377	3	-10	-2	1742	C.2146					
1	8	0	1111	0.1616	5	-6	-1	2465	C.1863	3	-12	-2	2177	0.2516					
0	2	0	3373	C.0396	5	-8	-1	2827	0.2137	4	-4	-2	2869	C.1337					
0	8	0	1269	C.1584	6	-6	-1	1986	C.2113	4	-7	-2	2671	C.1755					
0	10	0	4057	0.1980	6	-9	-1	1460	C.2496	4	-9	-2	2144	0.2082					
0	14	0	2892	C.2772	7	-6	-1	1586	C.2379	5	-5	-2	2338	C.1678					
0	16	0	2997	0.3168	7	-7	-1	1455	0.2484	6	-7	-2	3363	0.2153					
0	2	1	3030	C.0525	7	-8	-1	2244	0.2599	7	-4	-2	2056	C.2102					
0	3	1	2187	C.0686	7	-10	-1	2097	C.2858	7	-10	-2	1337	C.2777					
0	4	1	2866	0.0463	1	-9	-1	1213	C.1811	8	-9	-2	1932	0.2872					
0	8	1	987	C.1621	1	-10	-1	1113	C.2006	1	-11	-2	1175	C.2255					
0	11	1	1662	0.2205	4	-5	-1	946	C.1499	2	-10	-2	1293	C.2082					
0	12	1	1595	C.2401	5	-4	-1	1518	0.1639	3	-11	-2	1199	C.2330					
1	2	1	1122	C.0701	6	-5	-1	1575	C.2008	4	-8	-2	1064	C.1915					
1	3	1	3657	C.0829	7	-4	-1	1176	C.2208	0	1	3	2188	0.1051					
1	4	1	3425	C.0941	1	0	2	2268	C.0898	0	3	3	3401	0.1191					
1	5	1	2052	C.1147	2	0	2	3376	C.1158	0	6	3	2095	C.1574					
1	6	1	2442	C.1321	3	0	2	1861	C.1441	0	8	3	3381	C.1891					
1	7	1	2382	C.1502	5	0	2	3552	C.2038	1	1	3	1851	0.1246					
1	8	1	3297	0.1686	6	0	2	2779	C.2344	1	2	3	1450	0.1292					
1	10	1	2262	0.2063	0	3	2	1621	C.0909	1	4	3	4120	0.1463					
1	11	1	1944	0.2254	0	4	2	2765	C.1049	2	1	3	3165	C.1484					
1	12	1	1020	C.2445	0	5	2	1126	0.1206	2	8	3	2390	0.2162					
2	3	1	1346	C.1052	0	6	2	2876	C.1373	3	5	3	1756	C.1999					
2	4	1	1721	0.1175	0	7	2	2289	C.1547	3	10	3	2109	0.2633					
2	5	1	1437	0.1317	0	9	2	2125	0.1910	5	1	3	2740	0.2316					
2	8	1	2775	0.1806	0	10	2	2248	0.2096	5	-1	-3	4127	0.1374					
2	9	1	1106	C.1982	1	1	2	2405	0.0919	6	-1	-3	2632	C.1627					
2	12	1	2327	0.2530	1	3	2	2974	C.1076	7	-1	-3	2771	0.1900					
2	13	1	1536	0.2716	1	5	2	1476	C.1336	9	-1	-3	2866	C.2478					
2	14	1	1601	0.2905	1	7	2	2574	C.1651	3	-1	-3	1406	C.0984					
2	2	1	3679	0.0954	1	9	2	2746	0.1995	3	-2	-3	1115	C.1042					
2	1	1	2237	C.0890	1	13	2	1079	0.2726	4	-2	-3	4155	C.1202					

APPENDIX V

Structure Factors, $2\text{SbCl}_3 \cdot \text{C}_5\text{H}_5\text{N}$.

(Room Temperature, 25°C)

h, k, l, F_o, F_c (X 10)

Eliminated High Value Structure Factors (F_o)

(see Chapter VII)

1	0	1	214	-470
3	0	0	436	689
4	0	0	507	-939
1	0	-3	501	894
1	1	1	415	-258
1	1	0	407	-643
1	1	-2	460	646
3	-1	2	421	694
4	-1	2	530	243
5	-1	2	242	558
3	-1	-1	447	653
0	1	1	385	662
0	1	3	559	-902
0	2	-1	325	508
0	2	-4	731	959
2	-2	1	310	634
2	1	-4	425	571
1	-2	-1	358	538
7	-1	2	480	340
9	-1	2	400	271
3	2	-1	535	691

APPENDIX VI

PROGRAMME TO DETERMINE THE MEAN PLANE $aX + bY + Z = 0$

for a set of atoms with orthogonal Ångstrom coordinates:

$$X_i = x_i + y_i \cos \gamma + z_i \cos \beta$$

$$Y_i = y_i \sin \gamma - z_i \cos \alpha^* \sin \beta$$

$$Z_i = z_i \sin \alpha^* \sin \beta$$

where x_i, y_i, z_i are the triclinic Å coordinates of the atoms.

The X (orthogonal) axis is common with the x (triclinic)
axis, *and Y lies in the xy plane.*

The plane is defined in terms of angles θ, ϕ, ψ ,

describing rotation about X, Y, Z axes respectively, and by

shifts to the origin (in Å) X, Y, Z.

Rotation, θ° , about X is in a direction from Z to Y;

ϕ° about Y from X to Z; ψ° about Z from Y to X.

(FORTRAN IV ; I.B.M. 360/44)

C PROGRAMME FOR DETERMINATION OF MEAN PLANE AND ATOMIC DISTANCES
FROM PLANE.

```

      DIMENSION X(50),Y(50),Z(50),XORTH(50),YORTH(50),ZORTH(50)
      WRITE(6,3)
      K=0
99  READ(5,1) A,B,C,ALPHA,BETA,GAMMA,NATOM,NPLA,IP
      IF(A.EQ.0.0) GO TO 999
      READ(5,2) (X(I),Y(I),Z(I), I=1,NATOM)
      K=K+1
      WRITE(6,30) K
      FACT = 57.29582
      ALPHA=ALPHA/FACT
      BETA=BETA/FACT
      GAMMA=GAMMA/FACT
C ORTHOGONAL TRANSFORMATION OF COORDINATES
      ACOS=COS(ALPHA)
      BCOS=COS(BETA)
      GCOS=COS(GAMMA)
      BSIN=SIN(BETA)
      GSIN=SIN(GAMMA)
      RACOS=(BCOS*GCOS - ACOS)/BSIN*GSIN
      RASIN=SQRT(1. - RACOS*RACOS)
      F1=BSIN*RACOS
      F2=BSIN*RASIN
      DO 100 I=1,NATOM
      X(I)=X(I)*A
      Y(I)=Y(I)*B
      Z(I)=Z(I)*C
      XORTH(I)=X(I)+Y(I)*GCOS+Z(I)*BCOS
      YORTH(I)=Y(I)*GSIN- Z(I)*F1
100  ZORTH(I)=Z(I)*F2
C APPLY SHIFTS TO ORIGIN
      DO 400 I=2,NATOM
      XORTH(I)=XORTH(I) - XORTH(1)
      YORTH(I)=YORTH(I) - YORTH(1)
400  ZORTH(I)=ZORTH(I) - ZORTH(1)
C DETERMINATION OF MEAN PLANE OF COORDINATES
      E11=0.
      E22=0.
      E12=0.
      XK1=0.
      XK2=0.
      DO 200 I=2,NPLA
      E11=E11+XORTH(I)*XORTH(I)
      E22=E22+YORTH(I)*YORTH(I)
      E12=E12+XORTH(I)*YORTH(I)
      XK1=XK1+XORTH(I)*ZORTH(I)
200  XK2=XK2+YORTH(I)*ZORTH(I)
      DENOM=E11*E22 - E12*E12

```

```

      IF(DENOM.EQ.0.0) GO TO 301
      ROOTA = (E12*YK2 - E22*YK1)/DENOM
      ROOTB = (E11*YK2 - E12*YK1)/DENOM
      WRITE(6,4)
      WRITE(6,5) ROOTA,ROOTB
C DETERMINATION OF DISTANCES TO PLANE OF NON-PLANE ATOMS
      IF(NPLA.EQ.NATOM) GO TO 20
      ABC=SQRT(ROOTA*ROOTA + ROOTB*ROOTB + 1.)
      IOUT=NPLA+1
      WRITE(6,12)
      DO 300 I=IOUT,NATOM
      L=I-1
      DIST=(ROOTA*XORTH(I)+ROOTB*YORTH(I)+ZORTH(I))/ABC
      DIST=ABS(DIST)
      300 WRITE(6,8) L,DIST
C SHIFTS OF PLANE TO ORIGIN
      20 WRITE(6,16)
      WRITE(6,17) XORTH(I),YORTH(I),ZORTH(I)
C CALCULATION OF ANGULAR ROTATIONS OF PLANE
      WRITE(6,14)
      ROOT= -ROOTB/ROOTA
      PSI=ATAN(ROOT)
      SPSI=SIN(PSI)
      PHI=ATAN(SPSI/ROOTB)
C CALCULATION OF ROTATED SHIFTED COORDINATES
      CPSI=COS(PSI)
      CPHI=COS(PHI)
      SPHI=SIN(PHI)
      DO 500 I=2,NPLA
C APPLY PSI ROTN.
      XO=XORTH(I)
      YO=YORTH(I)
      XORTH(I)=XO*CPSI+YO*SPSI
      YORTH(I)=YO*CPSI-XO*SPSI
C APPLY PHI ROTN.
      XO=XORTH(I)
      ZO=ZORTH(I)
      XORTH(I)=XO*CPHI-ZO*SPHI
      500 ZORTH(I)=ZO*CPHI+XO*SPHI
      THETA=ATAN(ZORTH(I)/ YORTH(IP))
      CTH=COS(THETA)
      STH=SIN(THETA)
      PSI=PSI*FACT
      PHI=PHI*FACT
      THETA=THETA*FACT
      WRITE(6,15) THETA,PHI,PSI
C APPLY THETA ROTN.
      WRITE(6,9)
      DO 600 I=2,NPLA

```

```

      YO=YORTH(I)
      ZO=ZORTH(I)
      YORTH(I)=YO*CTH+ZO*STH
      ZORTH(I)=ZO*CTH-YO*STH
600 WRITE(6,10) XORTH(I),YORTH(I),ZORTH(I)
      WRITE(6,2000)
      GO TO 99
301 WRITE(6,19)
      GO TO 99
      1 FORMAT(3F7.3,3F7.2,3I3)
      2 FORMAT(10F8.5)
      3 FORMAT('1', ' MEAN PLANE AND ATOMIC DISTANCES FROM MEAN PLANE')
      4 FORMAT(' ', ' DEFINE EQUATION OF ORIGIN PLANE AS AX+BY+Z=0'//
      1 ' ORTHOGONAL ANGSTROM COEFFICIENTS'//)
      5 FORMAT(' ', 'A = ',E12.5,3X,'B = ',E12.5,3X,'C = 0.10000E 01'//)
12  FORMAT('0', ' DISTANCES TO PLANE FROM NON-PLANE ATOMS'//
      1 ' ATOM NUMBER',5X,' DIST. ANGSTROMS'//)
14  FORMAT(' ', ' ANGULAR ROTATIONS OF PLANE IN DEGREES'//)
      9 FORMAT(' ', ' ORTHOGONAL ROTATED ZEROED ANGSTROM COORDINATES',2X,
      1 ' X COORDS. ARE SHIFTS'//3X,' X',10X,' Y',10X,' Z'//)
10  FORMAT(' ',F9.5,3X,F9.5,3X,F9.5//)
      8 FORMAT(' ', ' ATOM',I2,' -PLANE',4X,F9.5//)
15  FORMAT(' ', 'THETA = ',F7.2,3X,'PHI = ',F7.2,3X,'PSI = ',F7.2//)
16  FORMAT('0', ' SHIFTS OF PLANE TO ORIGIN IN ANGSTROMS'//)
17  FORMAT(' ', ' X SHIFT = ',F8.4,' Y SHIFT = ',F8.4,3X,
      1 ' Z SHIFT = ',F8.4//)
19  FORMAT('-', ' PLANE IS PARALLEL TO C AXIS OF ORTHOGONAL CELL'//
      1 ' *** REDEFINE INPUT COORDINATES OF PLANE-ATOMS')
30  FORMAT('1', ' DATA SET',I2//)
2000 FORMAT('-', ' END OF DATA'/' *** PLANE REORIENTED')
999 CALL EXIT
      END

```

INPUT DATA.

A, B, C, ALPHA, BETA, GAMMA : Real cell dimensions.

NATOM : Total number of atoms.

NPLA : Number of atoms in plane.

IP : Atom to be oriented along Y axis (Z coord. = 0.0)

X(I), Y(I), Z(I) : Fractional coords. for all atoms.

X(1), Y(1), Z(1) : Fractional coords. of centre of planar molecule,
i.e. fractional shifts of plane to origin.

Terminate all data with blank card.